



HAL
open science

Asymptotic Modeling of the Electromagnetic Scattering by Small Spheres Perfectly Conducting

Justine Labat, Victor Péron, Sébastien Tordeux

► **To cite this version:**

Justine Labat, Victor Péron, Sébastien Tordeux. Asymptotic Modeling of the Electromagnetic Scattering by Small Spheres Perfectly Conducting. [Research Report] RR-9169, Université de Pau et des Pays de l'Adour; Inria Bordeaux Sud-Ouest; LMAP UMR CNRS 5142. 2018. hal-01762625v1

HAL Id: hal-01762625

<https://inria.hal.science/hal-01762625v1>

Submitted on 10 Apr 2018 (v1), last revised 22 Nov 2018 (v2)

HAL is a multi-disciplinary open access archive for the deposit and dissemination of scientific research documents, whether they are published or not. The documents may come from teaching and research institutions in France or abroad, or from public or private research centers.

L'archive ouverte pluridisciplinaire **HAL**, est destinée au dépôt et à la diffusion de documents scientifiques de niveau recherche, publiés ou non, émanant des établissements d'enseignement et de recherche français ou étrangers, des laboratoires publics ou privés.



Asymptotic Modeling of the Electromagnetic Scattering by Small Spheres Perfectly Conducting

Justine Labat, Victor Péron , Sébastien Tordeux

**RESEARCH
REPORT**

N° 9169

April 2018

Project-Teams Magique 3D, Inria
Bordeaux Sud-Ouest, UPPA-E2S,
LMAP UMR 5142



Asymptotic Modeling of the Electromagnetic Scattering by Small Spheres Perfectly Conducting

Justine Labat*, Victor Péron *, Sébastien Tordeux*

Project-Teams Magique 3D, Inria Bordeaux Sud-Ouest, UPPA-E2S, LMAP
UMR 5142

Research Report n° 9169 — April 2018 — 48 pages

Abstract: In this paper, we develop a method of matched asymptotic expansions for solving the time-harmonic electromagnetic scattering problem by a small sphere perfectly conducting. This method consists in defining an approximate solution using multi-scale expansions over far and near fields, related in a matching area. We make explicit the asymptotics up to the second order of approximation for the near-field expansion and up to the fifth order of approximation for the far-field expansion. We illustrate the results with numerical experiments which make evident the performance of the asymptotic models. The reference solution is an analytical solution computed thanks to Montjoie code.

Key-words: Asymptotic expansions, Maxwell's equations, Reduced models

* Team-Project Magique 3D, University of Pau and Pays de l'Adour, Inria Bordeaux Sud-Ouest, LMAP UMR CNRS 5142

**RESEARCH CENTRE
BORDEAUX – SUD-OUEST**

200 avenue de la Vieille Tour
33405 Talence Cedex

Modélisation asymptotique de la diffraction des ondes électromagnétiques par de petites sphères parfaitement conductrices

Résumé : Dans ce rapport, nous utilisons la méthode des développements asymptotiques raccordés afin d'approcher la solution du problème de diffraction d'ondes électromagnétiques par une petite sphère parfaitement conductrice. Cette méthode consiste à définir deux approximations locales de la solution en utilisant des développements multi-échelles, dits de champ proche et champ lointain. Ces développements sont ensuite raccordés dans une zone de transition. Nous effectuons les développements jusqu'à l'ordre deux pour le champ proche et jusqu'à l'ordre cinq pour le champ lointain. Nous illustrons ces résultats avec des expériences numériques qui mettent en évidence les ordres de convergence de ces développements, en fonction de la taille de l'obstacle. La solution de référence est une solution analytique calculée à l'aide du code Montjoie.

Mots-clés : Développements asymptotiques, Équations de Maxwell, Modèles réduits

1 Introduction

Many physical phenomena involve multiple electromagnetic scattering by small obstacles [7, 22, 38, 41]. All exact theories and numerical methods for computing the electromagnetic fields are based on solving Maxwell's equations either analytically or numerically. For scatterers of arbitrary shape, the use of numerical methods is required. When the scatterers are larger or comparable to the wavelength, classical numerical methods as continuous or discontinuous finite element methods and boundary element methods have been developed in [5, 18, 30] for solving the time-harmonic Maxwell's equations. However, these methods become very expensive, both in terms of computation time and memory capacity, when the scatterers are significantly small in comparison with the incident wavelength. That is partly due to the necessity of refining three-dimensional meshes as finer as the obstacles are small but also to the consideration of a low-frequency regime, where the refractive index is significantly smaller than one [34]. A recent method treating the multiple electromagnetic scattering proposed by Ganesh and Hawkins in [23], is based on a fully discrete spectrally accurate algorithm but their study is limited to obstacles of diameter larger than the incident wavelength.

Several methods can be considered in order to overcome difficulties related to the small obstacle size as local mesh refinement techniques or asymptotic analysis [15, 19, 24, 29]. An other spectral method which has been proposed in [4, 35], is based on a spectral approximation of the solution for solving the multiple acoustic scattering by small obstacles in two-dimensional domains. The asymptotic theory in singularly perturbed domains has turned out to be very efficient in numerical techniques. Dependence of solution on a small parameter is taken into consideration and the initial problem can be decomposed into a collection of elementary problems. Different methods bring out of this branch of analysis as the method of multiscale expansions [8, 32, 39] or the method of matched asymptotic expansions [12, 13, 28, 36]. Even if these methods lead to different iteration procedures for construction of the asymptotics, the approximations coincide locally [16]. Others asymptotic formulas for the perturbations in the tangential trace of the magnetic field caused by the presence of heterogeneities have been derived and rigorously justified by Ammari *et al.* in [3] and also in the Volkov's thesis [40]. In these works, a boundary integral equation point of view is approached. Moreover, an inverse problem is considered to determine both the physical properties and the location of the small obstacles [1, 2]. Only the first terms of the asymptotics are performed and it seems to be a difficult task to derive the next terms. In other word, there is no algorithm of construction for successive terms of the asymptotic expansions.

The matched asymptotic expansions consists in constructing distinct expansions of the solution in different regions with appropriate scales, and matching them in an intermediate region also called the matching area [37]. The justification of matching rules can be obtained from hypothesis on the structure of the uniform expansion in the whole domain [21]. This method allows to define local approximations of the solution at any order, relatively to the obstacle size but is difficult to justify rigorously [36]. This method is typically used for the case of one small obstacle that involves only two different expansions. The transition to the multiple scattering can be performed thanks to an appropriate model as Born or Foldy-Lax model [6, 10]. If obstacles are sufficiently distant, the principle of superposition given by the Born approximation can be taken into account. On the contrary, if interactions between obstacles cannot be neglected, the application of the Foldy theory should improve the previous one [20]. Some intermediate models between Born and Foldy approximations are compared in [11] for the multiple electromagnetic scattering by finitely many point-like obstacles. It is worth noting that the matched asymptotic expansions applied on the multiple electromagnetic scattering involve a such problem, in a punctured domain. From a viewpoint of *far field*, obstacles are reduced to point-like obstacles. The

physical nature of the equations is unchanged. In addition, we can employ this method to give explicit analytical solutions in specific geometries as spheres, spheroids or ellipsoids - in geometries for which a parametrization give us explicit eigenfunctions of the vectorial Laplace-Beltrami operator.

The search for an exact analytic solution goes traditionally through the solution of the vector Helmholtz equation for the electric field using the technique of separation of variables in one of the few parametrizations in which this equation is separable. The incident field is expanded in eigenfunctions that are regular in bounded domains, whereas the scattered field is expanded in eigenfunctions that are outgoing waves at infinity. The elementary problems identified by the method of matched asymptotic expansions are separable in the same coordinate system, either in *slow* or *fast* variable. However, the solutions of the elementary problems have not always the same physical nature. Actually, from a viewpoint of *near field*, created fields which contain the information of the perturbation, appear as in static regime.

This paper is organized as follows. In Section 2, we describe the problem that we consider and we present the main results that we have established. These results characterize the first terms of the asymptotic expansions for the electromagnetic scattering by a perfectly conducting small sphere. They are obtained thanks to the application of the method of matching asymptotic expansions and are performed at the second order for the near-field expansion and at the fifth order for the far-field expansion. Then, we give a physical interpretation of the first terms of the asymptotics through the idealistic notion of electric and magnetic multipoles. In Section 3, we display some numerical results which make evident the performance of the asymptotic models. From these local expansions, we construct a global approximation by truncating suitably the whole domain. In Section 4, we present the full method of matched asymptotic expansions applied on the electromagnetic scattering by a small sphere. It consists in defining an approximate solution using multi-scale expansions over far and near fields, related in a matching area. We make explicit the matching conditions thanks to the use of modal decomposition of the near-field and far-field terms that we have introduced in Appendix B. Then, we pursue the construction of the first terms of the far-field and near-field expansions based on the modal decomposition in spherical geometries. Finally, in Section 5, we extend our results to define a collected model which consists on gathering the terms, not with respect the δ -powers, but with respect to their nature, in terms of multipoles. Moreover, we propose a multiple scattering model in electromagnetism, based on the Born approximation.

2 Problem description and main result

2.1 Normalization of the equations

The propagation of time-harmonic electromagnetic waves of angular frequency ω in a homogeneous and isotropic dielectric with electric permittivity $\varepsilon > 0$ and magnetic permeability $\mu > 0$ is described by an incident wave $\Re\left[(\mathcal{E}^{\text{inc}}(\mathbf{x}), \mathcal{H}^{\text{inc}}(\mathbf{x})) \exp(-i\omega t)\right]$. The incident field $(\mathcal{E}^{\text{inc}}, \mathcal{H}^{\text{inc}})$ satisfies the time-harmonic Maxwell equations

$$\begin{cases} \operatorname{curl} \mathcal{E}^{\text{inc}} - i\omega\mu\mathcal{H}^{\text{inc}} = 0 & \text{in } \mathbb{R}^3 \\ \operatorname{curl} \mathcal{H}^{\text{inc}} + i\omega\varepsilon\mathcal{E}^{\text{inc}} = \mathcal{J} & \text{in } \mathbb{R}^3 \end{cases}$$

where the electric current density \mathcal{J} is a smooth vector field with compact support in \mathbb{R}^3 that is related to the electric charge density ρ through the charge conservation principle

$$-i\omega\rho + \operatorname{div} \mathcal{J} = 0 \quad \text{in } \mathbb{R}^3.$$

Remark 1. When \mathcal{J} is of class \mathcal{C}^∞ , then we can prove that \mathbf{E}^{inc} and \mathbf{H}^{inc} are also of class \mathcal{C}^∞ into any bounded sub-domain of \mathbb{R}^3 .

In Table 1, we introduce the classical electromagnetic fields, densities and potentials, with *calligraphic* symbols. Afterwards, we define a normalization and we denote the normalized quantities with *straight* symbols.

	Usual convention		Normalized quantities	
Electric field	\mathcal{E}	$[\text{Vm}^{-1}]$	\mathbf{E}	$= \varepsilon\mu^{\frac{1}{2}}\mathcal{E}$
Magnetic field	\mathcal{H}	$[\text{Am}^{-1}]$	\mathbf{H}	$= \varepsilon^{\frac{1}{2}}\mu\mathcal{H}$
Electric charge density	ρ	$[\text{Cm}^{-3}]$	ϱ	$= \mu^{\frac{1}{2}}\rho$
Electric current density	\mathcal{J}	$[\text{Am}^{-2}]$	\mathbf{j}	$= \mu^{\frac{1}{2}}\mathcal{J}$
Electric potential	\mathcal{V}	$[\text{V}]$	\mathbf{V}	$= \varepsilon\mu^{\frac{1}{2}}\mathcal{V}$
Magnetic potential	\mathcal{A}	$[\text{Vsm}^{-1}]$	\mathbf{A}	$= \varepsilon^{\frac{1}{2}}\mathcal{A}$

Table 1: Normalization of the electromagnetic quantities

Taking in account this normalization, the incident field $(\mathbf{E}^{\text{inc}}, \mathbf{H}^{\text{inc}})$, that is of class \mathcal{C}^∞ into any bounded domain of \mathbb{R}^3 , satisfies the time-harmonic Maxwell equations

$$\begin{cases} \mathbf{curl} \mathbf{E}^{\text{inc}} - i\kappa\mathbf{H}^{\text{inc}} = 0 & \text{in } \mathbb{R}^3 & (2.1a) \\ \mathbf{curl} \mathbf{H}^{\text{inc}} + i\kappa\mathbf{E}^{\text{inc}} = \mathbf{j} & \text{in } \mathbb{R}^3. & (2.1b) \end{cases}$$

The wave-number κ satisfies the dispersion relation

$$\kappa = \frac{\omega}{c} \quad (2.2)$$

with the wave-speed $c = (\mu\varepsilon)^{-\frac{1}{2}}$.

Remark 2. The charge conservation principle remains unchanged and we have $-i\omega\varrho + \text{div} \mathbf{j} = 0$.

Remark 3. For example, the incident field $(\mathbf{E}^{\text{inc}}, \mathbf{H}^{\text{inc}})$ can be an electromagnetic plane wave,

$$\mathbf{E}^{\text{inc}}(\mathbf{x}) = \mathbf{p} \exp(i\mathbf{k} \cdot \mathbf{x}); \quad \mathbf{H}^{\text{inc}}(\mathbf{x}) = \frac{1}{\kappa}(\mathbf{k} \times \mathbf{p}) \exp(i\mathbf{k} \cdot \mathbf{x}); \quad \text{with } \mathbf{k} \cdot \mathbf{p} = 0 \quad (2.3)$$

where the wave-vector \mathbf{k} that is proportional to the wave-number κ sets the angle of propagation and \mathbf{p} denotes the polarization vector.

2.2 Description of the scattering problem

In the presence of small obstacles with characteristic length δ , the incident field $(\mathbf{E}^{\text{inc}}, \mathbf{H}^{\text{inc}})$ is scattered and gives birth to a new field $(\mathbf{E}_\delta^{\text{tot}}, \mathbf{H}_\delta^{\text{tot}})$ which can be decomposed into the incident field and a scattered field $(\mathbf{E}_\delta, \mathbf{H}_\delta)$

$$\mathbf{E}_\delta^{\text{tot}} = \mathbf{E}^{\text{inc}} + \mathbf{E}_\delta; \quad \mathbf{H}_\delta^{\text{tot}} = \mathbf{H}^{\text{inc}} + \mathbf{H}_\delta.$$

Both the total field $(\mathbf{E}_\delta^{\text{tot}}, \mathbf{H}_\delta^{\text{tot}})$ and the scattered field $(\mathbf{E}_\delta, \mathbf{H}_\delta)$ have to satisfy Maxwell equations in the exterior domain of the obstacles with the same wave-number κ . The scattered field also needs to satisfy the outgoing Silver-Müller radiation condition at infinity

$$\lim_{r \rightarrow \infty} r(\mathbf{H}_\delta \times \hat{\mathbf{x}} - \mathbf{E}_\delta) = 0 \quad r = |\mathbf{x}|, \quad \hat{\mathbf{x}} = \frac{\mathbf{x}}{r}. \quad (2.4)$$

The created fields strongly depend on the geometry and the physical properties of obstacles. In this paper, we consider the multiple electromagnetic scattering by K spherical obstacles $\mathcal{B}(c_k, \delta)$, $k = 1, \dots, K$, perfectly conducting, each one being centered at c_k with small radius $\delta > 0$, see Figure 1. We assume that any distance \mathbf{d}_{jk} between two obstacles is not small in comparison

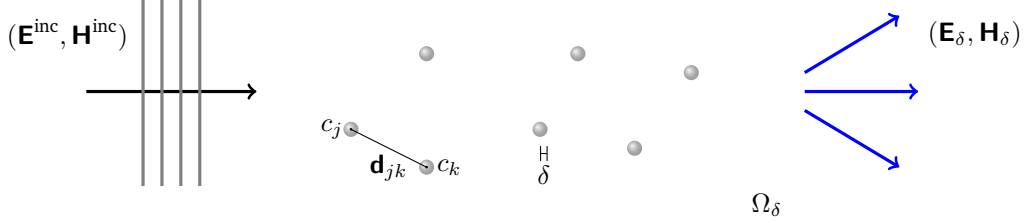


Figure 1: Domain of propagation

with λ . The domain of propagation Ω_δ is defined by

$$\Omega_\delta = \mathbb{R}^3 \setminus \bigcup_{k=1}^K \overline{\mathcal{B}(c_k, \delta)}. \quad (2.5)$$

The scattering problem reads as

$$\begin{cases} \mathbf{curl} \mathbf{E}_\delta - i\kappa \mathbf{H}_\delta = 0 & \text{in } \Omega_\delta & (2.6a) \\ \mathbf{curl} \mathbf{H}_\delta + i\kappa \mathbf{E}_\delta = 0 & \text{in } \Omega_\delta & (2.6b) \\ \mathbf{n} \times \mathbf{E}_\delta = -\mathbf{n} \times \mathbf{E}^{\text{inc}} & \text{on } \partial\Omega_\delta & (2.6c) \\ \mathbf{n} \cdot \mathbf{H}_\delta = -\mathbf{n} \cdot \mathbf{H}^{\text{inc}} & \text{on } \partial\Omega_\delta & (2.6d) \\ \lim_{r \rightarrow \infty} r(\mathbf{H}_\delta \times \hat{\mathbf{x}} - \mathbf{E}_\delta) = 0 & \text{uniformly in } \hat{\mathbf{x}} & (2.6e) \end{cases}$$

where \mathbf{n} denotes the outward-pointing normal unit vector of $\partial\Omega_\delta$. It is well-known that the electromagnetic scattering problem by a finite number of spheres is well-posed, see for instance [30, 31]. Moreover, the solution $(\mathbf{E}_\delta, \mathbf{H}_\delta)$ have an analytical decomposition into Ω_δ . In Appendix C, we recall some properties about its decomposition.

Remark 4. For lipschitz obstacles, the exterior Maxwell problem (2.6) has a unique solution $(\mathbf{E}_\delta, \mathbf{H}_\delta)$ in $\mathbf{H}_{\text{loc}}(\mathbf{curl}, \Omega_\delta)$ if the tangential trace of the electric field $\mathbf{n} \times \mathbf{E}_\delta$ on $\partial\Omega_\delta$ belongs to the Sobolev space

$$\mathbf{H}_t^{-\frac{1}{2}}(\text{div}_{\partial\Omega_\delta}, \partial\Omega_\delta) = \left\{ \mathbf{u} \in \mathbf{H}^{-\frac{1}{2}}(\partial\Omega_\delta), \text{div}_{\partial\Omega_\delta} \mathbf{u} \in H^{-\frac{1}{2}}(\partial\Omega_\delta) \text{ and } \mathbf{u} \cdot \mathbf{n} = 0 \text{ on } \partial\Omega_\delta \right\},$$

A characterization of this space for lipschitz domains is established in [9]. Moreover, this condition ensures that the normal trace of the magnetic field $\mathbf{n} \cdot \mathbf{H}_\delta$ on $\partial\Omega_\delta$ belongs to $H^{-\frac{1}{2}}(\partial\Omega_\delta)$. Then, well-posedness in $\mathbf{H}_{\text{loc}}(\mathbf{curl}, \Omega_\delta)$ derives from the Fredholm theory and can be proved thanks to a boundary integral equation posed on $\partial\Omega_\delta$ and the use of integral representation given by the Stratton-Chu formulas, see [14], or with an equivalent interior problem by equipping the fictive boundary with a transparent condition. These formulations are also equivalent to prove well-posedness of this problem into Sobolev weighted spaces for \mathbf{curl} and div , see [31], that allows to precise the behavior of the fields at infinity.

Remark 5. The numerical simulation of the scattering by small obstacles, using finite element methods (FEM, DG, HDG, . . .), can become very expensive or not affordable in terms of computation time and memory even in the context of mesh refinement and parallel computation. This is mainly due to the size of the linear system which should be inverted.

Afterwards, we introduce the results that we have established for $K = 1$ and $c_1 = 0$, *i.e.* for the scattering problem by one small sphere $\mathcal{B}(0, \delta)$ centered at the origin with small radius δ . We come back to the multiple scattering problem in Section 5. This is driven by the fact that the numerical validation confirms these results only for one small sphere. For any smooth vector field \mathbf{u} we denote $\gamma_n \mathbf{u}$ its normal trace on the unit sphere S^2 in \mathbb{R}^3 and $\gamma_t \mathbf{u}$ and $\gamma_\times \mathbf{u}$ its tangential traces on S^2 , defined by

$$\gamma_n \mathbf{u} = (\mathbf{e}_r \cdot \mathbf{u})|_{S^2}; \quad \gamma_\times \mathbf{u} = (\mathbf{e}_r \times \mathbf{u})|_{S^2}; \quad \gamma_t \mathbf{u} = (\gamma_\times \mathbf{u}) \times \mathbf{e}_r \quad (2.7)$$

where \mathbf{e}_r denotes the outward-pointing normal unit vector of S^2 .

2.3 The main result

In this section, we present the local approximations in far and near fields, for the solution to problem (2.6) that we have derived thanks to the method of matched asymptotic expansions.

2.3.1 Far-field approximation

Far from the obstacle, we prove that the exact solution has the following formal asymptotic expansion

$$\mathbf{E}_\delta = \delta^3 \tilde{\mathbf{E}}_3 + \delta^5 \tilde{\mathbf{E}}_5 + \dots; \quad \mathbf{H}_\delta = \delta^3 \tilde{\mathbf{H}}_3 + \delta^5 \tilde{\mathbf{H}}_5 + \dots \quad (2.8)$$

For any positive integer p , the far-field terms $(\tilde{\mathbf{E}}_p, \tilde{\mathbf{H}}_p)$ are defined in the asymptotic domain

$$\Omega^* = \mathbb{R}^3 \setminus \{0\}. \quad (2.9)$$

From this point of view, the scatterer is replaced by a point-like obstacle. Moreover, the third order far-field terms $(\tilde{\mathbf{E}}_3, \tilde{\mathbf{H}}_3)$ are given by

$$\begin{aligned} \tilde{\mathbf{E}}_3(\mathbf{x}) = & -\frac{\kappa^3}{2} h_1^{(1)}(\kappa r) \gamma_\times \mathbf{H}^{\text{inc}}(0) - \kappa^3 \frac{h_1^{(1)}(\kappa r) + \kappa r h_1^{(1)' }(\kappa r)}{i \kappa r} \gamma_t \mathbf{E}^{\text{inc}}(0) \\ & - 2\kappa^3 \frac{h_1^{(1)}(\kappa r)}{i \kappa r} \gamma_n \mathbf{E}^{\text{inc}}(0) \mathbf{e}_r \end{aligned} \quad (2.10a)$$

and

$$\begin{aligned} \tilde{\mathbf{H}}_3(\mathbf{x}) = & -\kappa^3 h_1^{(1)}(\kappa r) \gamma_\times \mathbf{E}^{\text{inc}}(0) + \frac{\kappa^3}{2} \frac{h_1^{(1)}(\kappa r) + \kappa r h_1^{(1)' }(\kappa r)}{i \kappa r} \gamma_t \mathbf{H}^{\text{inc}}(0) \\ & + \kappa^3 \frac{h_1^{(1)}(\kappa r)}{i \kappa r} \gamma_n \mathbf{H}^{\text{inc}}(0) \mathbf{e}_r \end{aligned} \quad (2.10b)$$

with $\mathbf{x} = r\hat{\mathbf{x}}$ and $h_n^{(1)}$ denotes the n -order spherical Hankel function of the first kind. The fifth order far-field terms ($\tilde{\mathbf{E}}_5, \tilde{\mathbf{H}}_5$) are given by

$$\begin{aligned} \tilde{\mathbf{E}}_5(\mathbf{x}) = & \frac{3\kappa^5}{10} h_1^{(1)}(\kappa r) \gamma_{\times} \mathbf{H}^{\text{inc}}(0) - \frac{3\kappa^5}{10} \frac{h_1^{(1)}(\kappa r) + \kappa r h_1^{(1)'}(\kappa r)}{i\kappa r} \gamma_t \mathbf{E}^{\text{inc}}(0) \\ & - \frac{3\kappa^5}{5} \frac{h_1^{(1)}(\kappa r)}{i\kappa r} \gamma_n (\mathbf{E}^{\text{inc}}(0)) \mathbf{e}_r - \frac{\kappa^4}{9} h_2^{(1)}(\kappa r) \gamma_{\times} \left(\mathbb{J}_{\mathbf{H}^{\text{inc}}}^{\text{sym}}(0) \mathbf{e}_r \right) \\ & - \frac{\kappa^4}{6} \frac{h_2^{(1)}(\kappa r) + \kappa r h_2^{(1)'}(\kappa r)}{i\kappa r} \gamma_t \left(\mathbb{J}_{\mathbf{E}^{\text{inc}}}^{\text{sym}}(0) \mathbf{e}_r \right) - \frac{\kappa^4}{2} \frac{h_2^{(1)}(\kappa r)}{i\kappa r} \gamma_n \left(\mathbb{J}_{\mathbf{E}^{\text{inc}}}(0) \mathbf{e}_r \right) \mathbf{e}_r \end{aligned} \quad (2.11a)$$

and

$$\begin{aligned} \tilde{\mathbf{H}}_5(\mathbf{x}) = & -\frac{3\kappa^5}{10} h_1^{(1)}(\kappa r) \gamma_{\times} \mathbf{E}^{\text{inc}}(0) - \frac{3\kappa^5}{10} \frac{h_1^{(1)}(\kappa r) + \kappa r h_1^{(1)'}(\kappa r)}{i\kappa r} \gamma_t \mathbf{H}^{\text{inc}}(0) \\ & - \frac{3\kappa^5}{5} \frac{h_1^{(1)}(\kappa r)}{i\kappa r} \gamma_n (\mathbf{H}^{\text{inc}}(0)) \mathbf{e}_r - \frac{\kappa^4}{6} h_2^{(1)}(\kappa r) \gamma_{\times} \left(\mathbb{J}_{\mathbf{E}^{\text{inc}}}^{\text{sym}}(0) \mathbf{e}_r \right) \\ & + \frac{\kappa^4}{9} \frac{h_2^{(1)}(\kappa r) + \kappa r h_2^{(1)'}(\kappa r)}{i\kappa r} \gamma_t \left(\mathbb{J}_{\mathbf{H}^{\text{inc}}}^{\text{sym}}(0) \mathbf{e}_r \right) + \frac{\kappa^4}{3} \frac{h_2^{(1)}(\kappa r)}{i\kappa r} \gamma_n \left(\mathbb{J}_{\mathbf{H}^{\text{inc}}}(0) \mathbf{e}_r \right) \mathbf{e}_r \end{aligned} \quad (2.11b)$$

where \mathbb{J}_{\diamond} denotes the Jacobian matrix of \diamond and $\mathbb{J}_{\diamond}^{\text{sym}} = \frac{1}{2}(\mathbb{J}_{\diamond} + \mathbb{J}_{\diamond}^{\top})$ the symmetric Jacobian of \diamond .

Remark 6. The fourth order far-field terms ($\tilde{\mathbf{E}}_4, \tilde{\mathbf{H}}_4$) are reduced to null-field.

For $P = 3, 4$ or 5 , let us introduce the vector fields ($\tilde{\mathbf{E}}_{\delta,P}, \tilde{\mathbf{H}}_{\delta,P}$) reading as the sum of the first far-field terms

$$\tilde{\mathbf{E}}_{\delta,P} = \sum_{p=3}^P \delta^p \tilde{\mathbf{E}}_p; \quad \tilde{\mathbf{H}}_{\delta,P} = \sum_{p=3}^P \delta^p \tilde{\mathbf{H}}_p. \quad (2.12)$$

The following conjecture is a transposition of the numerical results obtained in Section 3.3, which precises the expected order of convergence.

Conjecture 1. For $P = 3, 4$ or 5 , there exists $\delta_0 > 0$ such that for any $r_1 > r_0 > \delta_0$ there exists $c > 0$ such that for any positive $\delta < \delta_0$, we have

$$\|\mathbf{E}_{\delta} - \tilde{\mathbf{E}}_{\delta,P}\|_{\infty, \mathcal{C}(r_0, r_1)} \leq c \delta^{P-2} \|\mathbf{E}_{\delta}\|_{\infty, \mathcal{C}(r_0, r_1)}; \quad \|\mathbf{H}_{\delta} - \tilde{\mathbf{H}}_{\delta,P}\|_{\infty, \mathcal{C}(r_0, r_1)} \leq c \delta^{P-2} \|\mathbf{H}_{\delta}\|_{\infty, \mathcal{C}(r_0, r_1)}$$

and

$$\|\mathbf{E}_{\delta} - \tilde{\mathbf{E}}_{\delta,P}\|_{0, \mathcal{C}(r_0, r_1)} \leq c \delta^{P-2} \|\mathbf{E}_{\delta}\|_{0, \mathcal{C}(r_0, r_1)}; \quad \|\mathbf{H}_{\delta} - \tilde{\mathbf{H}}_{\delta,P}\|_{0, \mathcal{C}(r_0, r_1)} \leq c \delta^{P-2} \|\mathbf{H}_{\delta}\|_{0, \mathcal{C}(r_0, r_1)}$$

where $\mathcal{C}(r_0, r_1) = \{\mathbf{x} \in \mathbb{R}^3, r_0 < |\mathbf{x}| < r_1\}$, $\|\cdot\|_{0, \diamond}$ denotes the \mathbf{L}^2 -norm in \diamond and $\|\cdot\|_{\infty, \diamond}$ denotes the \mathbf{L}^{∞} -norm in \diamond . The constant c depends on δ_0, r_0 and r_1 but does not depend on δ .

Furthermore, thanks to the regularity of the analytical solution, we can establish the following conjecture that is a consequence of the previous one.

Conjecture 2. For any $P = 3, 4$ or 5 , there exists δ_0 such that for any $r_1 > r_0 > \delta_0$ there exists $c > 0$ such that for any positive $\delta < \delta_0$, we have

$$\|\mathbf{E}_{\delta} - \tilde{\mathbf{E}}_{\delta,P}\|_{\infty, \mathcal{C}(r_0, r_1)} \leq c \delta^{P+1}; \quad \|\mathbf{H}_{\delta} - \tilde{\mathbf{H}}_{\delta,P}\|_{\infty, \mathcal{C}(r_0, r_1)} \leq c \delta^{P+1}$$

and

$$\|\mathbf{E}_{\delta} - \tilde{\mathbf{E}}_{\delta,P}\|_{0, \mathcal{C}(r_0, r_1)} \leq c \delta^{P+1}; \quad \|\mathbf{H}_{\delta} - \tilde{\mathbf{H}}_{\delta,P}\|_{0, \mathcal{C}(r_0, r_1)} \leq c \delta^{P+1}.$$

2.3.2 Near-field approximation

Close to the obstacle, we prove that the exact solution have the formal asymptotic expansion

$$\mathbf{E}_\delta(\delta \cdot) = \widehat{\mathbf{E}}_0 + \delta \widehat{\mathbf{E}}_1 + \delta^2 \widehat{\mathbf{E}}_2 + \dots ; \quad \mathbf{H}_\delta(\delta \cdot) = \widehat{\mathbf{H}}_0 + \delta \widehat{\mathbf{H}}_1 + \delta^2 \widehat{\mathbf{H}}_2 + \dots$$

Here, for any positive integer p , the near-field terms $(\widehat{\mathbf{E}}_p, \widehat{\mathbf{H}}_p)$ are defined in fast variable $\mathbf{X} = \frac{\mathbf{x}}{\delta}$ in the dimensionless domain $\widehat{\Omega}$ given by

$$\widehat{\Omega} = \mathbb{R}^3 \setminus \overline{\mathcal{B}(0, 1)}. \quad (2.13)$$

The zeroth order near-field terms $(\widehat{\mathbf{E}}_0, \widehat{\mathbf{H}}_0)$ are given by

$$\widehat{\mathbf{E}}_0 = \frac{1}{\mathbb{R}^3} \left\{ 3\gamma_n(\mathbf{E}^{\text{inc}}(0))\widehat{x} - \mathbf{E}^{\text{inc}}(0) \right\}; \quad \widehat{\mathbf{H}}_0 = -\frac{1}{2\mathbb{R}^3} \left\{ 3\gamma_n(\mathbf{H}^{\text{inc}}(0))\widehat{x} - \mathbf{H}^{\text{inc}}(0) \right\} \quad (2.14)$$

with $\mathbf{X} = \mathbb{R}\widehat{x}$. The first order near-field terms $(\widehat{\mathbf{E}}_1, \widehat{\mathbf{H}}_1)$ are given by

$$\widehat{\mathbf{E}}_1 = \frac{1}{\mathbb{R}^4} \left\{ -\gamma_t(\mathbb{J}_{\mathbf{E}^{\text{inc}}}^{\text{sym}}(0)\widehat{x}) + \frac{3}{2}\gamma_n(\mathbb{J}_{\mathbf{E}^{\text{inc}}}(0)\widehat{x})\widehat{x} \right\} + \frac{i\kappa}{2\mathbb{R}^2} \gamma_\times(\mathbf{H}^{\text{inc}}(0)) \quad (2.15a)$$

$$\widehat{\mathbf{H}}_1 = \frac{1}{\mathbb{R}^4} \left\{ \frac{2}{3}\gamma_t(\mathbb{J}_{\mathbf{H}^{\text{inc}}}^{\text{sym}}(0)\widehat{x}) - \gamma_n(\mathbb{J}_{\mathbf{H}^{\text{inc}}}(0)\widehat{x})\widehat{x} \right\} - \frac{i\kappa}{\mathbb{R}^2} \gamma_\times(\mathbf{E}^{\text{inc}}(0)) \quad (2.15b)$$

The second order near-field terms $(\widehat{\mathbf{E}}_2, \widehat{\mathbf{H}}_2)$ are given by

$$\begin{aligned} \widehat{\mathbf{E}}_2 = \frac{1}{\mathbb{R}^5} \left\{ \frac{2}{3}\gamma_n(\widehat{x}^\top \mathbb{H}_{\mathbf{E}^{\text{inc}}}(0)\widehat{x})\widehat{x} + \frac{2\kappa^2}{15}\gamma_n(\mathbf{E}^{\text{inc}}(0))\widehat{x} - \frac{1}{2}\gamma_t(\widehat{x}^\top \mathbb{H}_{\mathbf{E}^{\text{inc}}}(0)\widehat{x}) \right. \\ \left. - \frac{i\kappa}{3}\gamma_\times(\mathbb{J}_{\mathbf{H}^{\text{inc}}}^{\text{sym}}(0)\widehat{x}) - \frac{\kappa^2}{5}\gamma_t(\mathbf{E}^{\text{inc}}(0)) \right\} + \frac{i\kappa}{3\mathbb{R}^3} \gamma_\times(\mathbb{J}_{\mathbf{H}^{\text{inc}}}(0)\widehat{x}) \\ \left. - \frac{3\kappa^2}{10\mathbb{R}^3} \left\{ \mathbf{E}^{\text{inc}}(0) - 3\gamma_n(\mathbf{E}^{\text{inc}}(0))\widehat{x} \right\} + \frac{\kappa^2}{2\mathbb{R}} \left\{ \mathbf{E}^{\text{inc}}(0) + \gamma_n(\mathbf{E}^{\text{inc}}(0))\widehat{x} \right\} \right\} \quad (2.16a) \end{aligned}$$

and

$$\begin{aligned} \widehat{\mathbf{H}}_2 = \frac{1}{\mathbb{R}^5} \left\{ -\frac{1}{2}\gamma_n(\widehat{x}^\top \mathbb{H}_{\mathbf{H}^{\text{inc}}}(0)\widehat{x})\widehat{x} - \frac{\kappa^2}{10}\gamma_n(\mathbf{H}^{\text{inc}}(0))\widehat{x} + \frac{3}{8}\gamma_t(\widehat{x}^\top \mathbb{H}_{\mathbf{H}^{\text{inc}}}(0)\widehat{x}) \right. \\ \left. - \frac{i\kappa}{4}\gamma_\times(\mathbb{J}_{\mathbf{E}^{\text{inc}}}^{\text{sym}}(0)\widehat{x}) + \frac{3\kappa^2}{20}\gamma_t(\mathbf{H}^{\text{inc}}(0)) \right\} + \frac{i\kappa}{2\mathbb{R}^3} \gamma_\times(\mathbb{J}_{\mathbf{E}^{\text{inc}}}(0)\widehat{x}) \\ \left. + \frac{3\kappa^2}{10\mathbb{R}^3} \left\{ 3\gamma_n(\mathbf{H}^{\text{inc}}(0))\widehat{x} - \mathbf{H}^{\text{inc}}(0) \right\} - \frac{\kappa^2}{4\mathbb{R}} \left\{ \mathbf{H}^{\text{inc}}(0) + \gamma_n(\mathbf{H}^{\text{inc}}(0))\widehat{x} \right\} \right\} \quad (2.16b) \end{aligned}$$

where \mathbb{H}_\diamond denotes the Hessian tensor of \diamond . For $P = 0, 1$ or 2 , let us introduce the vector fields $(\widehat{\mathbf{E}}_{\delta, P}, \widehat{\mathbf{H}}_{\delta, P})$ reading as the sum of the first near-field terms,

$$\widehat{\mathbf{E}}_{\delta, P} = \sum_{p=0}^P \delta^p \widehat{\mathbf{E}}_p; \quad \widehat{\mathbf{H}}_{\delta, P} = \sum_{p=0}^P \delta^p \widehat{\mathbf{H}}_p. \quad (2.17)$$

The following conjecture is a transposition of the numerical results obtained in Section 3.2, which precises the expected order of convergence.

Conjecture 3. For $P = 0, 1$ or 2 , there exist δ_0, R^* satisfying $R^* > \delta_0 > 0$ such that for any R_0 satisfying $1 < R_0 < R^*$, there exists $c > 0$ such that for any positive $\delta < \delta_0$, we have

$$\begin{aligned} \|\mathbf{E}_\delta(\delta \cdot) - \widehat{\mathbf{E}}_{\delta,P}\|_{\infty, \mathcal{C}(1, R_0)} &\leq c \delta^{P+1} \|\mathbf{E}_\delta(\delta \cdot)\|_{\infty, \mathcal{C}(1, R_0)} \\ \|\mathbf{H}_\delta(\delta \cdot) - \widehat{\mathbf{H}}_{\delta,P}\|_{\infty, \mathcal{C}(1, R_0)} &\leq c \delta^{P+1} \|\mathbf{H}_\delta(\delta \cdot)\|_{\infty, \mathcal{C}(1, R_0)} \end{aligned}$$

and

$$\begin{aligned} \|\mathbf{E}_\delta(\delta \cdot) - \widehat{\mathbf{E}}_{\delta,P}\|_{0, \mathcal{C}(1, R_0)} &\leq c \delta^{P+1} \|\mathbf{E}_\delta(\delta \cdot)\|_{0, \mathcal{C}(1, R_0)} \\ \|\mathbf{H}_\delta(\delta \cdot) - \widehat{\mathbf{H}}_{\delta,P}\|_{0, \mathcal{C}(1, R_0)} &\leq c \delta^{P+1} \|\mathbf{H}_\delta(\delta \cdot)\|_{0, \mathcal{C}(1, R_0)} \end{aligned}$$

where $\mathcal{C}(1, R_0) = \{\mathbf{X} \in \mathbb{R}^3, 1 < |\mathbf{X}| < R_0\}$.

Moreover, thanks to the regularity of the analytical solution, we can establish the following conjecture that is a consequence of the previous one.

Conjecture 4. For $P = 0, 1$ or 2 , there exist δ_0, R^* satisfying $R^* > \delta_0 > 0$ such that for any R_0 satisfying $1 < R_0 < R^*$, there exists $c > 0$ such that for any positive $\delta < \delta_0$, we have

$$\|\mathbf{E}_\delta(\delta \cdot) - \widehat{\mathbf{E}}_{\delta,P}\|_{\infty, \mathcal{C}(1, R_0)} \leq c \delta^{P+1}; \quad \|\mathbf{H}_\delta(\delta \cdot) - \widehat{\mathbf{H}}_{\delta,P}\|_{\infty, \mathcal{C}(1, R_0)} \leq c \delta^{P+1}$$

and

$$\|\mathbf{E}_\delta(\delta \cdot) - \widehat{\mathbf{E}}_{\delta,P}\|_{0, \mathcal{C}(1, R_0)} \leq c \delta^{P+\frac{5}{2}}; \quad \|\mathbf{H}_\delta(\delta \cdot) - \widehat{\mathbf{H}}_{\delta,P}\|_{0, \mathcal{C}(1, R_0)} \leq c \delta^{P+\frac{5}{2}}.$$

Remark 7. In the context of the multiple scattering by K spheres, the method of matched asymptotic expansions involves $K + 1$ expansions. Firstly, the far-field expansion is defined in the punctured domain $\mathbb{R}^3 \setminus \bigcup \{c_k\}$ and read as the superposition of the K scattered fields by the isolated obstacles. Our formula have to be translated to deduce the scattered field by an obstacle centered at c_k . In the other hand, the K near-field expansions, that are defined in the k -th fast variable $\mathbf{X}^{(k)} = \frac{\mathbf{x} - c_k}{\delta}$, are living in $\widehat{\Omega}$ again.

2.4 Physical interpretation

This section is based on results of the classical multipole theory in electromagnetism, see for instance [27, 33]. In Appendix A, we introduce the notion of electric and magnetic multipoles and we develop expressions of electromagnetic fields created in the presence of such kind of sources in static and time-harmonic regime. That allows to describe the first terms of the asymptotics in terms of multipoles.

2.4.1 First near-field terms

The zeroth order electric near-field term $\widehat{\mathbf{E}}_0$, given by (2.14), can be represented as an electric field created in the presence of an electric dipole of direction $4\pi \mathbf{E}^{\text{inc}}(0)$, in static regime and the zeroth order magnetic near-field term $\widehat{\mathbf{H}}_0$ as a magnetic field created in the presence of a magnetic dipole of direction $-2\pi \mathbf{H}^{\text{inc}}(0)$ in static regime again. According to (A.6)-(A.16), the zeroth order near-field terms can be put in the compact form

$$\widehat{\mathbf{E}}_0 = \mathbf{E}_{\text{dip}}^{\text{elec}}[4\pi \mathbf{E}^{\text{inc}}(0), \kappa = 0]; \quad \widehat{\mathbf{H}}_0 = \mathbf{H}_{\text{dip}}^{\text{mag}}[-2\pi \mathbf{H}^{\text{inc}}(0), \kappa = 0].$$

The first order electric near-field term $\widehat{\mathbf{E}}_1$ given by (2.15) is represented as a superposition of

- an electric field created in the presence of a filiform magnetic current in a magnetic dipole configuration in static regime, along the direction $-2\pi c \mathbf{curl} \mathbf{E}^{\text{inc}}(0) = -2\pi i\omega \mathbf{H}^{\text{inc}}(0)$, where ω denotes the angular frequency of the incident wave,
- an electric field created in the presence of an electric quadrupole along directions $(\mathbf{u}^E, \mathbf{v}^E)$, in static regime, satisfying the following system of equations

$$\begin{cases} u_i^E v_i^E - u_j^E v_j^E = -\frac{8\pi}{3} (\partial_i E_i^{\text{inc}}(0) - \partial_j E_j^{\text{inc}}(0)) & (i, j) \in \{(1, 2), (2, 3)\} \quad (2.18a) \\ u_i^E v_j^E + u_j^E v_i^E = -\frac{8\pi}{3} (\partial_i E_j^{\text{inc}}(0) + \partial_j E_i^{\text{inc}}(0)) & (i, j) \in \{(1, 2), (2, 3), (3, 1)\} \quad (2.18b) \end{cases}$$

where $\mathbf{u}^E = (u_1^E, u_2^E, u_3^E)$, $\mathbf{v}^E = (v_1^E, v_2^E, v_3^E)$ and $\partial_i E_j^{\text{inc}}$ denotes the i -th partial derivative of the j -th coordinate of \mathbf{E}^{inc} for $i, j = 1, 2, 3$.

The first order magnetic near-field term $\widehat{\mathbf{H}}_1$ given by (2.15) is represented as a superposition of

- a magnetic field created in the presence of a filiform electric current in an electric dipole configuration in static regime, along the direction $-4\pi c \mathbf{curl} \mathbf{H}^{\text{inc}}(0) = 4\pi i\omega \mathbf{E}^{\text{inc}}(0)$,
- a magnetic field created in the presence of a magnetic quadrupole along directions $(\mathbf{u}^H, \mathbf{v}^H)$, in static regime satisfying the following systems of equations

$$\begin{cases} u_i^H v_i^H - u_j^H v_j^H = \frac{16\pi}{9} (\partial_i H_i^{\text{inc}}(0) - \partial_j H_j^{\text{inc}}(0)) & (i, j) \in \{(1, 2), (2, 3)\} \quad (2.19a) \\ u_i^H v_j^H + u_j^H v_i^H = \frac{16\pi}{9} (\partial_i H_j^{\text{inc}}(0) + \partial_j H_i^{\text{inc}}(0)) & (i, j) \in \{(1, 2), (2, 3), (3, 1)\}. \quad (2.19b) \end{cases}$$

where $\partial_i H_j^{\text{inc}}$ denotes the i -th partial derivative of the j -th coordinate of \mathbf{H}^{inc} for $i, j = 1, 2, 3$.

Remark 8. The systems of equations (2.18) and (2.19) have an infinity of complex solutions. Indeed, if (\mathbf{u}, \mathbf{v}) is solution of one of them, then (\mathbf{v}, \mathbf{u}) or $(c\mathbf{u}, \frac{1}{c}\mathbf{v})$ for $c \neq 0$ is also solution. Actually, this formulation is only a physical interpretation and we have not the uniqueness for the quadrupole configuration.

According to (A.7)-(A.18) and (A.17)-(A.11), the first order near-field terms $\widehat{\mathbf{E}}_1$ and $\widehat{\mathbf{H}}_1$ can be put in the compact form

$$\begin{aligned} \widehat{\mathbf{E}}_1 &= \mathbf{E}_{\text{quad}}^{\text{elec}}[\mathbf{u}^E, \mathbf{v}^E, \kappa = 0] + \mathbf{E}_{\text{dip}}^{\text{mag}}[-2\pi i\omega \mathbf{H}^{\text{inc}}(0), \kappa = 0] \\ \widehat{\mathbf{H}}_1 &= \mathbf{H}_{\text{quad}}^{\text{mag}}[\mathbf{u}^H, \mathbf{v}^H, \kappa = 0] + \mathbf{H}_{\text{dip}}^{\text{elec}}[4\pi i\omega \mathbf{E}^{\text{inc}}(0), \kappa = 0]. \end{aligned}$$

Remark 9. The logical consequence is that the second order near-field terms $\widehat{\mathbf{E}}_2$ and $\widehat{\mathbf{H}}_2$ seem like a superposition of octopoles, quadrupoles and dipoles, but we have not performed the whole computation in this document.

2.4.2 First far-field terms

The third order electric far-field term $\widetilde{\mathbf{E}}_3$ can be represented as a superposition of

- an electric field in the presence of a time-harmonic electric dipole along direction $4\pi \mathbf{E}^{\text{inc}}(0)$,
- an electric field in the presence of a time-harmonic magnetic dipole along direction $-2\pi \mathbf{H}^{\text{inc}}(0)$.

The third order magnetic far-field term $\tilde{\mathbf{H}}_3$ can be represented as a superposition of

- a magnetic field in the presence of a time-harmonic magnetic dipole along direction $-2\pi\mathbf{H}^{\text{inc}}(0)$,
- a magnetic field in the presence of a time-harmonic electric dipole along direction $4\pi\mathbf{E}^{\text{inc}}(0)$.

According to (A.12)-(A.20) and (A.19)-(A.13), the third order far-field terms can be put in the compact form

$$\tilde{\mathbf{E}}_3 = \mathbf{E}_{\text{dip}}^{\text{elec}} [4\pi\mathbf{E}^{\text{inc}}(0), \kappa] + \mathbf{E}_{\text{dip}}^{\text{mag}} [-2\pi\mathbf{H}^{\text{inc}}(0), \kappa] \quad (2.20a)$$

$$\tilde{\mathbf{H}}_3 = \mathbf{H}_{\text{dip}}^{\text{elec}} [4\pi\mathbf{E}^{\text{inc}}(0), \kappa] + \mathbf{H}_{\text{dip}}^{\text{mag}} [-2\pi\mathbf{H}^{\text{inc}}(0), \kappa]. \quad (2.20b)$$

Remark 10. In a same way, we can prove that the fifth order far-field terms $\tilde{\mathbf{E}}_5$ and $\tilde{\mathbf{H}}_5$ can be represented as a superposition of dipoles and quadrupoles.

3 Numerical experiments

Numerical experiments allow to make evident the order of convergence of the near-field and far-field expansions that we have assumed in Conjecture 1 and 3. We compare these local approximations with a reference solution computed thanks to Montjoie code [18] into sub-domains independent of δ in the suitable system of coordinates. Moreover, we construct a global approximation of the solution thanks to the near-field and the far-field approximations. However, the numerical order of convergence that we obtained in the comparisons for the global approximation is non-optimal.

3.1 The reference solution

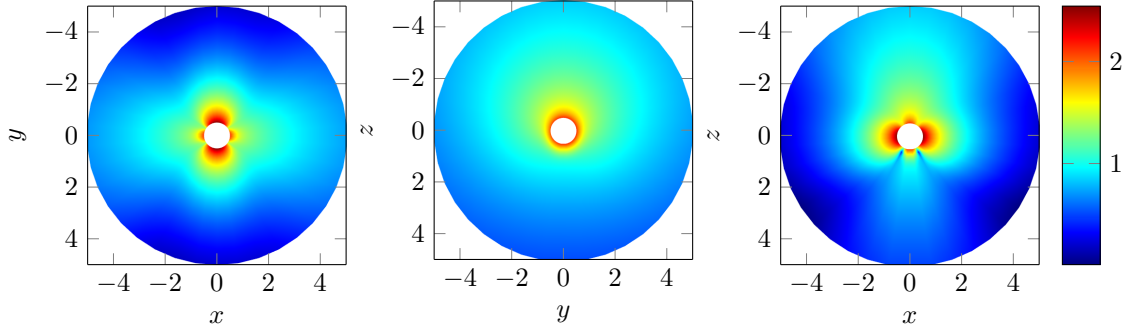
The spherical obstacle is enlightened by an electromagnetic plane wave $(\mathbf{E}^{\text{inc}}, \mathbf{H}^{\text{inc}})$ of wavelength λ defined in (2.3). The wave vector \mathbf{k} and the polarization vector \mathbf{p} are chosen such that

$$\mathbf{k} = \begin{pmatrix} 0 \\ 0 \\ -\kappa \end{pmatrix}; \quad \mathbf{p} = \begin{pmatrix} 1 \\ 0 \\ 0 \end{pmatrix}; \quad \kappa = \frac{2\pi}{\lambda}; \quad \lambda = 5. \quad (3.1)$$

Thereafter, we investigate the numerical order of convergence of the far-field and near-field approximations. The norms used in the comparison are the Sobolev norm \mathbf{L}^2 and the uniform norm \mathbf{L}^∞ of the difference between the reference solution and our approximations, into some domains of interest. To obtain the data, we calculate

- the reference solution $(\mathbf{E}_\delta^{\text{ref}}, \mathbf{H}_\delta^{\text{ref}})$ that is an analytical solution computed with Montjoie,
- the near-field approximation $(\hat{\mathbf{E}}_{\delta,P}, \hat{\mathbf{H}}_{\delta,P})$ or the far-field approximation $(\tilde{\mathbf{E}}_{\delta,P+3}, \tilde{\mathbf{H}}_{\delta,P+3})$ for $P = 0, 1$ or 2 , from (2.17) and (2.10),
- the absolute errors $\|\mathbf{E}_\delta^{\text{ref}} - \diamond\|$ and $\|\mathbf{H}_\delta^{\text{ref}} - \diamond\|$ or the relative errors $\|\mathbf{E}_\delta^{\text{ref}} - \diamond\|/\|\mathbf{E}_\delta^{\text{ref}}\|$ and $\|\mathbf{H}_\delta^{\text{ref}} - \diamond\|/\|\mathbf{H}_\delta^{\text{ref}}\|$ computed in the spherical coordinates using a Riemann sum for angles θ and φ and a trapezoidal rule for radius r ,

for a range of δ between 10^0 and 10^{-4} . In Figure 2, we draw cross sections of the x -coordinates of the reference electric field $\mathbf{E}_\delta^{\text{ref}}$ in a logarithmic scale in base 10, for $\delta = 0.5$.


 Figure 2: Cross sections of the x -coordinates of the scattered electric field in a logarithmic scale

3.2 Near-field approximation

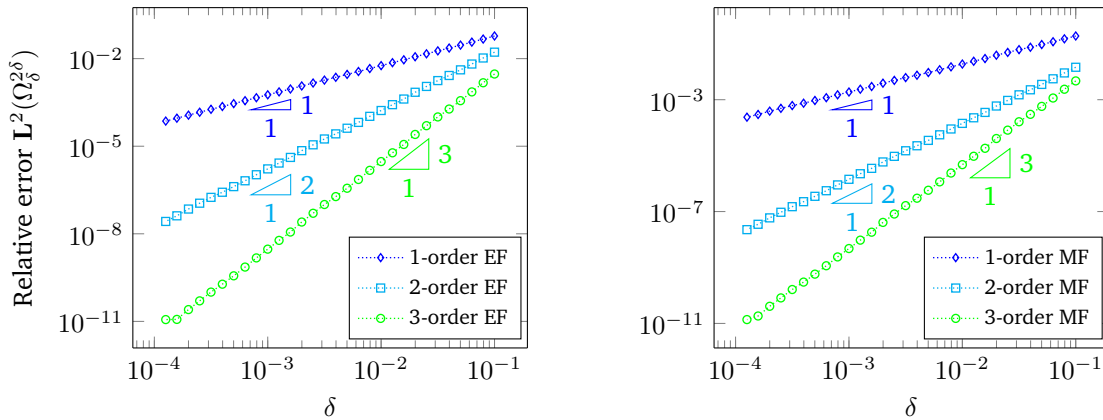
To illustrate the convergence results given by the near-field approximations, we introduce a subspace of $\widehat{\Omega}$ independent of δ in the fast variable,

$$\Omega_\delta^{2\delta} = \mathcal{B}(0, 2\delta) \setminus \overline{\mathcal{B}(0, \delta)}. \quad (3.2)$$

For the results in Figures 3 and 4, we investigate the numerical order of convergence for the \mathbf{L}^2 and \mathbf{L}^∞ norms of the near-field approximations into the domain $\Omega_\delta^{2\delta}$ with respect to the size of the obstacles δ such that

$$\delta \in \left\{ \frac{1}{10^p}, p = 1 : 0.1 : 4 \right\}. \quad (3.3)$$

Figure 3 makes evident the different orders of convergence for the near-field approximations $(\widehat{\mathbf{E}}_{\delta,0}, \widehat{\mathbf{H}}_{\delta,0})$, $(\widehat{\mathbf{E}}_{\delta,1}, \widehat{\mathbf{H}}_{\delta,1})$ and $(\widehat{\mathbf{E}}_{\delta,2}, \widehat{\mathbf{H}}_{\delta,2})$, using the \mathbf{L}^2 norm into the domain $\Omega_\delta^{2\delta}$. Figure 4 shows


 Figure 3: Relative \mathbf{L}^2 -errors for near-field approximations of the electric and magnetic fields

the same analysis but in the \mathbf{L}^∞ norm in the domain $\Omega_\delta^{2\delta}$.

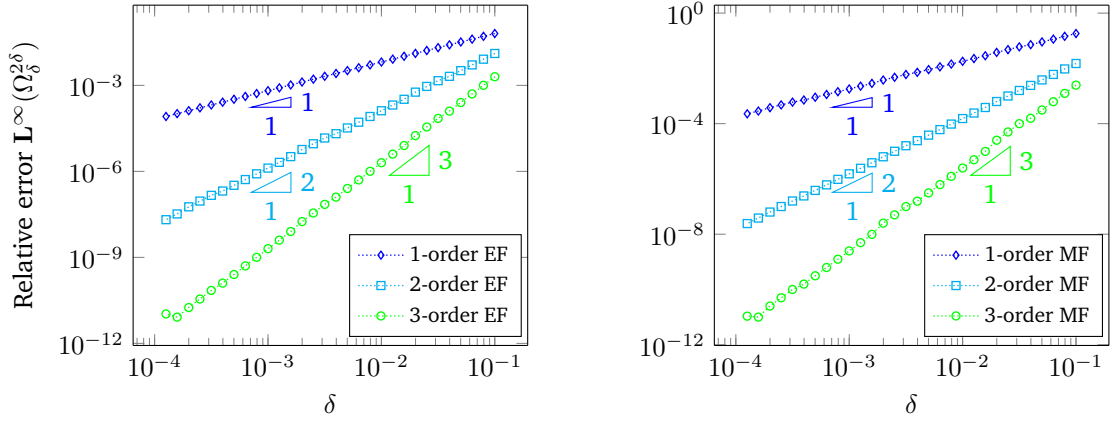


Figure 4: Relative L^∞ -errors for near-field approximations of the electric and magnetic fields

3.3 Far-field approximation

To illustrate the convergence results given by the far-field approximations, we introduce a subspace independent of δ ,

$$\Omega_\lambda^{2\lambda} = \mathcal{B}(0, 2\lambda) \setminus \overline{\mathcal{B}(0, \lambda)}. \quad (3.4)$$

For the results in Figures 5 and 6, we investigate the numerical order of convergence for the L^2 and L^∞ norms of the far-field approximation into the domain $\Omega_\lambda^{2\lambda}$ with respect to the size δ of the obstacles such that

$$\delta \in \left\{ \frac{1}{10^p}, p = 0.5 : 0.1 : 3.1 \right\}. \quad (3.5)$$

Figure 5 makes evident the different orders of convergence for the far-field approximation $(\delta^3 \tilde{\mathbf{E}}_3, \delta^3 \tilde{\mathbf{H}}_3)$, using the L^2 norm into the domain $\Omega_\lambda^{2\lambda}$. Figure 6 shows the same analysis but

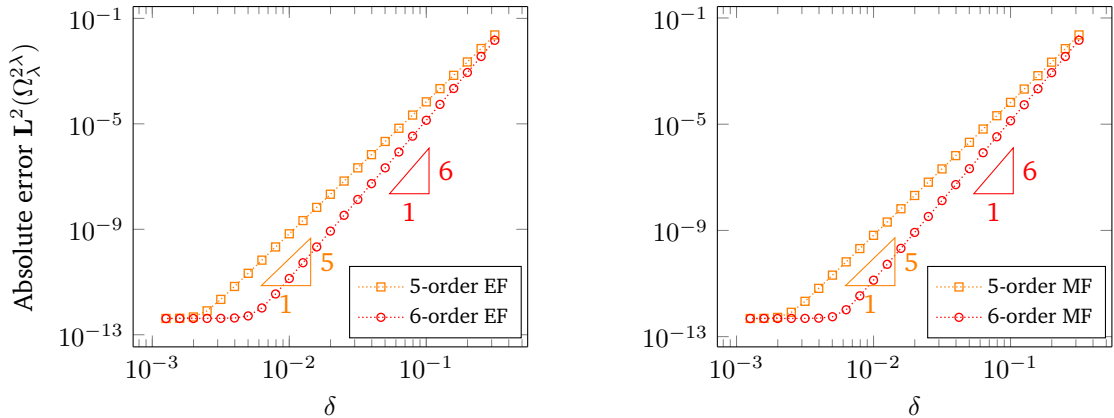
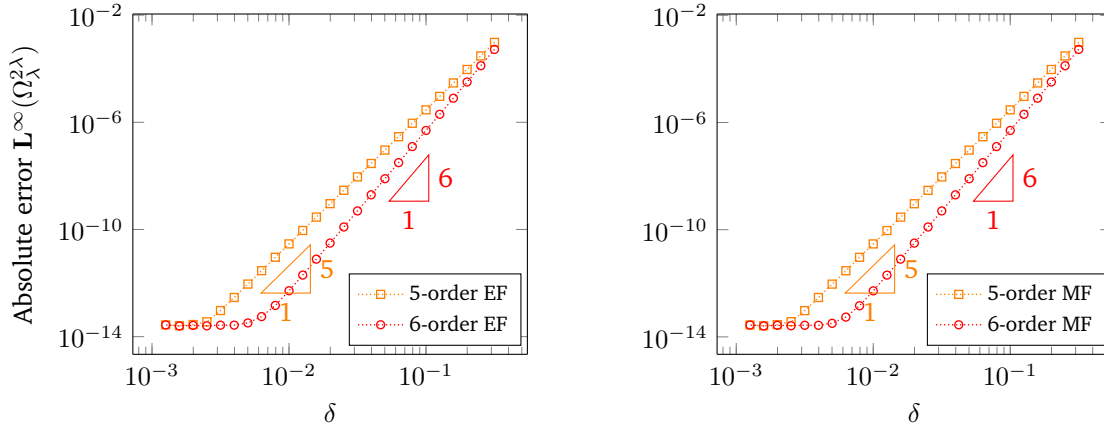


Figure 5: Absolute L^2 -errors for far-field approximations of the electric and magnetic fields

in the L^∞ norm into the domain $\Omega_\lambda^{2\lambda}$.

Figure 6: Absolute L^∞ -errors for far-field approximations of the electric and magnetic fields

3.4 A global approximation

From the local approximations $(\tilde{\mathbf{E}}_{\delta,P+3}, \tilde{\mathbf{H}}_{\delta,P+3})$ and $(\hat{\mathbf{E}}_{\delta,P}, \hat{\mathbf{H}}_{\delta,P})$ given by Equations (2.12) and (2.17) for $P = 0, 1$ and 2 , the derivation of a global approximation into the whole bounded domain

$$\Omega_\delta^\lambda = \{\mathbf{x} \in \mathbb{R}^3, \delta < |\mathbf{x}| < \lambda\} \quad (3.6)$$

goes through a combination of these both data. We introduce the sub-domains $\Omega_{\delta,\lambda}^F$ and Ω_δ^N of Ω_δ^λ , related to the validity of the far-field and near-field expansions, see Remarks 13 and 17,

$$\Omega_{\delta,\lambda}^F = \{\mathbf{x} \in \mathbb{R}^3, 2\sqrt{\lambda\delta} < |\mathbf{x}| < \lambda\}; \quad \Omega_\delta^N = \{\mathbf{x} \in \mathbb{R}^3, \delta < |\mathbf{x}| < \sqrt{\lambda\delta}\}. \quad (3.7)$$

A global approximation $(\mathbf{E}_{\delta,P}, \mathbf{H}_{\delta,P})$ for $P = 0, 1$ or 2 is then given by

- $(\mathbf{E}_{\delta,P}, \mathbf{H}_{\delta,P}) = (\hat{\mathbf{E}}_{\delta,P}, \hat{\mathbf{H}}_{\delta,P})$ in Ω_δ^N ,
- $(\mathbf{E}_{\delta,P}, \mathbf{H}_{\delta,P}) = (\tilde{\mathbf{E}}_{\delta,P+3}, \tilde{\mathbf{H}}_{\delta,P+3})$ in $\Omega_{\delta,\lambda}^F$,
- a combination of the two data in the matching area $\{\mathbf{x} \in \mathbb{R}^3, \sqrt{\lambda\delta} < |\mathbf{x}| < 2\sqrt{\lambda\delta}\}$.

We consider a cut-off smooth function $\chi_\delta : \mathbb{R}^+ \mapsto [0, 1]$ which is equal to 1 in neighborhood of the obstacle and equal to 0 far from the obstacle, in terms of distance. In these numerical experiments we choose $\chi_\delta = \chi(\frac{\cdot}{\sqrt{\lambda\delta}})$ where χ is such that

$$\chi \in \mathcal{C}^\infty(\mathbb{R}); \quad \chi(r) = \begin{cases} 1 & \text{if } r \leq 1 \\ 0 & \text{if } r \geq 2 \end{cases}; \quad \chi'(r) \leq 0 \text{ for any } r \geq 0. \quad (3.8)$$

A global approximation $(\mathbf{E}_{\delta,P}, \mathbf{H}_{\delta,P})$ of order $P = 0, 1$ and 2 is then defined for $\mathbf{x} \in \Omega_\delta^\lambda$ by

$$\begin{cases} \mathbf{E}_{\delta,P}(\mathbf{x}) = \chi_\delta(|\mathbf{x}|)\hat{\mathbf{E}}_{\delta,P}(\frac{\mathbf{x}}{\delta}) + (1 - \chi_\delta(|\mathbf{x}|))\tilde{\mathbf{E}}_{\delta,P+3}(\mathbf{x}) & (3.9a) \\ \mathbf{H}_{\delta,P}(\mathbf{x}) = \chi_\delta(|\mathbf{x}|)\hat{\mathbf{H}}_{\delta,P}(\frac{\mathbf{x}}{\delta}) + (1 - \chi_\delta(|\mathbf{x}|))\tilde{\mathbf{H}}_{\delta,P+3}(\mathbf{x}). & (3.9b) \end{cases}$$

Remark 11. The choices of the sub-domains Ω_δ^N and $\Omega_{\delta,\lambda}^F$ as well as the cut-off function χ_δ are non-optimal to make evident the order of convergence of the global approximation in the whole bounded domain Ω_δ^λ . Actually, the dependence on $\sqrt{\delta}$ in the sub-domains creates a factor scale in the error computation. Error estimates would enable to quantify this dependence.

For the results in Figure 7, we investigate the numerical order of convergence for the \mathbf{L}^2 and \mathbf{L}^∞ norms in the whole bounded domain Ω_δ^λ with respect to the size of the obstacles δ such that

$$\delta \in \left\{ \frac{1}{10^p}, p = 1 : 0.1 : 4 \right\}. \quad (3.10)$$

Figure 7 makes evident the different orders of convergence for the global approximations $(\mathbf{E}_{\delta,0}, \mathbf{H}_{\delta,0})$, $(\mathbf{E}_{\delta,1}, \mathbf{H}_{\delta,1})$ and $(\mathbf{E}_{\delta,2}, \mathbf{H}_{\delta,2})$, using the \mathbf{L}^2 norm in the whole bounded domain Ω_δ^λ for the electric and magnetic fields.

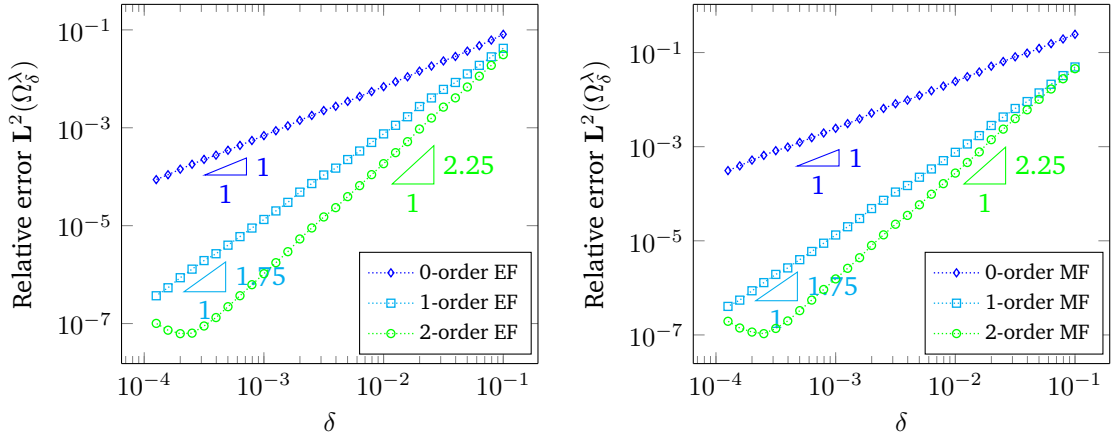


Figure 7: Relative \mathbf{L}^2 -errors for global approximations of the electric and magnetic fields

Remark 12. By virtue of Remark 11, the order of convergence is non-optimal for $(\mathbf{E}_{\delta,1}, \mathbf{H}_{\delta,1})$ and $(\mathbf{E}_{\delta,2}, \mathbf{H}_{\delta,2})$. We observe that the order is degrading between the first and the second order approximations.

4 The matched asymptotic expansions

In this section, we apply the method of matched asymptotic expansions to tackle the exterior time-harmonic Maxwell problem (2.6). Assuming that the obstacle size δ is significantly small in comparison with the incident wavelength $\lambda = \frac{2\pi}{\kappa}$, this method consists in defining an approximate solution using multi-scale expansions over far and near fields, related in a matching area. We introduce the geometrical setting, the problems satisfied by any term of the asymptotics at any order and the matching conditions applied on spectral coefficients. It is only in the last section that we focus on the first terms of the asymptotics.

4.1 Geometrical setting

Before postulating *Ansatz* of the far and near field expansions, we define the asymptotic domains where the expansions will be defined. The far-field domain Ω_δ^F is the exterior domain defined by

$$\Omega_\delta^F = \{\mathbf{x} \in \mathbb{R}^3, |\mathbf{x}| > \eta_\delta^F\} \quad \text{with } \lim_{\delta \rightarrow 0} \eta_\delta^F = 0. \quad (4.1)$$

The far-field expansion is then defined in Ω^* that is the limit of the far-field domain when δ tends to 0, see Figure 8,

$$\Omega^* = \lim_{\delta \rightarrow 0} \Omega_\delta^F = \mathbb{R}^3 \setminus \{0\}. \quad (4.2)$$

The definition of the near-field domain Ω_δ^N goes through the coordinate change $\mathbf{X} = \frac{\mathbf{x}}{\delta}$. Then, Ω_δ^N is the interior domain defined in fast variable by

$$\Omega_\delta^N = \{\mathbf{X} \in \mathbb{R}^3, \delta < \delta|\mathbf{X}| < \eta_\delta^N\} \quad \text{with } \lim_{\delta \rightarrow 0} \frac{\eta_\delta^N}{\delta} = +\infty. \quad (4.3)$$

The near-field expansion is then defined in $\widehat{\Omega}$ that is the near-field domain when δ tends to 0, see Figure 8 ,

$$\widehat{\Omega} = \lim_{\delta \rightarrow 0} \Omega_\delta^N = \mathbb{R}^3 \setminus \overline{\mathcal{B}(0, 1)}. \quad (4.4)$$

4.2 Far-field expansion

Far from the obstacle, the exact solution is approximated by the far-field expansion

$$\mathbf{E}_\delta(\mathbf{x}) \underset{\delta \rightarrow 0}{\sim} \sum_{p=0}^{\infty} \delta^p \widetilde{\mathbf{E}}_p(\mathbf{x}); \quad \mathbf{H}_\delta(\mathbf{x}) \underset{\delta \rightarrow 0}{\sim} \sum_{p=0}^{\infty} \delta^p \widetilde{\mathbf{H}}_p(\mathbf{x}) \quad (4.5)$$

where $\mathbf{x} = r\hat{x}$ is the spatial variable in spherical coordinates. This expansion begins at the third order since all previous terms are reduced to null-fields, see Remark 18. The set of $(\widetilde{\mathbf{E}}_p, \widetilde{\mathbf{H}}_p)$ with $p \geq 3$ is *singular* solution, reading as (B.18), of the time-harmonic Maxwell equations in Ω^* given by (4.2),

$$\begin{cases} \mathbf{curl} \widetilde{\mathbf{E}}_p - i\kappa \widetilde{\mathbf{H}}_p = 0 & \text{in } \Omega^* & (4.6a) \\ \mathbf{curl} \widetilde{\mathbf{H}}_p + i\kappa \widetilde{\mathbf{E}}_p = 0 & \text{in } \Omega^* & (4.6b) \\ \lim_{r \rightarrow \infty} r(\widetilde{\mathbf{H}}_p \times \hat{x} - \widetilde{\mathbf{E}}_p) = 0 & \text{uniformly in } \hat{x}. & (4.6c) \end{cases}$$

These problems are ill-posed in $\mathbf{H}_{\text{loc}}(\mathbf{curl}, \Omega^*)$ which is the space of vector fields \mathbf{u} such that

$$\forall \psi \in \mathcal{C}_c^\infty(\mathbb{R}^3), \psi = 0 \text{ in a neighbourhood of } 0, \psi \mathbf{u} \in \mathbf{L}^2(\mathbb{R}^3), \mathbf{curl}(\psi \mathbf{u}) \in \mathbf{L}^2(\mathbb{R}^3), \quad (4.7)$$

because it lacks a piece of information about their behavior at the origin. Actually, the terms $(\widetilde{\mathbf{E}}_p, \widetilde{\mathbf{H}}_p)$ are finite sums of multipoles that are explicitly known up to their spectral coefficients [30]. Obtaining these coefficients allows to define the far-field asymptotic expansion at any order.

Remark 13. The far-field expansion is defined in Ω^* but is a suitable approximation of the solution into the exterior domains Ω_δ^F , see (4.1). The proof goes through error estimates. For the numerical results in Section 3.4, we have chosen $\eta_\delta^F = (\delta\lambda)^{\frac{1}{2}}$.

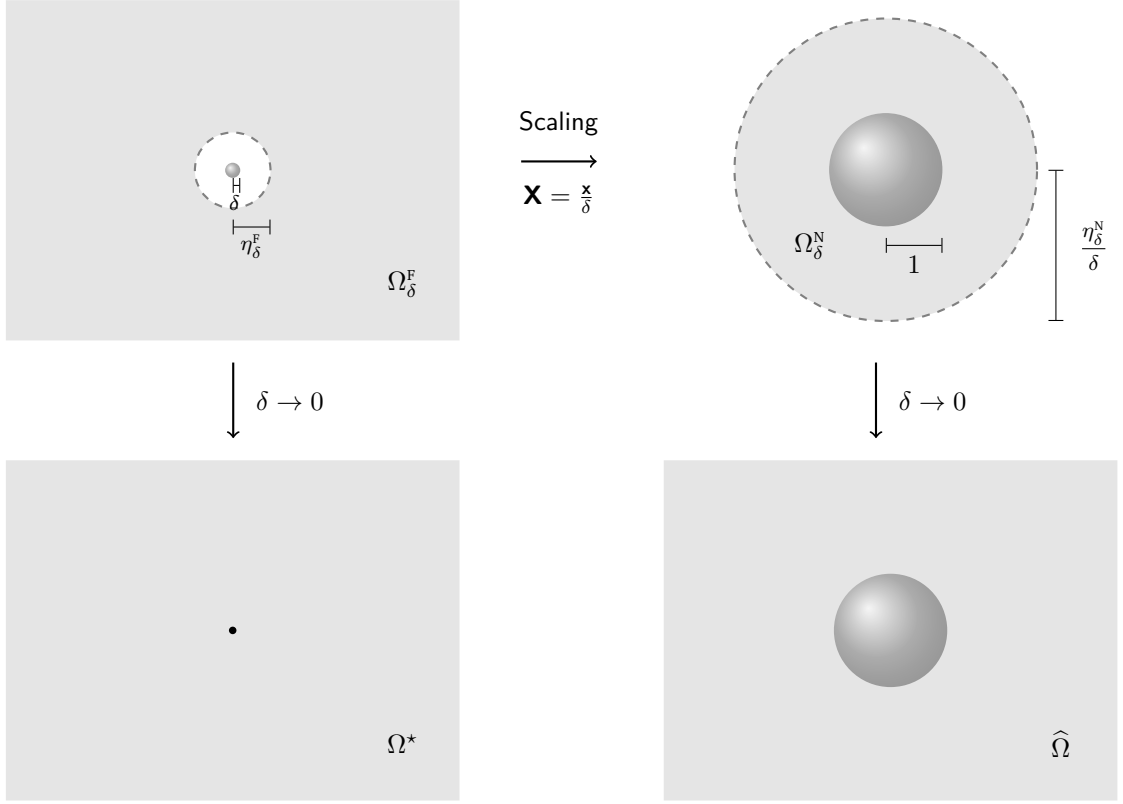


Figure 8: Far-field and near-field domains Ω_δ^F and Ω_δ^N and their limit Ω^* and $\widehat{\Omega}$

4.3 Near-field expansion

In the vicinity of the obstacle, the solution can be approximated by the near-field expansion

$$\mathbf{E}_\delta(\delta\mathbf{X}) \underset{\delta \rightarrow 0}{\sim} \sum_{p=0}^{\infty} \delta^p \widehat{\mathbf{E}}_p(\mathbf{X}); \quad \mathbf{H}_\delta(\delta\mathbf{X}) \underset{\delta \rightarrow 0}{\sim} \sum_{p=0}^{\infty} \delta^p \widehat{\mathbf{H}}_p(\mathbf{X}) \quad (4.8)$$

where $\mathbf{X} = \frac{\mathbf{x}}{\delta} = R\widehat{x}$ is the fast variable in spherical coordinates. The set of $(\widehat{\mathbf{E}}_p, \widehat{\mathbf{H}}_p)$ for $p \geq 0$ satisfies the nested Maxwell equations given by

$$\begin{cases} \operatorname{curl} \widehat{\mathbf{E}}_p = i\kappa \widehat{\mathbf{H}}_{p-1} & \text{in } \widehat{\Omega} \\ \operatorname{curl} \widehat{\mathbf{H}}_p = -i\kappa \widehat{\mathbf{E}}_{p-1} & \text{in } \widehat{\Omega} \end{cases} \quad (4.9a)$$

$$\quad (4.9b)$$

where $\widehat{\Omega}$ is defined in (4.4). In (4.9), we use the convention $\widehat{\mathbf{E}}_{-1} = \widehat{\mathbf{H}}_{-1} = 0$.

Remark 14. These equations are said *nested* because the problem of order p depends on the previous term, of order $p-1$. They can be read as Maxwell static problems with a non-homogeneous source term. Moreover, we can deduce from the problem of order $p+1$, complementary equations

for the divergence of the fields of order p , that are

$$\begin{cases} \operatorname{div} \widehat{\mathbf{E}}_p = 0 & \text{in } \widehat{\Omega} \\ \operatorname{div} \widehat{\mathbf{H}}_p = 0 & \text{in } \widehat{\Omega}. \end{cases} \quad (4.10a)$$

$$\quad (4.10b)$$

The boundary conditions are obtained by identifying the Taylor series expansion of the incident field in a neighborhood of the origin in the fast variable $\mathbf{X} = \frac{\mathbf{x}}{\delta}$,

$$\mathbf{E}^{\text{inc}}(\mathbf{x}) = \sum_{p=0}^{\infty} \delta^p \widehat{\mathbf{E}}_p^{\text{inc}}(\mathbf{X}); \quad \mathbf{H}^{\text{inc}}(\mathbf{x}) = \sum_{p=0}^{\infty} \delta^p \widehat{\mathbf{H}}_p^{\text{inc}}(\mathbf{X}) \quad (4.11)$$

where

$$\widehat{\mathbf{E}}_p^{\text{inc}}(\mathbf{X}) = \sum_{|\alpha|=p} \frac{1}{\alpha!} \mathbf{d}^\alpha \mathbf{E}^{\text{inc}}(0) \cdot \mathbf{X}^\alpha; \quad \widehat{\mathbf{H}}_p^{\text{inc}}(\mathbf{X}) = \sum_{|\alpha|=p} \frac{1}{\alpha!} \mathbf{d}^\alpha \mathbf{H}^{\text{inc}}(0) \cdot \mathbf{X}^\alpha, \quad (4.12)$$

with the boundary conditions satisfied by the near-field expansion. In particular, on the boundary $\partial\widehat{\Omega} = \mathcal{S}^2 = \widehat{\Gamma}$, we have

$$\begin{cases} \mathbf{e}_r \times \widehat{\mathbf{E}}_p = -\mathbf{e}_r \times \widehat{\mathbf{E}}_p^{\text{inc}} & \text{on } \widehat{\Gamma} \\ \mathbf{e}_r \cdot \widehat{\mathbf{H}}_p = -\mathbf{e}_r \cdot \widehat{\mathbf{H}}_p^{\text{inc}} & \text{on } \widehat{\Gamma}. \end{cases} \quad (4.13a)$$

$$\quad (4.13b)$$

Remark 15. The terms of order p depend on the zero value of the p -order derivative of the incident field.

The nested problems made up of the equations (4.9), (4.10) and (4.13) are ill-posed in the weighted Sobolev space \mathbf{W} defined by

$$\mathbf{W} = \left\{ \frac{\mathbf{u}}{(1 + R^2)^{\frac{1}{2}}} \in \mathbf{L}^2(\widehat{\Omega}), \operatorname{curl} \mathbf{u} \in \mathbf{L}^2(\widehat{\Omega}), \operatorname{div} \mathbf{u} = 0 \text{ in } \widehat{\Omega} \right\} \quad (4.14)$$

because it lacks a piece of information about the behavior of the *non-leading* terms towards the infinity.

Remark 16. The problem made up of the equations (4.9), (4.10) and (4.13) with $p = 0$ satisfied by $(\widehat{\mathbf{E}}_0, \widehat{\mathbf{H}}_0)$, is well-posed in the space \mathbf{W} . The terms $(\widehat{\mathbf{E}}_p, \widehat{\mathbf{H}}_p)$ for $p > 0$ can be described as a superposition of a regular solution $(\widehat{\mathbf{E}}_{p,0}, \widehat{\mathbf{H}}_{p,0})$ in \mathbf{W} of the homogeneous static Maxwell equations and a finite sum of growing vector fields, that are the non-leading terms, which are particular solutions of the nested equations and satisfying

$$\max_{|\mathbf{X}|=R} \left| \widehat{\mathbf{E}}_p(\mathbf{X}) - \widehat{\mathbf{E}}_{p,0}(\mathbf{X}) \right| = O(R^{p-3}); \quad \max_{|\mathbf{X}|=R} \left| \widehat{\mathbf{H}}_p(\mathbf{X}) - \widehat{\mathbf{H}}_{p,0}(\mathbf{X}) \right| = O(R^{p-3}). \quad (4.15)$$

These singularities also called *shadows* terms are produced by previous near-field terms. Then, the near-field problems can be solved by induction, where the computation of the shadows goes through previous terms and the computation of the leading term is done by solving a well-posed problem in \mathbf{W} .

Remark 17. The near-field expansion is defined in $\widehat{\Omega}$ but is a suitable approximation of the solution into the bounded domains Ω_δ^N , see (4.3). The proof goes through error estimates. For the numerical results in Section 3.4, we have chosen $\eta_\delta^N = 2(\delta\lambda)^{\frac{1}{2}}$.

4.4 Matching conditions

The far-field and near-field expansions are related thanks to a matching procedure which requires the behavior of $(\tilde{\mathbf{E}}_p, \tilde{\mathbf{H}}_p)$ close to the origin and the behavior of $(\hat{\mathbf{E}}_p, \hat{\mathbf{H}}_p)$ towards the infinity. In a formal way, for $p \geq 0$ we develop $(\tilde{\mathbf{E}}_p, \tilde{\mathbf{H}}_p)$ in a neighborhood of the origin as

$$\tilde{\mathbf{E}}_p(r\hat{x}) \underset{r \rightarrow 0}{\sim} \sum_{q=-\infty}^{+\infty} (\kappa r)^q \tilde{\mathbf{E}}_p^q(\hat{x}); \quad \tilde{\mathbf{H}}_p(r\hat{x}) \underset{r \rightarrow 0}{\sim} \sum_{q=-\infty}^{+\infty} (\kappa r)^q \tilde{\mathbf{H}}_p^q(\hat{x}) \quad (4.16)$$

and $(\hat{\mathbf{E}}_p, \hat{\mathbf{H}}_p)$ with fast variable $R = \frac{r}{\delta}$ in a neighborhood of infinity as

$$\hat{\mathbf{E}}_p(R\hat{x}) \underset{R \rightarrow +\infty}{\sim} \sum_{q=-\infty}^{+\infty} (\kappa R)^q \hat{\mathbf{E}}_p^q(\hat{x}); \quad \hat{\mathbf{H}}_p(R\hat{x}) \underset{R \rightarrow +\infty}{\sim} \sum_{q=-\infty}^{+\infty} (\kappa R)^q \hat{\mathbf{H}}_p^q(\hat{x}). \quad (4.17)$$

The two expansions are matched in the overlap area by using Equations (4.5), (4.8), (4.16) and (4.17). Then, the matching conditions read as

$$\begin{cases} (\tilde{\mathbf{E}}_p^q, \tilde{\mathbf{H}}_p^q) = (\hat{\mathbf{E}}_{p+q}^q, \hat{\mathbf{H}}_{p+q}^q) & -p \leq q < 0 \\ (\tilde{\mathbf{E}}_p^q, \tilde{\mathbf{H}}_p^q) = 0 & p < 0 \text{ or } q < -p. \end{cases} \quad (4.18a) \quad (4.18b)$$

These relations allow to determine entirely far-field terms. This step is formally expressed but fundamental to the justification of the approximate models. Modal decomposition of the solutions allow to define the angular terms $(\tilde{\mathbf{E}}_p^q, \tilde{\mathbf{H}}_p^q)$ and $(\hat{\mathbf{E}}_p^q, \hat{\mathbf{H}}_p^q)$ and make explicit these conditions through the spectral coefficients.

Proposition 1. *The formal matching conditions (4.18) are equivalent to*

$$\begin{cases} u_{n,m}^{(p),\times} = \frac{\kappa^{n+2}}{i n \mathfrak{h}_{n,-n-1}} \hat{h}_{n,m}^{(p-n-2)} & (4.19a) \\ u_{n,m}^{(p),t} = \frac{\kappa^{n+2}}{i n \mathfrak{h}_{n,-n-1}} \hat{e}_{n,m}^{(p-n-2)} & (4.19b) \end{cases}$$

for any $p \geq 0$, $n \geq 1$ and $-n \leq m \leq n$. The coefficients $u_{n,m}^{(p),\times}$ and $u_{n,m}^{(p),t}$ are from the modal decomposition (B.18)-(B.19) of the far-field terms $(\tilde{\mathbf{E}}_p, \tilde{\mathbf{H}}_p)$. The coefficients $\hat{e}_{n,m}^{(p-n-2)}$ and $\hat{h}_{n,m}^{(p-n-2)}$ are from the modal decomposition (B.21)-(B.22) of the regular part of the near-field terms $(\hat{\mathbf{E}}_{p-n-2,0}, \hat{\mathbf{H}}_{p-n-2,0})$. The coefficients $\mathfrak{h}_{n,\ell}$ come from the Laurent series expansion of the Hankel function of the first kind $h_n^{(1)}$, see Proposition 3.

Remark 18. The coefficients $u_{n,m}^{(p),\times}$ and $u_{n,m}^{(p),t}$ are equal to 0 when $p < 3$. That implies that the asymptotic far-field expansion starts at the third order.

Proof. Injecting expansions (B.20) of modal coefficients $\tilde{\diamond}_{n,m}^{(p),\times}$, $\tilde{\diamond}_{n,m}^{(p),t}$ and $\tilde{\diamond}_{n,m}^{(p),r}$ for $\diamond = e$ or h into the modal decomposition (B.18), we obtain the expansion in the vicinity of the origin of the far-field terms

$$\tilde{\mathbf{E}}_p = \sum_{q=-\infty}^{\infty} (\kappa r)^q \tilde{\mathbf{E}}_p^q(\hat{x}); \quad \tilde{\mathbf{H}}_p = \sum_{q=-\infty}^{\infty} (\kappa r)^q \tilde{\mathbf{H}}_p^q(\hat{x}),$$

where the angular coefficients $(\tilde{\mathbf{E}}_p^q, \tilde{\mathbf{H}}_p^q)$ are given by

$$\begin{aligned}\tilde{\mathbf{E}}_p^q &= \sum_{n=1}^{\infty} \sum_{m=-n}^n u_{n,m}^{\times} \mathfrak{h}_{n,q} \mathbf{curl}_{S^2} Y_{n,m} + u_{n,m}^t \frac{\mathfrak{h}_{n,q+1}}{i} \left[(q+2) \nabla_{S^2} Y_{n,m} + n(n+1) Y_{n,m} \mathbf{e}_r \right] \\ \tilde{\mathbf{H}}_p^q &= \sum_{n=1}^{\infty} \sum_{m=-n}^n -u_{n,m}^t \mathfrak{h}_{n,q} \mathbf{curl}_{S^2} Y_{n,m} + u_{n,m}^{\times} \frac{\mathfrak{h}_{n,q+1}}{i} \left[(q+2) \nabla_{S^2} Y_{n,m} + n(n+1) Y_{n,m} \mathbf{e}_r \right].\end{aligned}$$

On the other hand, injecting coefficients $\hat{\diamond}_{n,m}^{(p),\times}$, $\hat{\diamond}_{n,m}^{(p),t}$ and $\hat{\diamond}_{n,m}^{(p),r}$ for $\diamond = e$ or h into the modal decompositions of $(\hat{\mathbf{E}}_p, \hat{\mathbf{H}}_p)$, see Proposition 4, and making the index change $q = \ell - n - 2$, we obtain

$$\hat{\mathbf{E}}_p = \sum_{q=-\infty}^{\infty} (\kappa R)^q \hat{\mathbf{E}}_p^q(\hat{x}); \quad \hat{\mathbf{H}}_p = \sum_{q=-\infty}^{\infty} (\kappa R)^q \hat{\mathbf{H}}_p^q(\hat{x})$$

where the angular coefficients $(\hat{\mathbf{E}}_p^q, \hat{\mathbf{H}}_p^q)$ are given by

$$\begin{aligned}\hat{\mathbf{E}}_p^q &= \sum_{n=1}^{\infty} \sum_{m=-n}^n \left(-i\kappa^{n+2} \frac{1}{n \mathfrak{h}_{n,-n-1}} \hat{h}_{n,m}^{(p-q-n-2)} \right) \mathfrak{h}_{n,q} \mathbf{curl}_{S^2} Y_{n,m} \\ &\quad + \left(-i\kappa^{n+2} \frac{1}{n \mathfrak{h}_{n,-n-1}} \hat{e}_{n,m}^{(p-q-n-2)} \right) \frac{\mathfrak{h}_{n,q+1}}{i} \left[(q+2) \nabla_{S^2} Y_{n,m} + n(n+1) Y_{n,m} \mathbf{e}_r \right] \\ \hat{\mathbf{H}}_p^q &= \sum_{n=1}^{\infty} \sum_{m=-n}^n \left(i\kappa^{n+2} \frac{1}{n \mathfrak{h}_{n,-n-1}} \hat{h}_{n,m}^{(p-q-n-2)} \right) \mathfrak{h}_{n,q} \mathbf{curl}_{S^2} Y_{n,m} \\ &\quad + \left(-i\kappa^{n+2} \frac{1}{n \mathfrak{h}_{n,-n-1}} \hat{h}_{n,m}^{(p-q-n-2)} \right) \frac{\mathfrak{h}_{n,q+1}}{i} \left[(q+2) \nabla_{S^2} Y_{n,m} + n(n+1) Y_{n,m} \mathbf{e}_r \right].\end{aligned}$$

Finally, according to the matching conditions (4.18), we deduce (4.19). \square

Remark 19. The conditions (4.19) give us some pieces of information about the asymptotic expansions. Since we have assumed that the near-field expansion starts at the zeroth order, the coefficients $\hat{e}_{n,m}^{(p)}$ and $\hat{h}_{n,m}^{(p)}$ associated to an order $p < 0$ are equal to zero. In particular, conditions (4.19) imply that the coefficients $u_{n,m}^{(p),\times}$ and $u_{n,m}^{(p),t}$ are equal to zero when $n > p - 2$. Then, the modal decomposition (B.18) for the far-field of order $p \geq 3$ is a finite sum of multipoles which needs the knowledge of the near-field terms of order p' such that $0 \leq p' \leq p - 3$ to be calculated.

4.5 First terms of the asymptotics

In this section, we introduce the problems satisfied by the first terms of the asymptotics and we make explicit these terms. The near-field problems are solved by induction because the calculation of the near-field term of order p requires the knowledge of the previous near-field terms. In Figure 9, we illustrate the construction of the first near-field terms, where the arrows describe the different contributions in order to compute the current term.

Remark 20. The construction of the near-field terms does not depend on the far-field terms.

The far-field terms are found through their modal decomposition given by (B.18) where the series are actually finite sums going up to $n = p - 2$. In Figure 10, we illustrate the algorithm to construct the far-field terms.

Hereafter, we make explicit the near-field terms $(\hat{\mathbf{E}}_p, \hat{\mathbf{H}}_p)$ for $p = 0, 1, 2$ and the far-field terms $(\tilde{\mathbf{E}}_p, \tilde{\mathbf{H}}_p)$ for $p = 3, 4, 5$.

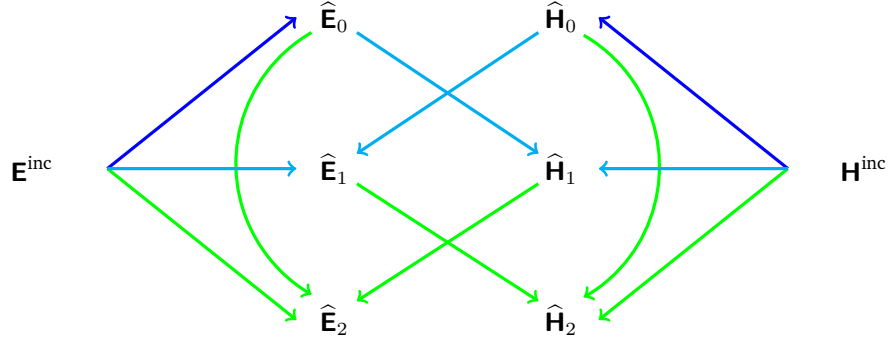


Figure 9: Construction of the near-field asymptotics (— Step 1, — Step 2, — Step 3)

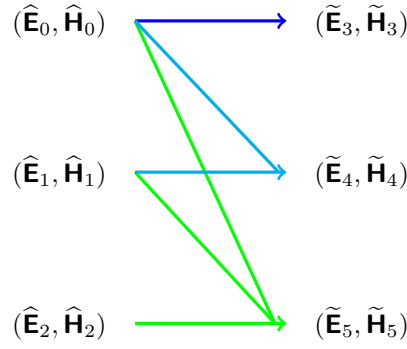


Figure 10: Construction of the far-field expansion (— Step 1, — Step 2, — Step 3)

4.5.1 Zeroth order near-field term

The zeroth order terms $\hat{\mathbf{E}}_0$ and $\hat{\mathbf{H}}_0$ are solutions of the homogeneous static Maxwell problems,

$$\begin{cases} \operatorname{curl} \hat{\mathbf{E}}_0 = 0 & \text{in } \hat{\Omega} & (4.20a) \\ \operatorname{div} \hat{\mathbf{E}}_0 = 0 & \text{in } \hat{\Omega} & (4.20b) \\ \mathbf{e}_r \times \hat{\mathbf{E}}_0 = -\mathbf{e}_r \times \mathbf{E}^{\text{inc}}(0) & \text{on } \hat{\Gamma} & (4.20c) \end{cases}$$

and

$$\begin{cases} \operatorname{curl} \hat{\mathbf{H}}_0 = 0 & \text{in } \hat{\Omega} & (4.21a) \\ \operatorname{div} \hat{\mathbf{H}}_0 = 0 & \text{in } \hat{\Omega} & (4.21b) \\ \mathbf{e}_r \cdot \hat{\mathbf{H}}_0 = -\mathbf{e}_r \cdot \mathbf{H}^{\text{inc}}(0) & \text{on } \hat{\Gamma}. & (4.21c) \end{cases}$$

The unique solution of (4.20)-(4.21) in \mathbf{W} , see (4.14), is

$$\hat{\mathbf{E}}_0 = \frac{1}{R^3} \left[3(\mathbf{E}^{\text{inc}}(0) \cdot \mathbf{e}_r) \mathbf{e}_r - \mathbf{E}^{\text{inc}}(0) \right]; \quad \hat{\mathbf{H}}_0 = -\frac{1}{2R^3} \left[3(\mathbf{H}^{\text{inc}}(0) \cdot \mathbf{e}_r) \mathbf{e}_r - \mathbf{H}^{\text{inc}}(0) \right].$$

4.5.2 First order near-field

The first order terms $\widehat{\mathbf{E}}_1$ and $\widehat{\mathbf{H}}_1$ are solutions of the nested Maxwell problems

$$\begin{cases} \mathbf{curl} \widehat{\mathbf{E}}_1 = i\kappa \widehat{\mathbf{H}}_0 & \text{in } \widehat{\Omega} & (4.23a) \\ \operatorname{div} \widehat{\mathbf{E}}_1 = 0 & \text{in } \widehat{\Omega} & (4.23b) \\ \mathbf{e}_r \times \widehat{\mathbf{E}}_1 = -\mathbf{e}_r \times \left(\mathbb{J}_{\mathbf{E}^{\text{inc}}}(0) \mathbf{e}_r \right) & \text{on } \widehat{\Gamma} & (4.23c) \end{cases}$$

and

$$\begin{cases} \mathbf{curl} \widehat{\mathbf{H}}_1 = -i\kappa \widehat{\mathbf{E}}_0 & \text{in } \widehat{\Omega} & (4.24a) \\ \operatorname{div} \widehat{\mathbf{H}}_1 = 0 & \text{in } \widehat{\Omega} & (4.24b) \\ \mathbf{e}_r \cdot \widehat{\mathbf{H}}_1 = -\mathbf{e}_r \cdot \left(\mathbb{J}_{\mathbf{H}^{\text{inc}}}(0) \mathbf{e}_r \right) & \text{on } \widehat{\Gamma}. & (4.24c) \end{cases}$$

These problems are ill-posed in \mathbf{W} . Let us decompose the solutions $(\widehat{\mathbf{E}}_1, \widehat{\mathbf{H}}_1)$ as a superposition of a field $(\widehat{\mathbf{E}}_{1,0}, \widehat{\mathbf{H}}_{1,0})$ satisfying homogeneous static Maxwell equations and a field $(\widehat{\mathbf{E}}_{1,1}, \widehat{\mathbf{H}}_{1,1})$ which is a particular solution of the nested problem (4.23)-(4.24),

$$\widehat{\mathbf{E}}_1 = \widehat{\mathbf{E}}_{1,0} + \widehat{\mathbf{E}}_{1,1}; \quad \widehat{\mathbf{H}}_1 = \widehat{\mathbf{H}}_{1,0} + \widehat{\mathbf{H}}_{1,1}. \quad (4.25)$$

The calculation of $\widehat{\mathbf{E}}_{1,1}$ and $\widehat{\mathbf{H}}_{1,1}$ go through their modal decomposition (B.26) with $p = 1$ and $\ell = 1$. According to the modal decomposition (B.29) of $\widehat{\mathbf{E}}_0$ and $\widehat{\mathbf{H}}_0$, their tangential traces on $\widehat{\Gamma}$ are given by

$$-\gamma_t \mathbf{E}^{\text{inc}}(0) = \gamma_t \widehat{\mathbf{E}}_0 = \sum_{m=-1}^1 \widehat{e}_{1,m}^{(0)} \nabla_{S^2} Y_{1,m}; \quad \frac{1}{2} \gamma_t \mathbf{H}^{\text{inc}}(0) = \gamma_t \widehat{\mathbf{H}}_0 = \sum_{m=-1}^1 \widehat{h}_{1,m}^{(0)} \nabla_{S^2} Y_{1,m}. \quad (4.26)$$

Then, according to the modal decomposition (B.32) of $\widehat{\mathbf{E}}_{1,1}$ and $\widehat{\mathbf{H}}_{1,1}$, we have

$$\begin{aligned} \widehat{\mathbf{E}}_{1,1} &= -\frac{i\kappa}{R^2} \sum_{m=-1}^1 \widehat{h}_{1,m}^{(0)} \mathbf{curl}_{S^2} Y_{1,m} = -\frac{i\kappa}{2R^2} \gamma_t \mathbf{H}^{\text{inc}}(0) \times \mathbf{e}_r \\ \widehat{\mathbf{H}}_{1,1} &= \frac{i\kappa}{R^2} \sum_{m=-1}^1 \widehat{e}_{1,m}^{(0)} \mathbf{curl}_{S^2} Y_{1,m} = -\frac{i\kappa}{R^2} \gamma_t \mathbf{E}^{\text{inc}}(0) \times \mathbf{e}_r. \end{aligned}$$

The leading terms $\widehat{\mathbf{E}}_{1,0}$ and $\widehat{\mathbf{H}}_{1,0}$ are solutions of the homogeneous static Maxwell problems,

$$\begin{cases} \mathbf{curl} \widehat{\mathbf{E}}_{1,0} = 0 & \text{in } \widehat{\Omega} & (4.27a) \\ \operatorname{div} \widehat{\mathbf{E}}_{1,0} = 0 & \text{in } \widehat{\Omega} & (4.27b) \\ \mathbf{e}_r \times \widehat{\mathbf{E}}_{1,0} = -\mathbf{e}_r \times \left(\mathbb{J}_{\mathbf{E}^{\text{inc}}}(0) \mathbf{e}_r \right) + \frac{i\kappa}{2} \gamma_t \mathbf{H}^{\text{inc}}(0) & \text{on } \widehat{\Gamma} & (4.27c) \end{cases}$$

and

$$\begin{cases} \mathbf{curl} \widehat{\mathbf{H}}_{1,0} = 0 & \text{in } \widehat{\Omega} & (4.28a) \\ \operatorname{div} \widehat{\mathbf{H}}_{1,0} = 0 & \text{in } \widehat{\Omega} & (4.28b) \\ \mathbf{e}_r \cdot \widehat{\mathbf{H}}_{1,0} = -\mathbf{e}_r \cdot \left(\mathbb{J}_{\mathbf{H}^{\text{inc}}}(0) \mathbf{e}_r \right) & \text{on } \widehat{\Gamma}. & (4.28c) \end{cases}$$

Remark 21. In (4.27), the term $\frac{i\kappa}{2}\mathbf{H}^{\text{inc}}(0) \times \mathbf{e}_r$ is also the antisymmetric part of the Jacobian operator applied on the vector field $\mathbf{E}^{\text{inc}}(0)$. In particular, we have

$$-\mathbf{e}_r \times \left(\mathbb{J}_{\mathbf{E}^{\text{inc}}}(0)\mathbf{e}_r \right) + \frac{i\kappa}{2}\gamma_t \mathbf{H}^{\text{inc}}(0) = -\mathbf{e}_r \times \left(\mathbb{J}_{\mathbf{E}^{\text{inc}}}^{\text{sym}}(0)\mathbf{e}_r \right) \quad (4.29)$$

where $\mathbb{J}^{\text{sym}} = \frac{1}{2}(\mathbb{J} + \mathbb{J}^\top)$ denotes the symmetric part of the Jacobian operator.

The unique solution of (4.27)-(4.28) in \mathbf{W} is

$$\begin{aligned} \widehat{\mathbf{E}}_{1,0} &= \frac{1}{R^4} \left[-\gamma_t \left(\mathbb{J}_{\mathbf{E}^{\text{inc}}}^{\text{sym}}(0)\mathbf{e}_r \right) + \frac{3}{2}\gamma_n \left(\mathbb{J}_{\mathbf{E}^{\text{inc}}}(0)\mathbf{e}_r \right) \mathbf{e}_r \right] \\ \widehat{\mathbf{H}}_{1,0} &= \frac{1}{R^4} \left[\frac{2}{3}\gamma_t \left(\mathbb{J}_{\mathbf{H}^{\text{inc}}}^{\text{sym}}(0)\mathbf{e}_r \right) - \gamma_n \left(\mathbb{J}_{\mathbf{H}^{\text{inc}}}(0)\mathbf{e}_r \right) \mathbf{e}_r \right]. \end{aligned}$$

4.5.3 Second order near-field

The second order terms $\widehat{\mathbf{E}}_2$ and $\widehat{\mathbf{H}}_2$ are solutions of the nested Maxwell problems

$$\begin{cases} \mathbf{curl} \widehat{\mathbf{E}}_2 = i\kappa \widehat{\mathbf{H}}_1 & \text{in } \widehat{\Omega} & (4.31a) \\ \mathbf{div} \widehat{\mathbf{E}}_2 = 0 & \text{in } \widehat{\Omega} & (4.31b) \\ \mathbf{e}_r \times \widehat{\mathbf{E}}_2 = -\mathbf{e}_r \times \left(\mathbf{e}_r^\top \mathbb{H}_{\mathbf{E}^{\text{inc}}}(0)\mathbf{e}_r \right) & \text{on } \widehat{\Gamma} & (4.31c) \end{cases}$$

and

$$\begin{cases} \mathbf{curl} \widehat{\mathbf{H}}_2 = -i\kappa \widehat{\mathbf{E}}_1 & \text{in } \widehat{\Omega} & (4.32a) \\ \mathbf{div} \widehat{\mathbf{H}}_2 = 0 & \text{in } \widehat{\Omega} & (4.32b) \\ \mathbf{e}_r \cdot \widehat{\mathbf{H}}_2 = -\mathbf{e}_r \cdot \left(\mathbf{e}_r^\top \mathbb{H}_{\mathbf{H}^{\text{inc}}}(0)\mathbf{e}_r \right) & \text{on } \widehat{\Gamma}. & (4.32c) \end{cases}$$

These problems are ill-posed in \mathbf{W} . Let us decompose the solutions $(\widehat{\mathbf{E}}_2, \widehat{\mathbf{H}}_2)$ as a superposition of a field $(\widehat{\mathbf{E}}_{2,0}, \widehat{\mathbf{H}}_{2,0})$ satisfying homogeneous static Maxwell equations and a couple of shadows $(\widehat{\mathbf{E}}_{2,1}, \widehat{\mathbf{H}}_{2,1})$ and $(\widehat{\mathbf{E}}_{2,2}, \widehat{\mathbf{H}}_{2,2})$ whose their sum is a particular solution of the nested problem (4.31)-(4.32),

$$\widehat{\mathbf{E}}_2 = \widehat{\mathbf{E}}_{2,0} + \widehat{\mathbf{E}}_{2,1} + \widehat{\mathbf{E}}_{2,2}; \quad \widehat{\mathbf{H}}_2 = \widehat{\mathbf{H}}_{2,0} + \widehat{\mathbf{H}}_{2,1} + \widehat{\mathbf{H}}_{2,2}. \quad (4.33)$$

The calculation of $(\widehat{\mathbf{E}}_{2,1}, \widehat{\mathbf{H}}_{2,1})$ and $(\widehat{\mathbf{E}}_{2,2}, \widehat{\mathbf{H}}_{2,2})$ goes through their modal decomposition (B.26) with $p = 2$ and $\ell = 1, 2$. According to the modal decomposition (B.29) of $\widehat{\mathbf{E}}_0$ and $\widehat{\mathbf{H}}_0$, their normal and tangential traces of $\widehat{\mathbf{E}}_0$ and $\widehat{\mathbf{H}}_0$ on $\widehat{\Gamma}$ are given by

$$2\gamma_n \mathbf{E}^{\text{inc}}(0) = \gamma_n \widehat{\mathbf{E}}_0 = \sum_{m=-1}^1 \widehat{e}_{1,m}^{(0)} Y_{1,m}; \quad -\gamma_n \mathbf{H}^{\text{inc}}(0) = \gamma_n \widehat{\mathbf{H}}_0 = \sum_{m=-1}^1 \widehat{h}_{1,m}^{(0)} Y_{1,m}. \quad (4.34)$$

Then, according to (4.26), (4.34) and the modal decomposition (B.26) for $p, \ell = 2$, the shadows $\widehat{\mathbf{E}}_{2,2}$ and $\widehat{\mathbf{H}}_{2,2}$ are given by

$$\begin{aligned} \widehat{\mathbf{E}}_{2,2} &= -\frac{\kappa^2}{R} \frac{\mathfrak{h}_{1,0}}{\mathfrak{h}_{1,-2}} \sum_{m=-1}^1 \widehat{e}_{1,m}^{(0)} \left[\nabla_{S^2} Y_{1,m} + 2Y_{1,m} \mathbf{e}_r \right] = \frac{\kappa^2}{2R} \left[\gamma_t \mathbf{E}^{\text{inc}}(0) + 2 \left(\gamma_n \mathbf{E}^{\text{inc}}(0) \right) \mathbf{e}_r \right] \\ \widehat{\mathbf{H}}_{2,2} &= -\frac{\kappa^2}{R} \frac{\mathfrak{h}_{1,0}}{\mathfrak{h}_{1,-2}} \sum_{m=-1}^1 \widehat{h}_{1,m}^{(0)} \left[\nabla_{S^2} Y_{1,m} + 2Y_{1,m} \mathbf{e}_r \right] = -\frac{\kappa^2}{2R} \left[\frac{1}{2} \gamma_t \mathbf{H}^{\text{inc}}(0) + \left(\gamma_n \mathbf{H}^{\text{inc}}(0) \right) \mathbf{e}_r \right]. \end{aligned} \quad \text{Inria}$$

According to the modal decomposition (B.31) of $\widehat{\mathbf{E}}_{1,0}$ and $\widehat{\mathbf{H}}_{1,0}$, their tangential traces on $\widehat{\Gamma}$ are given by

$$-\gamma_t \left(\mathbb{J}_{\mathbf{E}^{\text{inc}}}^{\text{sym}}(0) \mathbf{e}_r \right) = \gamma_t \widehat{\mathbf{E}}_{1,0} = \sum_{m=-2}^2 \widehat{e}_{2,m}^{(1)} \nabla_{S^2} Y_{2,m}; \quad \frac{2}{3} \gamma_t \left(\mathbb{J}_{\mathbf{H}^{\text{inc}}}^{\text{sym}}(0) \mathbf{e}_r \right) = \gamma_t \widehat{\mathbf{H}}_{1,0} = \sum_{m=-2}^2 \widehat{h}_{2,m}^{(1)} \nabla_{S^2} Y_{2,m}.$$

Then, according to the modal decomposition (B.26) for $p = 2$ and $\ell = 1$, the shadows $\widehat{\mathbf{E}}_{2,1}$ and $\widehat{\mathbf{H}}_{2,1}$ are given by

$$\begin{aligned} \widehat{\mathbf{E}}_{2,1} &= -\frac{i\kappa}{2R^3} \sum_{m=-2}^2 \widehat{h}_{2,m}^{(1)} \mathbf{curl}_{S^2} Y_{2,m} = -\frac{i\kappa}{3R^3} \left(\mathbb{J}_{\mathbf{H}^{\text{inc}}}^{\text{sym}}(0) \mathbf{e}_r \right) \times \mathbf{e}_r \\ \widehat{\mathbf{H}}_{2,1} &= \frac{i\kappa}{2R^3} \sum_{m=-2}^2 \widehat{e}_{2,m}^{(1)} \mathbf{curl}_{S^2} Y_{2,m} = -\frac{i\kappa}{2R^3} \left(\mathbb{J}_{\mathbf{E}^{\text{inc}}}^{\text{sym}}(0) \mathbf{e}_r \right) \times \mathbf{e}_r. \end{aligned}$$

The leading terms $\widehat{\mathbf{E}}_{2,0}$ and $\widehat{\mathbf{H}}_{2,0}$ are solutions of the homogeneous static Maxwell problems,

$$\begin{cases} \mathbf{curl} \widehat{\mathbf{E}}_{2,0} = 0 & \text{in } \widehat{\Omega} & (4.35a) \\ \text{div} \widehat{\mathbf{E}}_{2,0} = 0 & \text{in } \widehat{\Omega} & (4.35b) \\ \mathbf{e}_r \times \widehat{\mathbf{E}}_{2,0} = -\frac{1}{2} \mathbf{e}_r \times \left(\mathbf{e}_r^\top \mathbb{H}_{\mathbf{E}^{\text{inc}}}(0) \mathbf{e}_r \right) + \frac{i\kappa}{3} \gamma_t \left(\mathbb{J}_{\mathbf{H}^{\text{inc}}}^{\text{sym}}(0) \mathbf{e}_r \right) \\ \quad \quad \quad - \frac{\kappa^2}{2} \mathbf{e}_r \times \mathbf{E}^{\text{inc}}(0) & \text{on } \widehat{\Gamma} & (4.35c) \end{cases}$$

and

$$\begin{cases} \mathbf{curl} \widehat{\mathbf{H}}_{2,0} = 0 & \text{in } \widehat{\Omega} & (4.36a) \\ \text{div} \widehat{\mathbf{H}}_{2,0} = 0 & \text{in } \widehat{\Omega} & (4.36b) \\ \mathbf{e}_r \cdot \widehat{\mathbf{H}}_{2,0} = -\frac{1}{2} \mathbf{e}_r \cdot \left(\mathbf{e}_r^\top \mathbb{H}_{\mathbf{H}^{\text{inc}}}(0) \mathbf{e}_r \right) + \frac{\kappa^2}{2} \mathbf{e}_r \cdot \mathbf{H}^{\text{inc}}(0) & \text{on } \widehat{\Gamma}. & (4.36c) \end{cases}$$

The unique solution of (4.35) in \mathbf{W} is

$$\begin{aligned} \widehat{\mathbf{E}}_{2,0} &= \frac{1}{R^5} \left[-\frac{1}{2} \gamma_t \left(\mathbf{e}_r^\top \mathbb{H}_{\mathbf{E}^{\text{inc}}}(0) \mathbf{e}_r \right) + \frac{i\kappa}{3} \left(\mathbb{J}_{\mathbf{H}^{\text{inc}}}^{\text{sym}}(0) \mathbf{e}_r \right) \times \mathbf{e}_r - \frac{\kappa^2}{5} \gamma_t \mathbf{E}^{\text{inc}}(0) \right. \\ &\quad \left. - \frac{4}{3} \left\{ -\frac{1}{2} \gamma_n \left(\mathbf{e}_r^\top \mathbb{H}_{\mathbf{E}^{\text{inc}}}(0) \mathbf{e}_r \right) - \frac{\kappa^2}{10} \gamma_n \mathbf{E}^{\text{inc}}(0) \right\} \mathbf{e}_r \right] + \frac{3\kappa^2}{10R^3} \left[3 \left(\gamma_n \mathbf{E}^{\text{inc}}(0) \right) \mathbf{e}_r - \mathbf{E}^{\text{inc}}(0) \right]. \end{aligned}$$

The unique solution of (4.36) in \mathbf{W} is

$$\begin{aligned} \widehat{\mathbf{H}}_{2,0} &= \frac{1}{R^5} \left[-\frac{3}{4} \left\{ -\frac{1}{2} \gamma_t \left(\mathbf{e}_r^\top \mathbb{H}_{\mathbf{H}^{\text{inc}}}(0) \mathbf{e}_r \right) - \frac{i\kappa}{3} \left(\mathbb{J}_{\mathbf{E}^{\text{inc}}}^{\text{sym}}(0) \mathbf{e}_r \right) \times \mathbf{e}_r - \frac{\kappa^2}{5} \gamma_t \mathbf{H}^{\text{inc}}(0) \right\} \right. \\ &\quad \left. - \left\{ \frac{1}{2} \gamma_n \left(\mathbf{e}_r^\top \mathbb{H}_{\mathbf{H}^{\text{inc}}}(0) \mathbf{e}_r \right) + \frac{\kappa^2}{10} \gamma_n \mathbf{H}^{\text{inc}}(0) \right\} \mathbf{e}_r \right] + \frac{3\kappa^2}{10R^3} \left[3 \left(\gamma_n \mathbf{H}^{\text{inc}}(0) \right) \mathbf{e}_r - \mathbf{H}^{\text{inc}}(0) \right]. \end{aligned}$$

4.5.4 Far-field terms

The third, fourth and fifth order far-field terms are calculated thanks to their modal decomposition (B.18) where the series go up to $n = p - 2$ and the matching conditions (4.19), for $p = 3, 4, 5$. For $(\tilde{\mathbf{E}}_3, \tilde{\mathbf{H}}_3)$, we have

$$\begin{aligned} \tilde{\mathbf{E}}_3 = & \frac{\kappa^3}{i\mathfrak{h}_{1,-2}} h_1^{(1)}(\kappa r) \sum_{m=-1}^1 \widehat{h}_{1,m}^{(0)} \mathbf{curl}_{S^2} Y_{1,m} - \frac{\kappa^2}{\mathfrak{h}_{1,-2}} \frac{h_1^{(1)}(\kappa r) + \kappa r h_1^{(1)' }(\kappa r)}{r} \sum_{m=-1}^1 \widehat{e}_{1,m}^{(0)} \nabla_{S^2} Y_{1,m} \\ & - \frac{2\kappa^2}{\mathfrak{h}_{1,-2}} \frac{h_1^{(1)}(\kappa r)}{r} \sum_{m=-1}^1 \widehat{e}_{1,m}^{(0)} Y_{1,m} \mathbf{e}_r \end{aligned}$$

and

$$\begin{aligned} \tilde{\mathbf{H}}_3 = & -\frac{\kappa^3}{i\mathfrak{h}_{1,-2}} h_1^{(1)}(\kappa r) \sum_{m=-1}^1 \widehat{e}_{1,m}^{(0)} \mathbf{curl}_{S^2} Y_{1,m} - \frac{\kappa^2}{\mathfrak{h}_{1,-2}} \frac{h_1^{(1)}(\kappa r) + \kappa r h_1^{(1)' }(\kappa r)}{r} \sum_{m=-1}^1 \widehat{h}_{1,m}^{(0)} \nabla_{S^2} Y_{1,m} \\ & - \frac{2\kappa^2}{\mathfrak{h}_{1,-2}} \frac{h_1^{(1)}(\kappa r)}{r} \sum_{m=-1}^1 \widehat{h}_{1,m}^{(0)} Y_{1,m} \mathbf{e}_r. \end{aligned}$$

That is a sum of electromagnetic dipoles.

Remark 22. According to (4.26)-(4.34) The normal and tangential part of the electric and magnetic dipoles are given by

$$\begin{aligned} \sum_{m=-1}^1 \widehat{e}_{1,m}^{(0)} \nabla_{S^2} Y_{1,m} &= -\gamma_t \mathbf{E}^{\text{inc}}(0); & \sum_{m=-1}^1 \widehat{e}_{1,m}^{(0)} Y_{1,m} &= 2\gamma_n \mathbf{E}^{\text{inc}}(0) \\ \sum_{m=-1}^1 \widehat{h}_{1,m}^{(0)} \nabla_{S^2} Y_{1,m} &= \frac{1}{2} \gamma_t \mathbf{H}^{\text{inc}}(0); & \sum_{m=-1}^1 \widehat{h}_{1,m}^{(0)} Y_{1,m} &= -\gamma_n \mathbf{H}^{\text{inc}}(0). \end{aligned}$$

By substituting these expressions into the modal decomposition of $(\tilde{\mathbf{E}}_3, \tilde{\mathbf{H}}_3)$, we obtain the expected result.

For $(\tilde{\mathbf{E}}_4, \tilde{\mathbf{H}}_4)$, we have

$$\begin{aligned} \tilde{\mathbf{E}}_4 = & \frac{\kappa^4}{2i\mathfrak{h}_{2,-3}} h_2^{(1)}(\kappa r) \sum_{m=-2}^2 \widehat{h}_{2,m}^{(0)} \mathbf{curl}_{S^2} Y_{2,m} \\ & - \frac{\kappa^3}{2\mathfrak{h}_{2,-3}} \frac{h_2^{(1)}(\kappa r) + \kappa r h_2^{(1)' }(\kappa r)}{r} \sum_{m=-2}^2 \widehat{e}_{2,m}^{(0)} \nabla_{S^2} Y_{2,m} - \frac{3\kappa^3}{\mathfrak{h}_{2,-3}} \frac{h_2^{(1)}(\kappa r)}{r} \sum_{m=-2}^2 \widehat{e}_{2,m}^{(0)} Y_{2,m} \mathbf{e}_r \\ & + \frac{\kappa^3}{i\mathfrak{h}_{1,-2}} h_1^{(1)}(\kappa r) \sum_{m=-1}^1 \widehat{h}_{1,m}^{(1)} \mathbf{curl}_{S^2} Y_{1,m} - \frac{\kappa^2}{\mathfrak{h}_{1,-2}} \frac{h_1^{(1)}(\kappa r) + \kappa r h_1^{(1)' }(\kappa r)}{r} \sum_{m=-1}^1 \widehat{e}_{1,m}^{(1)} \nabla_{S^2} Y_{1,m} \\ & - \frac{2\kappa^2}{\mathfrak{h}_{1,-2}} \frac{h_1^{(1)}(\kappa r)}{r} \sum_{m=-1}^1 \widehat{e}_{1,m}^{(1)} Y_{1,m} \mathbf{e}_r \end{aligned} \quad \text{Inria}$$

and

$$\begin{aligned}\tilde{\mathbf{H}}_4 = & -\frac{\kappa^4}{2i\mathfrak{h}_{2,-3}} h_2^{(1)}(\kappa r) \sum_{m=-2}^2 \hat{e}_{2,m}^{(0)} \mathbf{curl}_{S^2} Y_{2,m} \\ & -\frac{\kappa^3}{2\mathfrak{h}_{2,-3}} \frac{h_2^{(1)}(\kappa r) + \kappa r h_2^{(1)' }(\kappa r)}{r} \sum_{m=-2}^2 \hat{h}_{2,m}^{(0)} \nabla_{S^2} Y_{2,m} - \frac{3\kappa^3}{\mathfrak{h}_{2,-3}} \frac{h_2^{(1)}(\kappa r)}{r} \sum_{m=-2}^2 \hat{h}_{2,m}^{(0)} Y_{2,m} \mathbf{e}_r \\ & -\frac{\kappa^3}{i n \mathfrak{h}_{1,-2}} h_1^{(1)}(\kappa r) \sum_{m=-1}^1 \hat{e}_{1,m}^{(1)} \mathbf{curl}_{S^2} Y_{1,m} - \frac{\kappa^2}{\mathfrak{h}_{1,-2}} \frac{h_1^{(1)}(\kappa r) + \kappa r h_1^{(1)' }(\kappa r)}{r} \sum_{m=-1}^1 \hat{h}_{1,m}^{(1)} \nabla_{S^2} Y_{1,m} \\ & -\frac{2\kappa^2}{\mathfrak{h}_{1,-2}} \frac{h_1^{(1)}(\kappa r)}{r} \sum_{m=-1}^1 \hat{h}_{1,m}^{(1)} Y_{1,m} \mathbf{e}_r.\end{aligned}$$

but $\hat{h}_{2,m}^{(0)} = \hat{e}_{2,m}^{(0)} = \hat{h}_{1,m}^{(1)} = \hat{e}_{1,m}^{(1)} = 0$ for any $-n \leq m \leq n$ ($n = 1$ or $n = 2$) according to (B.29)-(B.31). Then, we obtain

$$\tilde{\mathbf{E}}_4 = 0; \quad \tilde{\mathbf{H}}_4 = 0.$$

For $(\tilde{\mathbf{E}}_5, \tilde{\mathbf{H}}_5)$, noting that the sums of octopoles are reduced to null-fields according to (B.29), we have

$$\begin{aligned}\tilde{\mathbf{E}}_5 = & \frac{\kappa^4}{2i\mathfrak{h}_{2,-3}} h_2^{(1)}(\kappa r) \sum_{m=-2}^2 \hat{h}_{2,m}^{(1)} \mathbf{curl}_{S^2} Y_{2,m} \\ & + \frac{\kappa^4}{2i\mathfrak{h}_{2,-3}} \frac{h_2^{(1)}(\kappa r) + \kappa r h_2^{(1)' }(\kappa r)}{i\kappa r} \sum_{m=-2}^2 \hat{e}_{2,m}^{(1)} \nabla_{S^2} Y_{2,m} + \frac{3\kappa^4}{i\mathfrak{h}_{2,-3}} \frac{h_2^{(1)}(\kappa r)}{i\kappa r} \sum_{m=-2}^2 \hat{e}_{2,m}^{(1)} Y_{2,m} \mathbf{e}_r \\ & + \frac{\kappa^3}{i\mathfrak{h}_{1,-2}} h_1^{(1)}(\kappa r) \sum_{m=-1}^1 \hat{h}_{1,m}^{(2)} \mathbf{curl}_{S^2} Y_{1,m} + \frac{\kappa^3}{i\mathfrak{h}_{1,-2}} \frac{h_1^{(1)}(\kappa r) + \kappa r h_1^{(1)' }(\kappa r)}{i\kappa r} \sum_{m=-1}^1 \hat{e}_{1,m}^{(2)} \nabla_{S^2} Y_{1,m} \\ & + \frac{2\kappa^3}{i\mathfrak{h}_{1,-2}} \frac{h_1^{(1)}(\kappa r)}{i\kappa r} \sum_{m=-1}^1 \hat{e}_{1,m}^{(2)} Y_{1,m} \mathbf{e}_r\end{aligned}$$

and

$$\begin{aligned}\tilde{\mathbf{H}}_5 = & -\frac{\kappa^4}{2i\mathfrak{h}_{2,-3}} h_2^{(1)}(\kappa r) \sum_{m=-2}^2 \hat{e}_{2,m}^{(1)} \mathbf{curl}_{S^2} Y_{2,m} \\ & + \frac{\kappa^4}{2i\mathfrak{h}_{2,-3}} \frac{h_2^{(1)}(\kappa r) + \kappa r h_2^{(1)' }(\kappa r)}{i\kappa r} \sum_{m=-2}^2 \hat{h}_{2,m}^{(1)} \nabla_{S^2} Y_{2,m} + \frac{3\kappa^4}{i\mathfrak{h}_{2,-3}} \frac{h_2^{(1)}(\kappa r)}{i\kappa r} \sum_{m=-2}^2 \hat{h}_{2,m}^{(1)} Y_{2,m} \mathbf{e}_r \\ & -\frac{\kappa^3}{i\mathfrak{h}_{1,-2}} h_1^{(1)}(\kappa r) \sum_{m=-1}^1 \hat{e}_{1,m}^{(2)} \mathbf{curl}_{S^2} Y_{1,m} + \frac{\kappa^3}{i\mathfrak{h}_{1,-2}} \frac{h_1^{(1)}(\kappa r) + \kappa r h_1^{(1)' }(\kappa r)}{i\kappa r} \sum_{m=-1}^1 \hat{h}_{1,m}^{(2)} \nabla_{S^2} Y_{1,m} \\ & + \frac{2\kappa^2}{i\mathfrak{h}_{1,-2}} \frac{h_1^{(1)}(\kappa r)}{i\kappa r} \sum_{m=-1}^1 \hat{h}_{1,m}^{(2)} Y_{1,m} \mathbf{e}_r.\end{aligned}$$

That is a sum of electromagnetic dipoles and quadrupoles. The normal and tangential part of

the electric and magnetic dipoles are given by

$$\begin{aligned} \sum_{m=-1}^1 \widehat{e}_{1,m}^{(2)} \nabla_{S^2} Y_{1,m} &= -\frac{3\kappa^2}{10} \gamma_t(\mathbf{E}^{\text{inc}}(0)); & \sum_{m=-1}^1 \widehat{e}_{1,m}^{(2)} Y_{1,m} &= -\frac{3\kappa^2}{10} \gamma_n(\mathbf{E}^{\text{inc}}(0)) \\ \sum_{m=-1}^1 \widehat{h}_{1,m}^{(2)} \nabla_{S^2} Y_{1,m} &= -\frac{3\kappa^2}{10} \gamma_t(\mathbf{H}^{\text{inc}}(0)); & \sum_{m=-1}^1 \widehat{h}_{1,m}^{(2)} Y_{1,m} &= -\frac{3\kappa^2}{10} \gamma_n(\mathbf{H}^{\text{inc}}(0)). \end{aligned}$$

The normal and tangential part of the electric and magnetic quadrupoles are given by

$$\begin{aligned} \sum_{m=-2}^2 \widehat{e}_{2,m}^{(1)} \nabla_{S^2} Y_{2,m} &= -\gamma_t(\mathbb{J}_{\mathbf{E}^{\text{inc}}}^{\text{sym}}(0) \mathbf{e}_r); & \sum_{m=-2}^2 \widehat{e}_{2,m}^{(1)} Y_{2,m} &= -\frac{1}{2} \gamma_n(\mathbb{J}_{\mathbf{E}^{\text{inc}}}^{\text{sym}}(0) \mathbf{e}_r) \\ \sum_{m=-2}^2 \widehat{h}_{2,m}^{(1)} \nabla_{S^2} Y_{2,m} &= \frac{2}{3} \gamma_t(\mathbb{J}_{\mathbf{H}^{\text{inc}}}^{\text{sym}}(0) \mathbf{e}_r); & \sum_{m=-2}^2 \widehat{h}_{2,m}^{(1)} Y_{2,m} &= \frac{1}{3} \gamma_n(\mathbb{J}_{\mathbf{H}^{\text{inc}}}^{\text{sym}}(0) \mathbf{e}_r). \end{aligned}$$

It suffices to substitute these expressions into the modal decomposition of $(\widetilde{\mathbf{E}}_5, \widetilde{\mathbf{H}}_5)$ given herein-above in order to obtain the result.

5 Conclusion and perspectives

In this report, we have applied the method of matched asymptotic expansions to the electromagnetic scattering by a small sphere. We have performed the near-field expansion at the second order and the far-field expansion at the fifth order. We have tackled the subject from a formal point of view by validating numerically our results, which have several direct applications. Here, we develop the following ones:

- the derivation of collected models,
- the application of the Born theory to the multiple scattering.

Finally, we end this section with the on-going works and the perspectives.

5.1 Collected models

The main interest of asymptotic analysis lies in describing the leading behavior of the solution when one of their parameters tends to zero or to infinity. For the numerical analysis, the information is exploitable if we can indeed calculate this leading term, hoping that this computation will be less expensive than the one of the exact solution. In the case of the sphere, we have indeed been able to compute explicitly the first terms but we can remark that the computation of the exact solution is less costly than the one of the approximate solution on a refined mesh. Nevertheless, our method allows us to calculate the solution on uniform and enough coarse meshes, that is clearly a benefit on the necessity of using refined meshes depending on the small parameter. In order to decrease the computation time of the approximate solution, we can consider a collected model which consists in assembling the different terms, not with respect to the δ -power but with respect to their nature (dipole, quadrupole, ...). From a far-field point of view, the dipole collected model reads as

$$\begin{aligned} \mathbf{E}_\delta^{\text{Col}} &= \left[-\frac{(\kappa\delta)^3}{2} + \frac{3(\kappa\delta)^5}{10} \right] h_1^{(1)}(\kappa r) \gamma_\times(\mathbf{H}^{\text{inc}}(0)) \\ &\quad - \left[(\kappa\delta)^3 + \frac{3(\kappa\delta)^5}{10} \right] \frac{h_1^{(1)}(\kappa r) + \kappa r h_1^{(1)'}(\kappa r)}{i\kappa r} \gamma_t(\mathbf{E}^{\text{inc}}(0)) - 2 \left[(\kappa\delta)^3 + \frac{3(\kappa\delta)^5}{10} \right] \frac{h_1^{(1)}(\kappa r)}{i\kappa r} \gamma_n(\mathbf{E}^{\text{inc}}(0)) \mathbf{e}_r \end{aligned}$$

and

$$\begin{aligned} \mathbf{H}_\delta^{\text{Col}} = & - \left[(\kappa\delta)^3 + \frac{3(\kappa\delta)^5}{10} \right] h_1^{(1)}(\kappa r) \gamma_\times (\mathbf{E}^{\text{inc}}(0)) \\ & + \left[\frac{(\kappa\delta)^3}{2} - \frac{3(\kappa\delta)^5}{10} \right] \frac{h_1^{(1)}(\kappa r) + \kappa r h_1^{(1)'}(\kappa r)}{i\kappa r} \gamma_t (\mathbf{H}^{\text{inc}}(0)) + 2 \left[\frac{(\kappa\delta)^3}{2} - \frac{3(\kappa\delta)^5}{10} \right] \frac{h_1^{(1)}(\kappa r)}{i\kappa r} \gamma_n (\mathbf{H}^{\text{inc}}(0)) \mathbf{e}_r \end{aligned}$$

where γ_\times , γ_t and γ_n are defined by (2.7). This approximation improves the first approximation ($\delta^3 \tilde{\mathbf{E}}_3, \delta^3 \tilde{\mathbf{H}}_3$) and its computation time is unchanged because it is only the dipole amplitude which have changed. According to (A.12)-(A.13) and (A.19)-(A.20), the previous expressions can be written in the compact form

$$\begin{aligned} \mathbf{E}_\delta^{\text{Col}} = & \delta^3 \left\{ \mathbf{E}_{\text{dip}}^{\text{elec}} \left[4\pi \left(1 + \frac{3(\kappa\delta)^2}{10} \right) \mathbf{E}^{\text{inc}}(0) \right] + \mathbf{E}_{\text{dip}}^{\text{mag}} \left[-2\pi \left(1 - \frac{3(\kappa\delta)^2}{5} \right) \mathbf{H}^{\text{inc}}(0) \right] \right\} \\ \mathbf{H}_\delta^{\text{Col}} = & \delta^3 \left\{ \mathbf{H}_{\text{dip}}^{\text{elec}} \left[4\pi \left(1 + \frac{3(\kappa\delta)^2}{10} \right) \mathbf{E}^{\text{inc}}(0) \right] + \mathbf{H}_{\text{dip}}^{\text{mag}} \left[-2\pi \left(1 - \frac{3(\kappa\delta)^2}{5} \right) \mathbf{H}^{\text{inc}}(0) \right] \right\} \end{aligned}$$

In Figure 11, we illustrate the performance of this collected model, given by $(\mathbf{E}_\delta^{\text{Col}}, \mathbf{H}_\delta^{\text{Col}})$ and we compare this one to the first approximation ($\delta^3 \tilde{\mathbf{E}}_3, \delta^3 \tilde{\mathbf{H}}_3$).

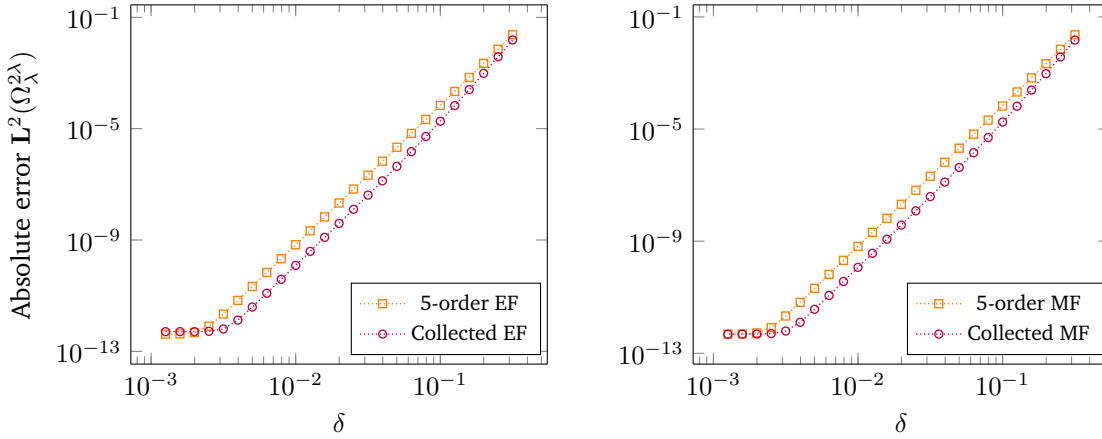


Figure 11: Absolute L^2 -errors for far-field approximations of the electric and magnetic fields

In pre-asymptotic regime, we can remark that the order of convergence for the collected approximation is close to six but the error does not decrease a lot in comparison with the first approximation ($\delta^3 \tilde{\mathbf{E}}_3, \delta^3 \tilde{\mathbf{H}}_3$). Actually, in the fifth order far-field term, the predominant term when δ is enough large is given by the dipolar term while the predominant term is the quadrupolar term when δ is small. For the same computation cost, the error decreases with a factor approximately equal to 6.0.

5.2 Born approximation

The extension to the multiple scattering can be done directly thanks to the Born model. It consists in superposing the scattered fields by the K isolated obstacles centered in c_k , $k = 1, \dots, K$. Interactions between obstacles are neglected. By considering this approximation, the third order

far-field terms are given by

$$\begin{aligned} \tilde{\mathbf{E}}_3^{\text{Born}}(\mathbf{x}) = \kappa^3 \sum_{k=1}^K \left\{ -\frac{1}{2} h_1^{(1)}(\kappa|\mathbf{x} - c_k|) \gamma_{\times} \mathbf{H}^{\text{inc}}(c_k) \right. \\ \left. - \frac{h_1^{(1)}(\kappa|\mathbf{x} - c_k|) + \kappa|\mathbf{x} - c_k| h_1^{(1)}(\kappa|\mathbf{x} - c_k|)}{i\kappa|\mathbf{x} - c_k|} \gamma_t \mathbf{E}^{\text{inc}}(c_k) - 2 \frac{h_1^{(1)}(\kappa|\mathbf{x} - c_k|)}{i\kappa|\mathbf{x} - c_k|} \gamma_n(\mathbf{E}^{\text{inc}}(c_k)) \mathbf{e}_r^{(k)} \right\} \end{aligned}$$

and

$$\begin{aligned} \tilde{\mathbf{H}}_3^{\text{Born}}(\mathbf{x}) = \kappa^3 \sum_{k=1}^K \left\{ -h_1^{(1)}(\kappa|\mathbf{x} - c_k|) \gamma_{\times} \mathbf{E}^{\text{inc}}(c_k) \right. \\ \left. + \frac{1}{2} \frac{h_1^{(1)}(\kappa|\mathbf{x} - c_k|) + \kappa|\mathbf{x} - c_k| h_1^{(1)}(\kappa|\mathbf{x} - c_k|)}{i\kappa|\mathbf{x} - c_k|} \gamma_t \mathbf{H}^{\text{inc}}(c_k) + \frac{h_1^{(1)}(\kappa|\mathbf{x} - c_k|)}{i\kappa|\mathbf{x} - c_k|} \gamma_n(\mathbf{H}^{\text{inc}}(c_k)) \mathbf{e}_r^{(k)} \right\} \end{aligned}$$

where $\mathbf{e}_r^{(k)}$ denotes the unit vector $\frac{\mathbf{x} - c_k}{|\mathbf{x} - c_k|}$. In Figure 12, we illustrate this formulation for $K = 13$ obstacles, where the physical parameters are given in Section 3. We draw cross sections of the x and y -coordinates of the approximate electric field given by $\delta^3 \tilde{\mathbf{E}}_3^{\text{Born}}$, in a logarithmic scale.

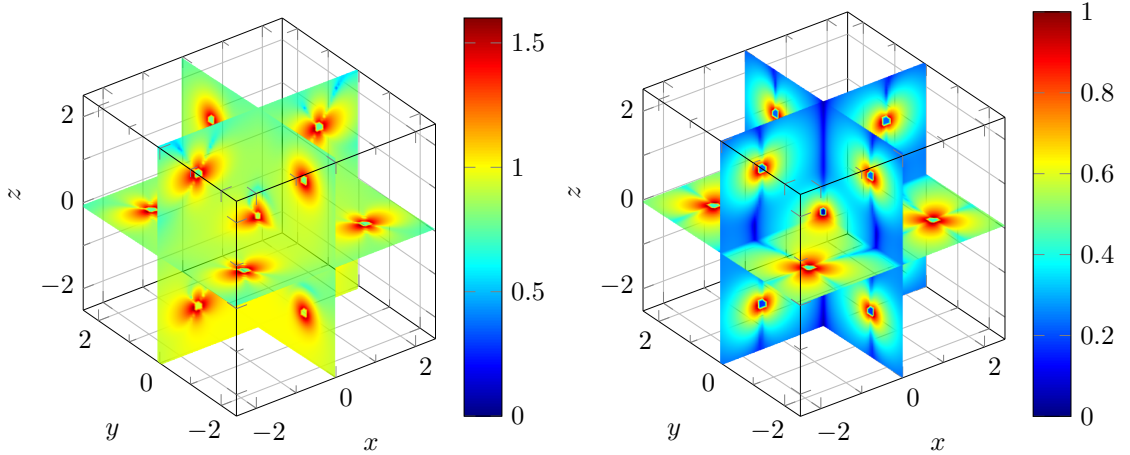


Figure 12: Cross sections of the x and y -coordinates of the scattered electric field in a logarithmic scale

By virtue of (2.20), the previous expressions can be put into the compact form,

$$\begin{aligned} \tilde{\mathbf{E}}_3^{\text{Born}}(\mathbf{x}) &= \sum_{k=1}^K \mathbf{E}_{\text{dip}}^{\text{elec}}[4\pi \mathbf{E}^{\text{inc}}(c_k)](\mathbf{x} - c_k) + \mathbf{E}_{\text{dip}}^{\text{mag}}[-2\pi \mathbf{H}^{\text{inc}}(c_k)](\mathbf{x} - c_k) \\ \tilde{\mathbf{H}}_3^{\text{Born}}(\mathbf{x}) &= \sum_{k=1}^K \mathbf{H}_{\text{dip}}^{\text{elec}}[4\pi \mathbf{E}^{\text{inc}}(c_k)](\mathbf{x} - c_k) + \mathbf{H}_{\text{dip}}^{\text{mag}}[-2\pi \mathbf{H}^{\text{inc}}(c_k)](\mathbf{x} - c_k). \end{aligned}$$

Moreover, each of the K near-field expansions are defined in the fast variable $\mathbf{X}^{(k)}$ centered around the k -th obstacle,

$$\mathbf{X}^{(k)} = \frac{\mathbf{x} - c_k}{\delta}. \quad (5.1)$$

For any $k = 1, \dots, K$, the near-field terms $(\widehat{\mathbf{E}}_p^{(k)}, \widehat{\mathbf{H}}_p^{(k)})$ are the same than for one obstacle except the awareness of translations. However, the Born model is restricted to very small obstacles, that are sufficiently far enough away from each other.

5.3 Other perspectives

A better approximation for the multiple scattering is the Foldy-Lax model which takes into account the interactions between the obstacles. Actually, the total scattered field is obtained by considering the superposition of scattered fields generated by the incident field and by considering also all the isolated scattered fields as new sources for the other obstacles. The scattering problem related to this model is set by looking for an approximation of the scattered field as a superposition of K unknowns electromagnetic dipoles

$$\begin{aligned}\mathbf{E}_\delta^{\text{Foldy}} &= \sum_{k=1}^K \left\{ \mathbf{E}_{\text{dip}}^{\text{elec}}[\mathbf{d}_k^{\text{E}}](\mathbf{x} - c_k) + \mathbf{E}_{\text{dip}}^{\text{mag}}[\mathbf{d}_k^{\text{H}}](\mathbf{x} - c_k) \right\} \\ \mathbf{H}_\delta^{\text{Foldy}} &= \sum_{k=1}^K \left\{ \mathbf{H}_{\text{dip}}^{\text{elec}}[\mathbf{d}_k^{\text{E}}](\mathbf{x} - c_k) + \mathbf{H}_{\text{dip}}^{\text{mag}}[\mathbf{d}_k^{\text{H}}](\mathbf{x} - c_k) \right\}\end{aligned}$$

whose directions can be written thanks to the collected model,

$$\mathbf{d}_k^{\text{E}} = 4\pi \left(1 + \frac{3(\kappa\delta)^2}{10}\right) \mathbf{w}_k^{\text{E}}(c_k); \quad \mathbf{d}_k^{\text{H}} = -2\pi \left(1 - \frac{3(\kappa\delta)^2}{5}\right) \mathbf{w}_k^{\text{H}}(c_k).$$

The vector fields $\mathbf{w}_k^{\text{E}}(c_k)$ and $\mathbf{w}_k^{\text{H}}(c_k)$ can be determined by solving the following linear systems

$$\begin{aligned}\mathbf{w}_k^{\text{E}}(c_k) &= \delta^3 \left\{ \mathbf{E}^{\text{inc}}(c_k) + \sum_{\substack{\ell=1 \\ \ell \neq k}}^K \mathbf{E}_{\text{dip}}^{\text{elec}}[4\pi \mathbf{w}_\ell^{\text{E}}(c_\ell)](c_k - c_\ell) + \mathbf{E}_{\text{dip}}^{\text{mag}}[-2\pi \mathbf{w}_\ell^{\text{H}}(c_\ell)](c_k - c_\ell) \right\} \quad k = 1, \dots, K \\ \mathbf{w}_k^{\text{H}}(c_k) &= \delta^3 \left\{ \mathbf{H}^{\text{inc}}(c_k) + \sum_{\substack{\ell=1 \\ \ell \neq k}}^K \mathbf{H}_{\text{dip}}^{\text{elec}}[4\pi \mathbf{w}_\ell^{\text{E}}(c_\ell)](c_k - c_\ell) + \mathbf{H}_{\text{dip}}^{\text{mag}}[-2\pi \mathbf{w}_\ell^{\text{H}}(c_\ell)](c_k - c_\ell) \right\} \quad k = 1, \dots, K.\end{aligned}$$

We are still investigating the Foldy-Lax model for electromagnetic waves. Our next objective is to compare numerically the two models, Born and Foldy, with a spectral method looking like the Ganesh's method in [23] but adapted to small obstacles as in [4]. In addition, the proofs of existence and uniqueness for solutions of the elementary problems as well as the convergence proofs justifying the asymptotic expansions have to be developed in order to validate theoretically our results. The theoretical aspects will be performed in a later paper. Finally, another perspective is the extension to the time-dependant domain. Thanks to the identification of the time-harmonic symbol $-i\omega$ with the partial time-derivative ∂_t , we can plan to adapt this work on the Maxwell's equations in time-dependant domain, that have been already done for the wave equation in [28] in contrast with the Helmholtz equation in [6].

Appendices

A Multipole theory in electromagnetism

If fields are associated with forces, potentials are associated with energy and work. In the presence of a charge distribution ρ and a current distribution \mathcal{J} in the free-space with a time-harmonic dependency, electromagnetic fields $(\mathcal{E}, \mathcal{H})$ are generated and can be described by their potential decomposition

$$\mathcal{E} = -\nabla\mathcal{V} + i\omega\mathcal{A}; \quad \mathcal{H} = \frac{1}{\mu} \mathbf{curl} \mathcal{A} \quad (\text{A.1})$$

where the electric potential \mathcal{V} and magnetic potential \mathcal{A} are given by

$$\mathcal{V}(\mathbf{x}) = \frac{1}{4\pi\epsilon} \int_{\mathbb{R}^3} \exp(i\kappa|\mathbf{x} - \mathbf{y}|) \frac{\rho(\mathbf{y})}{|\mathbf{x} - \mathbf{y}|} d\mathbf{y}; \quad \mathcal{A}(\mathbf{x}) = \frac{\mu}{4\pi} \int_{\mathbb{R}^3} \exp(i\kappa|\mathbf{x} - \mathbf{y}|) \frac{\mathcal{J}(\mathbf{y})}{|\mathbf{x} - \mathbf{y}|} d\mathbf{y}.$$

According to Equation (A.1), applying the normalization of Table 1, the normalized electromagnetic fields (\mathbf{E}, \mathbf{H}) read as

$$\mathbf{E} = -\nabla V + i\kappa\mathbf{A}; \quad \mathbf{H} = \mathbf{curl} \mathbf{A} \quad (\text{A.2})$$

where the electric potential V and the magnetic potential \mathbf{A} are given by

$$V(\mathbf{x}) = \frac{1}{4\pi} \int_{\mathbb{R}^3} \exp(i\kappa|\mathbf{x} - \mathbf{y}|) \frac{\varrho(\mathbf{y})}{|\mathbf{x} - \mathbf{y}|} d\mathbf{y}; \quad \mathbf{A}(\mathbf{x}) = \frac{1}{4\pi c} \int_{\mathbb{R}^3} \exp(i\kappa|\mathbf{x} - \mathbf{y}|) \frac{\mathbf{j}(\mathbf{y})}{|\mathbf{x} - \mathbf{y}|} d\mathbf{y}. \quad (\text{A.3})$$

Remark 23. These formulas are also valid in electrostatics or magnetostatics, *i.e.* with $\omega = 0$ and where we deal with the following equations

$$\mathbf{curl} \mathbf{E} = 0 \text{ and } \text{div} \mathbf{E} = \varrho \quad \text{or} \quad \mathbf{curl} \mathbf{H} = \frac{\mathbf{j}}{c} \text{ and } \text{div} \mathbf{H} = 0. \quad (\text{A.4})$$

A.1 Electric multipoles

A N -point charge distribution is an idealistic configuration for electric charge distributions. It can be represented as a combination of Dirac distributions $\delta_{\mathbf{x}_k}$ at points \mathbf{x}_k for $k \in [1, N]$ with charge amplitudes q_k that are constants in static or time-harmonic regime,

$$\varrho(\mathbf{x}) = \sum_{k=1}^N q_k \delta_{\mathbf{x}_k}(\mathbf{x}). \quad (\text{A.5})$$

The electric multipoles stem from an asymptotic process describing an ideal electric charge distribution. An electric multipole of order 2^N , or electric dipole for $N = 1$, electric quadrupole for $N = 2$, electric octopole and so forth, is obtained in bringing together a 2^N -point charge such that:

- there are 2^{N-1} positive charges ($+q$) and 2^{N-1} opposite ones ($-q$) such that the geometric centers of the positive charges and the negative ones are blended.
- the charge amplitudes are given by $q = \frac{q_0}{\epsilon^N}$, where q_0 is measured in Coulomb and any distance between two opposite charges is proportional to ϵ .

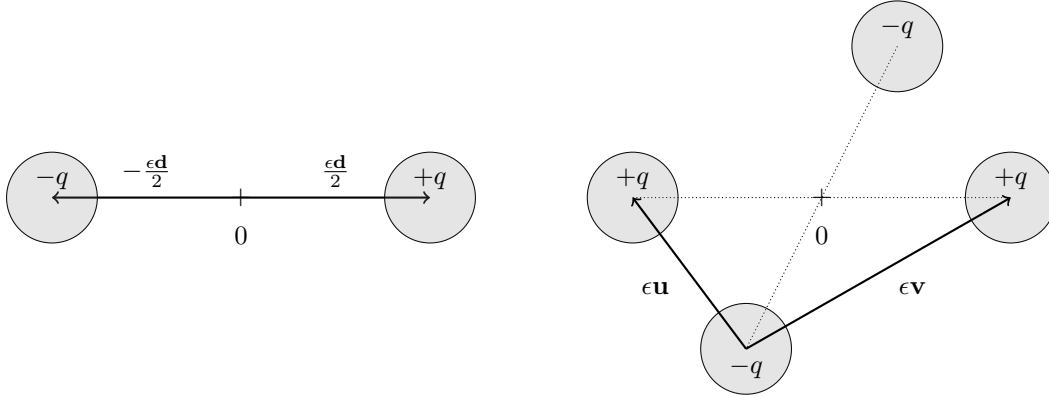


Figure 13: Electrostatic dipole on the left ; Electrostatic quadrupole on the right

By *in bringing together*, we mean that any distance between two charges are tending towards 0, while the amplitudes are tending towards ∞ . In Figure 13, we schematize an electrostatic dipole and quadrupole, where we have denoted by ϵ the parameter supposed to tend to 0.

Electric fields are produced through a such configuration thanks to the relation $\mathbf{E} = -\nabla V_\varrho$ where V_ϱ is the scalar electric potential induced by ϱ in a multipolar configuration. In particular, Equations (A.2)-(A.3) with $\kappa = 0$ allow to deduce a general form of the electric field $\mathbf{E}_{\text{dip}}^{\text{elec}}$ created in the presence of an electric dipole centered at the origin along a direction \mathbf{d} ,

$$\mathbf{E}_{\text{dip}}^{\text{elec}}[\mathbf{d}, \kappa = 0](r, \theta, \varphi) = \frac{q_0}{4\pi r^3} \left\{ 3(\mathbf{d} \cdot \mathbf{e}_r(\theta, \varphi))\mathbf{e}_r(\theta, \varphi) - \mathbf{d} \right\} \quad (\text{A.6})$$

where $\mathbf{e}_r = (\sin \theta \cos \varphi, \sin \theta \sin \varphi, \cos \theta)^\top$. Moreover, the electric field $\mathbf{E}_{\text{quad}}^{\text{elec}}$ created in the presence of an electric quadrupole centered at the origin along directions (\mathbf{u}, \mathbf{v}) , in a static regime, can be represented as

$$\begin{aligned} \mathbf{E}_{\text{quad}}^{\text{elec}}[\mathbf{u}, \mathbf{v}, \kappa = 0](r, \theta, \varphi) = & \frac{3q_0}{16\pi r^4} \left\{ [(\mathbf{u} \cdot \mathbf{v}) - 3(\mathbf{u} \cdot \mathbf{e}_r)(\mathbf{v} \cdot \mathbf{e}_r)]\mathbf{e}_r \right. \\ & \left. + [(\mathbf{u} \cdot \mathbf{e}_r)(\mathbf{v} \cdot \mathbf{e}_\theta) + (\mathbf{v} \cdot \mathbf{e}_r)(\mathbf{u} \cdot \mathbf{e}_\theta)]\mathbf{e}_\theta + [(\mathbf{u} \cdot \mathbf{e}_r)(\mathbf{v} \cdot \mathbf{e}_\varphi) + (\mathbf{v} \cdot \mathbf{e}_r)(\mathbf{u} \cdot \mathbf{e}_\varphi)]\mathbf{e}_\varphi \right\} \quad (\text{A.7}) \end{aligned}$$

where $(\mathbf{e}_r, \mathbf{e}_\theta, \mathbf{e}_\varphi)$ denotes the spherical coordinate system.

Remark 24. The formula (A.6) can be found in [27, Section 1.16] as well as a discussion about multipole of superior order, but in general, we do not find the formula (A.7) in the literature. The computation of $\mathbf{E}_{\text{quad}}^{\text{elec}}$ goes through its potential decomposition (A.2) with

$$V_{\text{quad}}[\mathbf{u}, \mathbf{v}, \kappa = 0] = \lim_{\epsilon \rightarrow 0} \frac{q(\epsilon)}{4\pi} \left[\frac{1}{|\mathbf{x} - c_1(\epsilon)|} + \frac{1}{|\mathbf{x} - c_2(\epsilon)|} - \frac{1}{|\mathbf{x} - c_3(\epsilon)|} - \frac{1}{|\mathbf{x} - c_4(\epsilon)|} \right] \quad (\text{A.8})$$

where $c_k(\epsilon)$ denotes the center of the k -th charge. In the configuration of Figure 13, the centers read as $c_1(\epsilon) = \frac{\epsilon \mathbf{d}_1}{2}$, $c_2(\epsilon) = -\frac{\epsilon \mathbf{d}_1}{2}$, $c_3(\epsilon) = \frac{\epsilon \mathbf{d}_2}{2}$, $c_4(\epsilon) = -\frac{\epsilon \mathbf{d}_2}{2}$ with $\mathbf{d}_2 - \mathbf{d}_1 = \mathbf{u}$ and $\mathbf{d}_2 + \mathbf{d}_1 = \mathbf{v}$. Moreover, the charge q is given by $q(\epsilon) = \frac{q_0}{\epsilon^2}$.

In classical magnetostatics, the presence of an electric current distribution \mathbf{j} on a system of electric dipole, drag the creation of a magnetic field. A filiform electric current distribution is described by a curve γ and a constant intensity I_γ ,

$$I_\gamma = \int_S \mathbf{j} \cdot \mathbf{n} \, ds, \quad (\text{A.9})$$

where S denotes any wire section, ds its surface element and \mathbf{n} its unit normal vector oriented with respect to γ , see Figure 14. For γ parametrized along a direction \mathbf{d} as in Figure 14, this current affects the vectorial magnetic potential as

$$\mathbf{A}_{\text{dip}}[\mathbf{d}, \kappa = 0] = \lim_{\epsilon \rightarrow 0} \frac{I_\gamma}{4\pi c} \left(\int_{-\frac{\epsilon}{2}}^{\frac{\epsilon}{2}} \frac{1}{|\mathbf{x} - s\mathbf{d}|} ds \right) \mathbf{d}. \quad (\text{A.10})$$

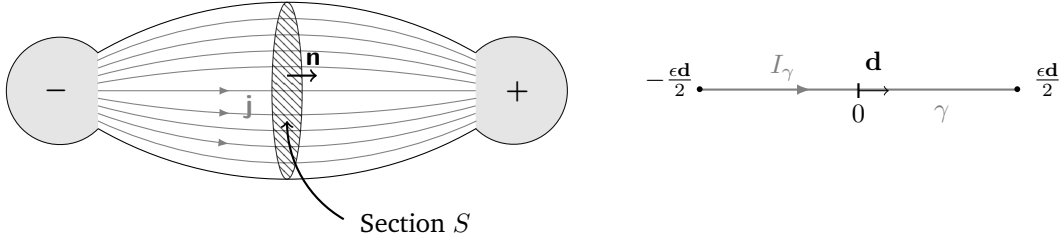


Figure 14: Filiform current between two opposite charges

In particular, Equations (A.2)-(A.10) allow to deduce a general form for the magnetic field $\mathbf{H}_{\text{dip}}^{\text{elec}}$ created in the presence of a filiform electric current of intensity I_γ between two opposite electric point charges along the direction \mathbf{d} ,

$$\mathbf{H}_{\text{dip}}^{\text{elec}}[\mathbf{d}, \kappa = 0](r, \theta, \varphi) = \frac{I_\gamma}{4\pi cr^2} (\mathbf{d} \times \mathbf{e}_r). \quad (\text{A.11})$$

In the time-harmonic regime, the charge conservation principle involves the creation of currents in the presence of charges and reciprocally the creation of charges in the presence of currents. In particular, the charge q is linked with the current intensity I_γ as $I_\gamma = -i\omega q$. The presence of an electric dipole along a direction \mathbf{d} generates electromagnetic fields ($\mathbf{E}_{\text{dip}}^{\text{elec}}, \mathbf{H}_{\text{dip}}^{\text{elec}}$). The two following expressions generalize the previous ones that are expressed for $\kappa \neq 0$. According to Equations (A.2)-(A.3) and Remark 2, electromagnetic fields read as

$$\mathbf{E}_{\text{dip}}^{\text{elec}}[\mathbf{d}, \kappa](r, \theta, \varphi) = \frac{\exp(i\kappa r)}{4\pi r} \left\{ \left(\frac{3}{r^2} - \frac{3i\kappa}{r} - \kappa^2 \right) (\mathbf{d} \cdot \mathbf{e}_r) \mathbf{e}_r + \left(-\frac{1}{r^2} + \frac{i\kappa}{r} + \kappa^2 \right) \mathbf{d} \right\} \quad (\text{A.12})$$

and

$$\mathbf{H}_{\text{dip}}^{\text{elec}}[\mathbf{d}, \kappa](r, \theta, \varphi) = \frac{\exp(i\kappa r)}{4\pi r} \left(\frac{1}{r} - i\kappa \right) (-i\kappa \mathbf{d}) \times \mathbf{e}_r. \quad (\text{A.13})$$

A.2 Magnetic multipoles

The notion of magnetic multipole, although very controversial in classical physics and running counter to the existing theory, enriches the theoretical background of Maxwell's equations. Theoretically, it consists in adding magnetic sources to the Maxwell's system - a magnetic charge density ν and a magnetic current density \mathbf{m} - related with a similar *magnetic* charge conservation principle $-i\omega\nu + \text{div } \mathbf{m} = 0$. These densities become sources for the following equations

$$\text{div } \mathbf{H} = \nu \quad \text{and} \quad \text{curl } \mathbf{E} - i\kappa \mathbf{H} = -\frac{\mathbf{m}}{c}. \quad (\text{A.14})$$

In this case, when we consider that the two other equations are homogeneous, we would have

$$\mathbf{H} = -\nabla V_\nu + i\kappa \mathbf{A}_m \quad \text{and} \quad \mathbf{E} = -\mathbf{curl} \mathbf{A}_m. \quad (\text{A.15})$$

By analogy with the previous section, the magnetic fields $\mathbf{H}_{\text{dip}}^{\text{mag}}$ and $\mathbf{H}_{\text{quad}}^{\text{mag}}$ created in the presence of a magnetic dipole/quadrupole depending on respective directions \mathbf{d}_ν and $(\mathbf{u}_\nu, \mathbf{v}_\nu)$ have the following representations in static regime

$$\mathbf{H}_{\text{dip}}^{\text{mag}}[\mathbf{d}_\nu, \kappa = 0](r, \theta, \varphi) = \frac{n_0}{4\pi r^3} \left\{ 3(\mathbf{d}_\nu \cdot \mathbf{e}_r) \mathbf{e}_r - \mathbf{d}_\nu \right\} \quad (\text{A.16})$$

and

$$\begin{aligned} \mathbf{H}_{\text{quad}}^{\text{mag}}[\mathbf{u}_\nu, \mathbf{v}_\nu, \kappa = 0](r, \theta, \varphi) = & \frac{3n_0}{16\pi r^4} \left\{ [(\mathbf{u}_\nu \cdot \mathbf{v}_\nu) - 3(\mathbf{u}_\nu \cdot \mathbf{e}_r)(\mathbf{v}_\nu \cdot \mathbf{e}_r)] \mathbf{e}_r \right. \\ & \left. + [(\mathbf{u}_\nu \cdot \mathbf{e}_r)(\mathbf{v}_\nu \cdot \mathbf{e}_\theta) + (\mathbf{v}_\nu \cdot \mathbf{e}_r)(\mathbf{u}_\nu \cdot \mathbf{e}_\theta)] \mathbf{e}_\theta + [(\mathbf{u}_\nu \cdot \mathbf{e}_r)(\mathbf{v}_\nu \cdot \mathbf{e}_\varphi) + (\mathbf{v}_\nu \cdot \mathbf{e}_r)(\mathbf{u}_\nu \cdot \mathbf{e}_\varphi)] \mathbf{e}_\varphi \right\}. \end{aligned} \quad (\text{A.17})$$

Moreover, the electric field $\mathbf{E}_{\text{dip}}^{\text{mag}}$ created in the presence of a filiform magnetic current density \mathbf{m} between two opposite magnetic point charges of direction \mathbf{d}_m in static regime reads as

$$\mathbf{E}_{\text{dip}}^{\text{mag}}[\mathbf{d}_m, \kappa = 0](r, \theta, \varphi) = -\frac{I_\gamma}{4\pi c r^2} (\mathbf{d} \times \mathbf{e}_r). \quad (\text{A.18})$$

Finally, the electromagnetic fields ($\mathbf{E}_{\text{dip}}^{\text{mag}}, \mathbf{H}_{\text{dip}}^{\text{mag}}$) created in the presence of a time-harmonic magnetic dipole along a direction \mathbf{d} , are given by

$$\mathbf{H}_{\text{dip}}^{\text{mag}}[\mathbf{d}, \kappa](r, \theta, \varphi) = \frac{\exp(i\kappa r)}{4\pi r} \left\{ \left(\frac{3}{r^2} - \frac{3i\kappa}{r} - \kappa^2 \right) (\mathbf{d} \cdot \mathbf{e}_r) \mathbf{e}_r + \left(-\frac{1}{r^2} + \frac{i\kappa}{r} + \kappa^2 \right) \mathbf{d} \right\} \quad (\text{A.19})$$

and

$$\mathbf{E}_{\text{dip}}^{\text{mag}}[\mathbf{d}, \kappa](r, \theta, \varphi) = -\frac{\exp(i\kappa r)}{4\pi r} \left(\frac{1}{r} - i\kappa \right) (-i\kappa \mathbf{d}) \times \mathbf{e}_r. \quad (\text{A.20})$$

B Solutions of time-harmonic and nested Maxwell equations

B.1 Well-known properties on the scattering by spheres

Modal decomposition of solutions of Maxwell equations results from the spectral decomposition of tangential vector fields in $\mathbf{L}^2(S^2)$, where S^2 is the unit sphere. A tangential vector field $\boldsymbol{\lambda}$ in $\mathbf{L}^2(S_\rho)$ reads as a series which converges into $\mathbf{L}^2(S_\rho)$

$$\boldsymbol{\lambda} = \sum_{n=1}^{\infty} \sum_{m=-n}^n \lambda_{n,m}^\times \nabla_{S^2} Y_{n,m} + \lambda_{n,m}^t \mathbf{curl}_{S^2} Y_{n,m} \quad (\text{B.1})$$

where S_ρ denotes the sphere of radius ρ , see for instance [17, 30, 31]. The coefficients $\lambda_{n,m}^\times$ and $\lambda_{n,m}^t$ are defined as the projections of $\boldsymbol{\lambda}$ onto the orthogonal basis of the tangential vector fields in $\mathbf{L}^2(S^2)$, composed of vectorial spherical harmonics $\nabla_{S^2} Y_{n,m}$ and $\mathbf{curl}_{S^2} Y_{n,m}$

$$\lambda_{n,m}^\times = \frac{1}{n(n+1)} \int_{S_\rho} \boldsymbol{\lambda} \cdot \nabla_{S^2} \overline{Y_{n,m}}(\hat{x}) \, ds; \quad \lambda_{n,m}^t = \frac{1}{n(n+1)} \int_{S_\rho} \boldsymbol{\lambda} \cdot \mathbf{curl}_{S^2} \overline{Y_{n,m}}(\hat{x}) \, ds. \quad (\text{B.2})$$

The spherical harmonics $Y_{n,m}$ constitute an orthonormal basis of $L^2(\mathcal{S}^2)$, see [31],

$$Y_{n,m}(\theta, \varphi) = \sqrt{\frac{2n+1}{4\pi} \frac{(n-|m|)!}{(n+|m|)!}} P_{n,|m|}(\cos \theta) \exp(im\varphi). \quad (\text{B.3})$$

For any integer $m \in [0, n]$, $P_{n,m}$ is the m -th Legendre function of order n defined for $t \in [-1, 1]$ by

$$P_{n,m}(t) = (1-t^2)^{\frac{m}{2}} \left(\frac{d}{dt} \right)^m P_n(t) \quad (\text{B.4})$$

where $t \mapsto P_n(t)$ is the Legendre polynomial of order n

$$P_n(t) = \frac{(-1)^n}{2^n n!} \left(\frac{d}{dt} \right)^n (1-t^2)^n. \quad (\text{B.5})$$

The tangential operators $\nabla_{\mathcal{S}^2}$ and $\mathbf{curl}_{\mathcal{S}^2}$ are given in spherical coordinates by

$$\nabla_{\mathcal{S}^2} = \partial_\theta \mathbf{e}_\theta + \frac{1}{\sin \theta} \partial_\varphi \mathbf{e}_\varphi; \quad \mathbf{curl}_{\mathcal{S}^2} = \nabla_{\mathcal{S}^2} \times \mathbf{e}_r = \frac{1}{\sin \theta} \partial_\varphi \mathbf{e}_\theta - \partial_\theta \mathbf{e}_\varphi. \quad (\text{B.6a})$$

Proposition 2. *The vectorial spherical harmonics $\nabla_{\mathcal{S}^2} Y_{n,m}$ and $\mathbf{curl}_{\mathcal{S}^2} Y_{n,m}$ are the eigenvectors with multiplicity $2n+1$ associated to the eigenvalues $-n(n+1)$ of the vectorial Laplace-Beltrami operator $\Delta_{\mathcal{S}^2}$ defined on the unit sphere, reading as*

$$\Delta_{\mathcal{S}^2} = \nabla_{\mathcal{S}^2}(\text{div}_{\mathcal{S}^2}) - \mathbf{curl}_{\mathcal{S}^2}(\mathbf{curl}_{\mathcal{S}^2}), \quad (\text{B.7})$$

where surface operators $\text{div}_{\mathcal{S}^2}$ and $\mathbf{curl}_{\mathcal{S}^2}$ are respectively dual operators of $\nabla_{\mathcal{S}^2}$ and $\mathbf{curl}_{\mathcal{S}^2}$ for the pivot space $L^2(\mathcal{S}_\rho)$. In particular, the following properties hold

1. $\|\nabla_{\mathcal{S}^2} Y_{n,m}\|_{0,\mathcal{S}^2}^2 = \|\mathbf{curl}_{\mathcal{S}^2} Y_{n,m}\|_{0,\mathcal{S}^2}^2 = n(n+1)$;
2. the vectorial spherical harmonics are orthogonal in pairs and for $(n, m) \neq (n', m')$, we have

$$\int_{\mathcal{S}^2} \nabla_{\mathcal{S}^2} Y_{n,m} \cdot \nabla_{\mathcal{S}^2} \overline{Y_{n',m'}} \, ds = \int_{\mathcal{S}^2} \mathbf{curl}_{\mathcal{S}^2} Y_{n,m} \cdot \mathbf{curl}_{\mathcal{S}^2} \overline{Y_{n',m'}} \, ds = 0. \quad (\text{B.8})$$

The tangential trace decomposition (B.1) in $\mathbf{L}^2(\mathcal{S}^2)$ is the first step to determine modal decomposition of solutions of time-harmonic Maxwell equations. The second one is the use Debye potentials, see [30], which introduces a link between a scalar solution u of Helmholtz equation and vectorial solutions of time-harmonic Maxwell equations given by

$$(\mathbf{curl}(u\mathbf{x}), \frac{1}{i\kappa} \mathbf{curl} \mathbf{curl}(u\mathbf{x})). \quad (\text{B.9})$$

When u is a singular solution of Helmholtz equation, u can be represented as the series which converges in $L^2_{\text{loc}}(\mathbb{R}^3 \setminus \{0\})$,

$$u = \sum_{n=0}^{\infty} \sum_{m=-n}^n u_{n,m} h_n^{(1)}(\kappa r) Y_{n,m}(\hat{x}), \quad (\text{B.10})$$

where $L^2_{\text{loc}}(\mathbb{R}^3 \setminus \{0\})$ is the space of scalar functions u such that

$$\forall \psi \in \mathcal{C}_c^\infty(\mathbb{R}^3), \quad \psi = 0 \text{ in a neighborhood of } 0, \quad \psi u \in L^2(\mathbb{R}^3). \quad (\text{B.11})$$

The function $h_n^{(1)}$ denotes the n -order spherical Hankel function of first kind and we have the following properties:

Proposition 3. For any $n \geq 0$, the spherical Hankel function of the first kind $h_n^{(1)}$ is defined as $h_n^{(1)} = j_n + iy_n$, where j_n denotes the spherical Bessel function of order n and y_n the spherical Neumann function of order n . Both are solutions of the spherical Bessel differential equation in \mathbb{C}^* ,

$$\frac{d}{dr} \left(r^2 \frac{du}{dr} \right) + \kappa^2 r^2 u = n(n+1)u. \quad (\text{B.12})$$

The spherical Bessel functions are smooth nearby 0 whereas the Neumann functions are singular. Moreover, the spherical Hankel function can be described as a Laurent series expansion in a neighborhood of 0 as

$$h_n^{(1)}(z) = \sum_{\ell=-n-1}^{\infty} \mathfrak{h}_{n,\ell} z^\ell. \quad (\text{B.13})$$

The coefficients $\mathfrak{h}_{n,\ell}$ read as

$$\mathfrak{h}_{n,\ell} = \begin{cases} j_{n,\ell} & \text{if } \ell - n \text{ is even and } \ell \geq n \\ i \mathfrak{y}_{n,\ell} & \text{if } \ell - n \text{ is odd and } \ell \geq -n - 1 \\ 0 & \text{otherwise} \end{cases} \quad (\text{B.14})$$

where $j_{n,\ell}$ and $\mathfrak{y}_{n,\ell}$ are coefficients into series expansions of j_n and y_n given by

$$j_{n,\ell} = \begin{cases} \frac{\sqrt{\pi}}{2^{\ell+1}} \frac{(-1)^{\frac{\ell-n}{2}}}{(\frac{\ell-n}{2})! \Gamma(\frac{\ell+n+1}{2} + 1)} & \text{if } \ell - n \text{ is even and } \ell \geq n \\ 0 & \text{otherwise} \end{cases}$$

$$\mathfrak{y}_{n,\ell} = \begin{cases} (-1)^{n+1} \frac{\sqrt{\pi}}{2^{\ell+1}} \frac{(-1)^{\frac{\ell+n+1}{2}}}{(\frac{\ell+n+1}{2})! \Gamma(\frac{\ell-n}{2} + 1)} & \text{if } \ell - n \text{ is odd and } \ell \geq -n - 1 \\ 0 & \text{otherwise} \end{cases}$$

with Γ denotes the Euler gamma function, see [25] for more details.

The coefficients $u_{n,m}$ in (B.10) are defined as the projections of u onto the basis of $L^2(\mathcal{S}^2)$ composed of $Y_{n,m}$ on every sphere \mathcal{S}_ρ of radius $\rho > 0$

$$u_{n,m} = \frac{1}{h_n^{(1)}(\kappa\rho)} \int_{\mathcal{S}_\rho} u(\mathbf{x}) \overline{Y_{n,m}(\hat{x})} ds. \quad (\text{B.15})$$

Then, the associated Maxwell solution \mathbf{u} is also singular and reads as the following series which converges in $\mathbf{H}_{\text{loc}}(\mathbf{curl}, \mathbb{R}^3 \setminus \{0\})$,

$$\mathbf{u} = \sum_{n=0}^{\infty} \sum_{m=-n}^n \left\{ u_{n,m}^\times \mathbf{curl} (h_n^{(1)}(\kappa r) Y_{n,m}(\hat{x}) \mathbf{x}) + \frac{u_{n,m}^t}{i\kappa} \mathbf{curl} \mathbf{curl} (h_n^{(1)}(\kappa r) Y_{n,m}(\hat{x}) \mathbf{x}) \right\}. \quad (\text{B.16})$$

The complex magnitudes $u_{n,m}^\times$ and $u_{n,m}^t$ are defined as the projections of $\mathbf{n} \times \mathbf{u}$ onto the basis of tangential vector fields in $L^2(\mathcal{S}^2)$ on every sphere \mathcal{S}_ρ of radius $\rho > 0$

$$u_{n,m}^\times = -\frac{\lambda_{n,m}^\times}{h_n^{(1)}(\kappa\rho)}; \quad u_{n,m}^t = -\frac{i\kappa\rho\lambda_{n,m}^t}{h_n^{(1)}(\kappa\rho) + \kappa\rho h_n^{(1)'}(\kappa\rho)}, \quad (\text{B.17})$$

with $\lambda_{n,m}^\times$ and $\lambda_{n,m}^t$ are spectral coefficients (B.2) with $\boldsymbol{\lambda} = \mathbf{n} \times \mathbf{u}$.

B.2 Solutions of time-harmonic Maxwell equations as series

A singular solution $(\tilde{\mathbf{E}}_p, \tilde{\mathbf{H}}_p)$ with $p \geq 3$ of the time-harmonic Maxwell equations reads as the following series which converges into $\mathbf{H}_{\text{loc}}(\mathbf{curl}, \mathbb{R}^3 \setminus \{0\})$, see for instance [30],

$$\tilde{\mathbf{E}}_p = \sum_{n=1}^{\infty} \sum_{m=-n}^n \tilde{e}_{n,m}^{(p),\times}(r) \mathbf{curl}_{\mathbb{S}^2} Y_{n,m} + \tilde{e}_{n,m}^{(p),t}(r) \nabla_{\mathbb{S}^2} Y_{n,m} + \tilde{e}_{n,m}^{(p),r}(r) Y_{n,m} \mathbf{e}_r \quad (\text{B.18a})$$

$$\tilde{\mathbf{H}}_p = \sum_{n=1}^{\infty} \sum_{m=-n}^n \tilde{h}_{n,m}^{(p),\times}(r) \mathbf{curl}_{\mathbb{S}^2} Y_{n,m} + \tilde{h}_{n,m}^{(p),t}(r) \nabla_{\mathbb{S}^2} Y_{n,m} + \tilde{h}_{n,m}^{(p),r}(r) Y_{n,m} \mathbf{e}_r. \quad (\text{B.18b})$$

Convergence results are detailed in [26]. The radial coefficients are defined as projections of the vector fields onto the basis of $\mathbf{L}^2(\mathbb{S}^2)$ composed of $\mathbf{curl}_{\mathbb{S}^2} Y_{n,m}$, $\nabla_{\mathbb{S}^2} Y_{n,m}$ and onto $Y_{n,m} \mathbf{e}_r$

$$\begin{aligned} \tilde{e}_{n,m}^{(p),\times} &= \frac{1}{n(n+1)} \int_{\mathbb{S}^2} \tilde{\mathbf{E}}_p(r, \hat{x}) \cdot \mathbf{curl}_{\mathbb{S}^2} \overline{Y_{n,m}} \, ds; & \tilde{h}_{n,m}^{(p),\times} &= \frac{1}{n(n+1)} \int_{\mathbb{S}^2} \tilde{\mathbf{H}}_p(r, \hat{x}) \cdot \mathbf{curl}_{\mathbb{S}^2} \overline{Y_{n,m}} \, ds; \\ \tilde{e}_{n,m}^{(p),t} &= \frac{1}{n(n+1)} \int_{\mathbb{S}^2} \tilde{\mathbf{E}}_p(r, \hat{x}) \cdot \nabla_{\mathbb{S}^2} \overline{Y_{n,m}} \, ds; & \tilde{h}_{n,m}^{(p),t} &= \frac{1}{n(n+1)} \int_{\mathbb{S}^2} \tilde{\mathbf{H}}_p(r, \hat{x}) \cdot \nabla_{\mathbb{S}^2} \overline{Y_{n,m}} \, ds; \\ \tilde{e}_{n,m}^{(p),r} &= \int_{\mathbb{S}^2} \tilde{\mathbf{E}}_p(r, \hat{x}) \cdot \mathbf{e}_r \overline{Y_{n,m}} \, ds; & \tilde{h}_{n,m}^{(p),r} &= \int_{\mathbb{S}^2} \tilde{\mathbf{H}}_p(r, \hat{x}) \cdot \mathbf{e}_r \overline{Y_{n,m}} \, ds. \end{aligned}$$

According to Eq. (B.16), these projections can be expressed thanks to the Hankel functions $h_n^{(1)}$

$$\tilde{e}_{n,m}^{(p),\times} = u_{n,m}^{(p),\times} h_n^{(1)}(\kappa r); \quad \tilde{h}_{n,m}^{(p),\times} = -u_{n,m}^{(p),t} h_n^{(1)}(\kappa r) \quad (\text{B.19a})$$

$$\tilde{e}_{n,m}^{(p),t} = \frac{u_{n,m}^{(p),t}}{i\kappa r} (h_n^{(1)}(\kappa r) + \kappa r h_n^{(1)' }(\kappa r)); \quad \tilde{h}_{n,m}^{(p),t} = \frac{u_{n,m}^{(p),\times}}{i\kappa r} (h_n^{(1)}(\kappa r) + \kappa r h_n^{(1)' }(\kappa r)) \quad (\text{B.19b})$$

$$\tilde{e}_{n,m}^{(p),r} = \frac{n(n+1)u_{n,m}^{(p),t}}{i\kappa r} h_n^{(1)}(\kappa r); \quad \tilde{h}_{n,m}^{(p),r} = \frac{n(n+1)u_{n,m}^{(p),\times}}{i\kappa r} h_n^{(1)}(\kappa r) \quad (\text{B.19c})$$

where the complex magnitudes $u_{n,m}^{(p),\times}$ and $u_{n,m}^{(p),t}$ are modal coefficients (B.17) with $\mathbf{u} = \tilde{\mathbf{E}}_p$. The magnitudes $u_{n,m}^{(p),\times}$ and $u_{n,m}^{(p),t}$ are not only defined through the spectral decomposition of $\tilde{\mathbf{E}}_p$ but are also related to the modal decomposition of near-field terms using the matching conditions (4.18). These conditions allow to establish that in (B.18), only a finite number of coefficients are not equal to zero. To give details of this dependence, the study of behavior of the far-field terms $(\tilde{\mathbf{E}}_p, \tilde{\mathbf{H}}_p)$ is required. That goes through a Laurent series expansion of the Hankel functions of the first kind $h_n^{(1)}$. According to Proposition 3, the radial coefficients $\tilde{\diamond}_{n,m}^{(p),\times}$, $\tilde{\diamond}_{n,m}^{(p),t}$ and $\tilde{\diamond}_{n,m}^{(p),r}$ for $\diamond = e$ or h can be described as Laurent series expansions in a neighborhood of 0 as

$$\tilde{e}_{n,m}^{(p),\times} = u_{n,m}^{(p),\times} \sum_{\ell=-n-1}^{\infty} \mathfrak{h}_{n,\ell}(\kappa r)^\ell; \quad \tilde{h}_{n,m}^{(p),\times} = -u_{n,m}^{(p),t} \sum_{\ell=0}^{\infty} \mathfrak{h}_{n,\ell}(\kappa r)^\ell \quad (\text{B.20a})$$

$$\tilde{e}_{n,m}^{(p),t} = u_{n,m}^{(p),t} \sum_{\ell=-n-2}^{\infty} \frac{\mathfrak{h}_{n,\ell+1}}{i}(\ell+2)(\kappa r)^\ell; \quad \tilde{h}_{n,m}^{(p),t} = u_{n,m}^{(p),\times} \sum_{\ell=-n-2}^{\infty} \frac{\mathfrak{h}_{n,\ell+1}}{i}(\ell+2)(\kappa r)^\ell \quad (\text{B.20b})$$

$$\frac{\tilde{e}_{n,m}^{(p),r}}{n(n+1)} = u_{n,m}^{(p),t} \sum_{\ell=-n-2}^{\infty} \frac{\mathfrak{h}_{n,\ell+1}}{i}(\kappa r)^\ell; \quad \frac{\tilde{h}_{n,m}^{(p),r}}{n(n+1)} = u_{n,m}^{(p),\times} \sum_{\ell=-n-2}^{\infty} \frac{\mathfrak{h}_{n,\ell+1}}{i}(\kappa r)^\ell. \quad (\text{B.20c})$$

B.3 Solutions of the static and nested Maxwell equations as series

B.3.1 Solutions of the static Maxwell equations as series

A regular solution $(\widehat{\mathbf{E}}_{p,0}, \widehat{\mathbf{H}}_{p,0})$ with $p \geq 0$ of the homogeneous static Maxwell equations in the exterior domain $\widehat{\Omega}$ reads as the following series which converges into $\mathbf{H}(\mathbf{curl}, \widehat{\Omega})$,

$$\widehat{\mathbf{E}}_{p,0}(\mathbf{X}) = \sum_{n=1}^{\infty} \sum_{m=-n}^n \frac{\widehat{e}_{n,m}^{(p)}}{R^{n+2}} \left(\nabla_{S^2} Y_{n,m}(\widehat{x}) - (n+1)Y_{n,m}(\widehat{x})\mathbf{e}_r \right) \quad (\text{B.21a})$$

$$\widehat{\mathbf{H}}_{p,0}(\mathbf{X}) = \sum_{n=1}^{\infty} \sum_{m=-n}^n \frac{\widehat{h}_{n,m}^{(p)}}{R^{n+2}} \left(\nabla_{S^2} Y_{n,m}(\widehat{x}) - (n+1)Y_{n,m}(\widehat{x})\mathbf{e}_r \right). \quad (\text{B.21b})$$

The spectral coefficients $\widehat{e}_{n,m}^{(p)}$ are defined as projections of $\widehat{\mathbf{E}}_{p,0}$ onto the vectorial spherical harmonics $\nabla_{S^2} Y_{n,m}$ on the unit sphere S^2 ,

$$\widehat{e}_{n,m}^{(p)} = \frac{1}{n(n+1)} \int_{S^2} (\mathbf{e}_r \times \widehat{\mathbf{E}}_{p,0}) \cdot \mathbf{curl}_{S^2} \overline{Y_{n,m}} \, ds.$$

The others coefficients $\widehat{h}_{n,m}^{(p)}$ are projections of $\widehat{\mathbf{H}}_{p,0}$ onto the basis vector fields $Y_{n,m}\mathbf{e}_r$ on S^2 ,

$$\widehat{h}_{n,m}^{(p)} = -\frac{1}{n+1} \int_{S^2} (\mathbf{e}_r \cdot \widehat{\mathbf{H}}_{p,0}) \overline{Y_{n,m}} \, ds.$$

In order to obtain the boundary conditions (4.13) and apply the calculation of these coefficients in practice, we require the following recursive relations for any $p \geq 0$,

$$\begin{aligned} \widehat{e}_{n,m}^{(p)} = -\frac{1}{n(n+1)} \sum_{|\alpha|=p} \frac{1}{\alpha!} \int_{S^2} (\mathbf{e}_r \times (d^\alpha \mathbf{E}^{\text{inc}}(0) \cdot \mathbf{e}_r^\alpha)) \cdot \mathbf{curl}_{S^2} \overline{Y_{n,m}} \, ds \\ - \sum_{\ell=1}^p \kappa^\ell \frac{\ell-n}{n} \frac{\mathfrak{h}_{n,\ell-n-1}}{\mathfrak{h}_{n,-n-1}} \widehat{e}_{n,m}^{(p-\ell)} \end{aligned} \quad (\text{B.22a})$$

and

$$\widehat{h}_{n,m}^{(p)} = \frac{1}{n+1} \sum_{|\alpha|=p} \frac{1}{\alpha!} \int_{S^2} (\mathbf{e}_r \cdot (d^\alpha \mathbf{H}^{\text{inc}}(0) \cdot \mathbf{e}_r^\alpha)) \overline{Y_{n,m}} \, ds - \sum_{\ell=1}^p \kappa^\ell \frac{\mathfrak{h}_{n,\ell-n-1}}{\mathfrak{h}_{n,-n-1}} \widehat{h}_{n,m}^{(p-\ell)}. \quad (\text{B.22b})$$

The coefficients $\mathfrak{h}_{n,\ell}$ denote the coefficients before the ℓ -power of r into the expansion as Laurent series of the n -order Hankel function $h_n^{(1)}$ of the first kind, see Proposition 3.

Remark 25. Expressions in equations (B.21) define a regular solution of the homogeneous static Maxwell equations in exterior domain $\widehat{\Omega}$. To show that, we go through intrinsic expressions of the rotational and the divergence of a smooth vector field $\mathbf{u} = u_r \mathbf{e}_r + \mathbf{u}_t$, given by

$$\mathbf{curl} \, \mathbf{u} = \frac{1}{R} \mathbf{curl}_{S^2} \mathbf{u}_t + \frac{1}{R} \mathbf{curl}_{S^2} u_r + \frac{1}{R} \partial_R [\mathbf{R} \mathbf{e}_r \times \mathbf{u}_t] ; \quad \text{div} \, \mathbf{u} = \frac{1}{R^2} \partial_R [R^2 u_r] + \frac{1}{R} \text{div}_{S^2} \mathbf{u}_t \quad (\text{B.23})$$

where the operators \mathbf{curl}_{S^2} and div_{S^2} denote respectively the dual operators of \mathbf{curl}_{S^2} and ∇_{S^2} for the pivot space $\mathbf{L}^2(S^2)$. Since the following properties hold

$$\mathbf{curl}_{S^2} \nabla_{S^2} Y_{n,m} = 0 ; \quad \mathbf{e}_r \times \nabla_{S^2} Y_{n,m} = -\mathbf{curl}_{S^2} Y_{n,m} ; \quad \text{div}_{S^2} \nabla_{S^2} Y_{n,m} = -n(n+1)Y_{n,m} \quad (\text{B.24})$$

we observe that $(\widehat{\mathbf{E}}_{p,0}, \widehat{\mathbf{H}}_{p,0})$ satisfies

$$\left\{ \begin{array}{l} \operatorname{curl} \widehat{\mathbf{E}}_{p,0} = \frac{1}{R} \sum_{n=1}^{\infty} \sum_{m=-n}^n \frac{\widehat{e}_{n,m}^{(p)}}{R^{n+2}} [-(n+1) \operatorname{curl}_{S^2} Y_{n,m} - (n+1) \mathbf{e}_r \times \nabla_{S^2} Y_{n,m}] = 0 \quad ; \\ \operatorname{curl} \widehat{\mathbf{H}}_{p,0} = \frac{1}{R} \sum_{n=1}^{\infty} \sum_{m=-n}^n \frac{\widehat{h}_{n,m}^{(p)}}{R^{n+2}} [-(n+1) \operatorname{curl}_{S^2} Y_{n,m} - (n+1) \mathbf{e}_r \times \nabla_{S^2} Y_{n,m}] = 0 \quad ; \\ \operatorname{div} \widehat{\mathbf{E}}_{p,0} = \frac{1}{R^2} \sum_{n=1}^{\infty} \sum_{m=-n}^n \frac{\widehat{e}_{n,m}^{(p)}}{R^{n+1}} [n(n+1) Y_{n,m} + \operatorname{div}_{S^2} \nabla_{S^2} Y_{n,m}] = 0 \quad ; \\ \operatorname{div} \widehat{\mathbf{H}}_{p,0} = \frac{1}{R^2} \sum_{n=1}^{\infty} \sum_{m=-n}^n \frac{\widehat{h}_{n,m}^{(p)}}{R^{n+1}} [n(n+1) Y_{n,m} + \operatorname{div}_{S^2} \nabla_{S^2} Y_{n,m}] = 0 \quad . \end{array} \right.$$

B.3.2 Solutions of the nested Maxwell equations as series

Proposition 4. For any $p \geq 0$, a solution $(\widehat{\mathbf{E}}_p, \widehat{\mathbf{H}}_p)$ of the nested Maxwell equations reads as the following series which converges into $\mathbf{H}_{\text{loc}}(\operatorname{curl}, \mathbb{R}^3 \setminus \overline{\mathcal{B}(0,1)})$

$$\widehat{\mathbf{E}}_p = \sum_{\ell=0}^p \widehat{\mathbf{E}}_{p,\ell} ; \quad \widehat{\mathbf{H}}_p = \sum_{\ell=0}^p \widehat{\mathbf{H}}_{p,\ell} \quad (\text{B.25})$$

where

$$\widehat{\mathbf{E}}_{p,\ell} = \sum_{n=1}^{\infty} \sum_{m=-n}^n \widehat{e}_{n,m,\ell}^{(p),\times}(\mathbb{R}) \operatorname{curl}_{S^2} Y_{n,m} + \widehat{e}_{n,m,\ell}^{(p),t}(\mathbb{R}) \nabla_{S^2} Y_{n,m} + \widehat{e}_{n,m,\ell}^{(p),r}(\mathbb{R}) Y_{n,m} \mathbf{e}_r \quad (\text{B.26a})$$

$$\widehat{\mathbf{H}}_{p,\ell} = \sum_{n=1}^{\infty} \sum_{m=-n}^n \widehat{h}_{n,m,\ell}^{(p),\times}(\mathbb{R}) \operatorname{curl}_{S^2} Y_{n,m} + \widehat{h}_{n,m,\ell}^{(p),t}(\mathbb{R}) \nabla_{S^2} Y_{n,m} + \widehat{h}_{n,m,\ell}^{(p),r}(\mathbb{R}) Y_{n,m} \mathbf{e}_r. \quad (\text{B.26b})$$

The radial coefficients are given by

$$\begin{aligned} \widehat{e}_{n,m,\ell}^{(p),\times} &= -\frac{i\kappa^\ell}{R^{n+2-\ell}} \frac{1}{n} \frac{\mathfrak{h}_{n,\ell-n-2}}{\mathfrak{h}_{n,-n-1}} \widehat{h}_{n,m}^{(p-\ell)} \quad ; \quad \widehat{h}_{n,m,\ell}^{(p),\times} = \frac{i\kappa^\ell}{R^{n+2-\ell}} \frac{1}{n} \frac{\mathfrak{h}_{n,\ell-n-2}}{\mathfrak{h}_{n,-n-1}} \widehat{e}_{n,m}^{(p-\ell)} \quad ; \\ \widehat{e}_{n,m,\ell}^{(p),t} &= -\frac{\kappa^\ell}{R^{n+2-\ell}} \frac{\ell-n}{n} \frac{\mathfrak{h}_{n,\ell-n-1}}{\mathfrak{h}_{n,-n-1}} \widehat{e}_{n,m}^{(p-\ell)} \quad ; \quad \widehat{h}_{n,m,\ell}^{(p),t} = -\frac{\kappa^\ell}{R^{n+2-\ell}} \frac{\ell-n}{n} \frac{\mathfrak{h}_{n,\ell-n-1}}{\mathfrak{h}_{n,-n-1}} \widehat{h}_{n,m}^{(p-\ell)} \quad ; \\ \widehat{e}_{n,m,\ell}^{(p),r} &= -\frac{\kappa^\ell}{R^{n+2-\ell}} \frac{\mathfrak{h}_{n,\ell-n-1}}{\mathfrak{h}_{n,-n-1}} (n+1) \widehat{e}_{n,m}^{(p-\ell)} \quad ; \quad \widehat{h}_{n,m,\ell}^{(p),r} = -\frac{\kappa^\ell}{R^{n+2-\ell}} \frac{\mathfrak{h}_{n,\ell-n-1}}{\mathfrak{h}_{n,-n-1}} (n+1) \widehat{h}_{n,m}^{(p-\ell)} \quad . \end{aligned}$$

Remark 26. In (B.26), the series with $\ell = 0$ correspond to the series expansions of $(\widehat{\mathbf{E}}_{p,0}, \widehat{\mathbf{H}}_{p,0})$, according to the following identities

$$\begin{aligned} \widehat{e}_{n,m,0}^{(p),\times} &= 0 ; & \widehat{e}_{n,m,0}^{(p),t} &= \frac{\widehat{e}_{n,m}^{(p)}}{R^{n+2}} ; & \widehat{e}_{n,m,0}^{(p),r} &= -\frac{n+1}{R^{n+2}} \widehat{e}_{n,m}^{(p)} ; \\ \widehat{h}_{n,m,0}^{(p),\times} &= 0 ; & \widehat{h}_{n,m,0}^{(p),t} &= \frac{\widehat{h}_{n,m}^{(p)}}{R^{n+2}} ; & \widehat{h}_{n,m,0}^{(p),r} &= -\frac{n+1}{R^{n+2}} \widehat{h}_{n,m}^{(p)} . \end{aligned}$$

Remark 27. The sub-terms $(\widehat{\mathbf{E}}_{p,\ell}, \widehat{\mathbf{H}}_{p,\ell})$ are built such that they satisfy *sub-nested* Maxwell equations in the following sense

$$\operatorname{curl} \widehat{\mathbf{E}}_{p,\ell} = i\kappa \widehat{\mathbf{H}}_{p-1,\ell-1} \text{ in } \widehat{\Omega} ; \quad \operatorname{curl} \widehat{\mathbf{H}}_{p,\ell} = -i\kappa \widehat{\mathbf{E}}_{p-1,\ell-1} \text{ in } \widehat{\Omega}. \quad (\text{B.27})$$

In (B.27), we use the convention $\widehat{\mathbf{E}}_{p,\ell} = \widehat{\mathbf{H}}_{p,\ell} = 0$ if $p < 0$ or $\ell < 0$. If each sub-term $(\widehat{\mathbf{E}}_{p,\ell}, \widehat{\mathbf{H}}_{p,\ell})$ satisfies the equations (B.27) then the near-field term $(\widehat{\mathbf{E}}_p, \widehat{\mathbf{H}}_p)$ defined as (B.25) satisfies the nested Maxwell equations (4.9).

Proof of Proposition 4. The family $(\widehat{\mathbf{E}}_{p,\ell}, \widehat{\mathbf{H}}_{p,\ell})$ satisfies the nested Maxwell equations (B.27). Actually, we apply operators (B.23) on the previous series in order to compare them to the modal coefficients of $(i\kappa\widehat{\mathbf{H}}_{p-1,\ell-1}, -i\kappa\widehat{\mathbf{E}}_{p-1,\ell-1})$,

$$\begin{aligned} \mathbf{curl} \widehat{\mathbf{E}}_{p,\ell} &= \\ & \sum_{n=1}^{\infty} \sum_{m=-n}^n (\mathbf{curl} \widehat{\mathbf{E}}_{p,\ell})_{n,m}^{\times} \mathbf{curl}_{S^2} Y_{n,m} + (\mathbf{curl} \widehat{\mathbf{E}}_{p,\ell})_{n,m}^t \nabla_{S^2} Y_{n,m} + (\mathbf{curl} \widehat{\mathbf{E}}_{p,\ell})_{n,m}^r Y_{n,m} \mathbf{e}_r \\ \mathbf{curl} \widehat{\mathbf{H}}_{p,\ell} &= \\ & \sum_{n=1}^{\infty} \sum_{m=-n}^n (\mathbf{curl} \widehat{\mathbf{H}}_{p,\ell})_{n,m}^{\times} \mathbf{curl}_{S^2} Y_{n,m} + (\mathbf{curl} \widehat{\mathbf{H}}_{p,\ell})_{n,m}^t \nabla_{S^2} Y_{n,m} + (\mathbf{curl} \widehat{\mathbf{H}}_{p,\ell})_{n,m}^r Y_{n,m} \mathbf{e}_r \end{aligned}$$

where the modal coefficients of $(\mathbf{curl} \widehat{\mathbf{E}}_{p,\ell}, \mathbf{curl} \widehat{\mathbf{H}}_{p,\ell})$ are given by

$$\begin{aligned} (\mathbf{curl} \widehat{\mathbf{E}}_{p,\ell})_{n,m}^{\times} &= \frac{1}{R} \widehat{e}_{n,m,\ell}^{(p),r} - \frac{1}{R} \partial_R [\mathcal{R} \widehat{e}_{n,m,\ell}^{(p),t}]; & (\mathbf{curl} \widehat{\mathbf{H}}_{p,\ell})_{n,m}^{\times} &= \frac{1}{R} \widehat{h}_{n,m,\ell}^{(p),r} - \frac{1}{R} \partial_R [\mathcal{R} \widehat{h}_{n,m,\ell}^{(p),t}]; \\ (\mathbf{curl} \widehat{\mathbf{E}}_{p,\ell})_{n,m}^t &= \frac{1}{R} \partial_R [\mathcal{R} \widehat{e}_{n,m,\ell}^{(p),\times}]; & (\mathbf{curl} \widehat{\mathbf{H}}_{p,\ell})_{n,m}^t &= \frac{1}{R} \partial_R [\mathcal{R} \widehat{h}_{n,m,\ell}^{(p),\times}]; \\ (\mathbf{curl} \widehat{\mathbf{E}}_{p,\ell})_{n,m}^r &= \frac{n(n+1)}{R} \widehat{e}_{n,m,\ell}^{(p),\times}; & (\mathbf{curl} \widehat{\mathbf{H}}_{p,\ell})_{n,m}^r &= \frac{n(n+1)}{R} \widehat{h}_{n,m,\ell}^{(p),\times}. \end{aligned}$$

That is due to the properties (B.24) and also to the following one

$$\mathbf{curl}_{S^2} \mathbf{curl}_{S^2} Y_{n,m} = n(n+1) Y_{n,m}. \quad (\text{B.28})$$

Expanding radial coefficients of $(\mathbf{curl} \widehat{\mathbf{E}}_{p,\ell}, \mathbf{curl} \widehat{\mathbf{H}}_{p,\ell})$, we observe that

$$\begin{aligned} (\mathbf{curl} \widehat{\mathbf{E}}_{p,\ell})_{n,m}^t &= i\kappa \frac{-\kappa^{\ell-1}}{R^{n+2-(\ell-1)}} \frac{(\ell-1)-n}{n} \frac{\mathfrak{h}_{n,(\ell-1)-n-1}}{\mathfrak{h}_{n,-n-1}} \widehat{h}_{n,m}^{(p-\ell)} = i\kappa \widehat{e}_{n,m,\ell-1}^{(p-1),t} \\ (\mathbf{curl} \widehat{\mathbf{E}}_{p,\ell})_{n,m}^r &= i\kappa \frac{\kappa^{\ell-1}}{R^{n+2-(\ell-1)}} \frac{\mathfrak{h}_{(\ell-1)-n-1}}{\mathfrak{h}_{n,-n-1}} (n+1) \widehat{h}_{n,m}^{(p-\ell)} = i\kappa \widehat{e}_{n,m,\ell-1}^{(p-1),r} \\ (\mathbf{curl} \widehat{\mathbf{H}}_{p,\ell})_{n,m}^t &= -i\kappa \frac{-\kappa^{\ell-1}}{R^{n+2-(\ell-1)}} \frac{(\ell-1)-n}{n} \frac{\mathfrak{h}_{n,(\ell-1)-n-1}}{\mathfrak{h}_{n,-n-1}} \widehat{e}_{n,m}^{(p-\ell)} = -i\kappa \widehat{h}_{n,m,\ell-1}^{(p-1),t} \\ (\mathbf{curl} \widehat{\mathbf{H}}_{p,\ell})_{n,m}^r &= -i\kappa \frac{-\kappa^{\ell-1}}{R^{n+2-(\ell-1)}} \frac{\mathfrak{h}_{(\ell-1)-n-1}}{\mathfrak{h}_{n,-n-1}} (n+1) \widehat{e}_{n,m}^{(p-\ell)} = -i\kappa \widehat{h}_{n,m,\ell-1}^{(p-1),r} \end{aligned}$$

and

$$\begin{aligned} (\mathbf{curl} \widehat{\mathbf{E}}_{p,\ell})_{n,m}^{\times} &= i\kappa \frac{i\kappa^{\ell-1}}{R^{n+2-(\ell-1)}} \frac{1}{n} \frac{\ell(1+2n-\ell)\mathfrak{h}_{n,\ell-n-1}}{\mathfrak{h}_{n,-n-1}} \widehat{e}_{n,m}^{(p-\ell)} \\ (\mathbf{curl} \widehat{\mathbf{H}}_{p,\ell})_{n,m}^{\times} &= -i\kappa \frac{-i\kappa^{\ell-1}}{R^{n+2-(\ell-1)}} \frac{1}{n} \frac{\ell(1+2n-\ell)\mathfrak{h}_{n,\ell-n-1}}{\mathfrak{h}_{n,-n-1}} \widehat{h}_{n,m}^{(p-\ell)}. \end{aligned}$$

Furthermore, we have $\ell(1+2n-\ell)\mathfrak{h}_{n,\ell-n-1} = \mathfrak{h}_{n,\ell-n-3}$ and then, the set of shadows $(\widehat{\mathbf{E}}_{p,\ell}, \widehat{\mathbf{H}}_{p,\ell})$ satisfies the nested Maxwell equations (B.27). Finally, the sum of shadows satisfies the property (4.15) because $n+2-\ell \geq 3-p$ for any $n \geq 1$ and $\ell \leq p$. \square

B.3.3 First terms of the near-field expansion as finite sums

The decomposition for solutions of tie-harmonic Maxwell equations can be extended to more complex geometries as well as these ones for the time-harmonic Maxwell equations, but in general the series are infinite, see [26, 30]. In the case of the scattering by a sphere, in particular considering the boundary conditions (4.13), these series are actually finite sums. The following corollary that is a consequence of (B.21) and (4.13), characterizes the zeroth order near-field term $(\widehat{\mathbf{E}}_0, \widehat{\mathbf{H}}_0)$ as a finite sum of dipoles.

Corollary 1. *The zeroth order near-field term $(\widehat{\mathbf{E}}_0, \widehat{\mathbf{H}}_0)$ have the following modal decomposition*

$$\widehat{\mathbf{E}}_0 = \frac{1}{\mathbb{R}^3} \sum_{m=-1}^1 \widehat{e}_{1,m}^{(0)} \left[\nabla_{S^2} Y_{1,m} - 2Y_{1,m} \mathbf{e}_r \right]; \quad \widehat{\mathbf{H}}_0 = \frac{1}{\mathbb{R}^3} \sum_{m=-1}^1 \widehat{h}_{1,m}^{(0)} \left[\nabla_{S^2} Y_{1,m} - 2Y_{1,m} \mathbf{e}_r \right]. \quad (\text{B.29})$$

The result is due to the following lemma in which we decompose a vector field in the basis of the spherical harmonics. Then, we observe that in (B.21), there is only a finite number of radial coefficients $\widehat{e}_{n,m}^{(0)}$ and $\widehat{h}_{n,m}^{(0)}$ not equal to zero. In particular, it is for $n = 1$.

Lemma 1. *Let \mathbf{u} be a constant vector field of \mathbb{R}^3 . Let us denote (u_1, u_2, u_3) its coordinates in the canonical basis of \mathbb{R}^3 . The normal and tangential traces of \mathbf{u} on S^2 read in the basis of spherical harmonics as*

$$\gamma_n \mathbf{u} = \frac{u_1 + iu_2}{2} \sqrt{\frac{8\pi}{3}} Y_{1,-1} + \frac{u_1 - iu_2}{2} \sqrt{\frac{8\pi}{3}} Y_{1,1} + u_3 \sqrt{\frac{4\pi}{3}} Y_{1,0} \quad (\text{B.30a})$$

$$\gamma_t \mathbf{u} = \frac{u_1 + iu_2}{2} \sqrt{\frac{8\pi}{3}} \nabla_{S^2} Y_{1,-1} + \frac{u_1 - iu_2}{2} \sqrt{\frac{8\pi}{3}} \nabla_{S^2} Y_{1,1} + u_3 \sqrt{\frac{4\pi}{3}} \nabla_{S^2} Y_{1,0}. \quad (\text{B.30b})$$

The following corollary characterizes the first order near-field terms $(\widehat{\mathbf{E}}_1, \widehat{\mathbf{H}}_1)$ as a finite sum of dipoles and quadrupoles.

Corollary 2. *The leading part of the first order near-field term $(\widehat{\mathbf{E}}_{1,0}, \widehat{\mathbf{H}}_{1,0})$ have the following modal decomposition*

$$\widehat{\mathbf{E}}_{1,0} = \frac{1}{\mathbb{R}^4} \sum_{m=-2}^2 \widehat{e}_{2,m}^{(1)} \left[\nabla_{S^2} Y_{2,m} - 3Y_{2,m} \mathbf{e}_r \right]; \quad \widehat{\mathbf{H}}_{1,0} = \frac{1}{\mathbb{R}^4} \sum_{m=-2}^2 \widehat{h}_{2,m}^{(1)} \left[\nabla_{S^2} Y_{2,m} - 3Y_{2,m} \mathbf{e}_r \right]. \quad (\text{B.31})$$

The associated shadows $(\widehat{\mathbf{E}}_{1,1}, \widehat{\mathbf{H}}_{1,1})$ have the following modal decomposition

$$\widehat{\mathbf{E}}_{1,1} = -\frac{i\kappa}{\mathbb{R}^2} \sum_{m=-1}^1 \widehat{h}_{1,m}^{(0)} \mathbf{curl}_{S^2} Y_{1,m}; \quad \widehat{\mathbf{H}}_{1,1} = \frac{i\kappa}{\mathbb{R}^2} \sum_{m=-1}^1 \widehat{e}_{1,m}^{(0)} \mathbf{curl}_{S^2} Y_{1,m}. \quad (\text{B.32})$$

The result is due to the following lemma in which we decompose a vector field reading as $\mathbf{M}\mathbf{e}_r$, where \mathbf{M} is a constant matrix, in the basis of the spherical harmonics. Then, we observe that in (B.25)-(B.26), there is only a finite number of radial coefficients $\widehat{e}_{n,m}^{(1)}$ and $\widehat{h}_{n,m}^{(1)}$ not equal to zero. In particular, it is for $n = 2$.

Lemma 2. *Let \mathbf{M} be a constant matrix of size 3×3 . Let us denote $(m_{i,j})$ its coordinates relatively to the canonical basis of \mathbb{R}^3 . The normal and tangential traces of the vector field $\mathbf{M}\mathbf{e}_r$ on S^2 read in*

the basis of spherical harmonics as

$$\begin{aligned}\gamma_n(\mathbf{M}\mathbf{e}_r) &= \frac{m_{1,1} - m_{2,2}}{2} \sqrt{\frac{8\pi}{15}} (Y_{2,2} + Y_{2,-2}) + \frac{m_{1,2} + m_{2,1}}{2i} \sqrt{\frac{8\pi}{15}} (Y_{2,2} - Y_{2,-2}) + \\ &\quad \frac{m_{1,3} + m_{3,1}}{2} \sqrt{\frac{8\pi}{15}} (Y_{2,1} + Y_{2,-1}) + \frac{m_{2,3} + m_{3,2}}{2i} \sqrt{\frac{8\pi}{15}} (Y_{2,1} - Y_{2,-1}) + \frac{m_{3,3}}{2} \sqrt{\frac{16\pi}{5}} Y_{2,0}. \\ \gamma_t(\mathbf{M}\mathbf{e}_r) &= \frac{2m_{3,3} - m_{1,1} + m_{2,2}}{2} \sqrt{\frac{4\pi}{45}} \nabla_{S^2} Y_{2,0} + \frac{m_{1,1} - m_{2,2}}{4} \sqrt{\frac{8\pi}{15}} (\nabla_{S^2} Y_{2,-2} + \nabla_{S^2} Y_{2,2}) \\ &\quad + \frac{m_{1,3} + m_{3,1}}{4} \sqrt{\frac{8\pi}{15}} (\nabla_{S^2} Y_{2,-1} + \nabla_{S^2} Y_{2,1}) + \frac{m_{2,3} + m_{3,2}}{4i} \sqrt{\frac{8\pi}{15}} (\nabla_{S^2} Y_{2,1} - \nabla_{S^2} Y_{2,-1}) \\ &\quad + \frac{m_{1,2} + m_{2,1}}{4i} \sqrt{\frac{8\pi}{15}} (\nabla_{S^2} Y_{2,2} - \nabla_{S^2} Y_{2,-2}) + \frac{m_{3,1} - m_{1,3}}{4i} \sqrt{\frac{8\pi}{3}} (\mathbf{curl}_{S^2} Y_{1,1} - \mathbf{curl}_{S^2} Y_{1,-1}) \\ &\quad + \frac{m_{3,2} - m_{2,3}}{4} \sqrt{\frac{8\pi}{3}} (\mathbf{curl}_{S^2} Y_{1,1} + \mathbf{curl}_{S^2} Y_{1,-1}) + \frac{m_{2,1} - m_{1,2}}{2} \sqrt{\frac{4\pi}{3}} \mathbf{curl}_{S^2} Y_{1,0}.\end{aligned}$$

C Analytical solution of the scattering problem by one small sphere

In this section, we develop the Taylor expansion of the analytical solution of the electromagnetic scattering by a small sphere. The result validates the expression of the far-field expansion $(\delta^3 \tilde{\mathbf{E}}_3, \delta^3 \tilde{\mathbf{H}}_3)$. In a first time, we recall some results about regular solutions of Maxwell expansions in order to introduce the modal decomposition of the incident field.

C.1 Analytical decomposition of the incident field

The incident electromagnetic fields $(\mathbf{E}^{\text{inc}}, \mathbf{H}^{\text{inc}})$ are regular solutions of the time-harmonic Maxwell equations, in any bounded domain of \mathbb{R}^3 . Then, we can decompose these ones into the basis of regular solutions of the Maxwell equations, related to the spherical Bessel functions j_n , see [30],

$$\begin{aligned}\mathbf{E}^{\text{inc}}(\mathbf{x}) &= \sum_{n=1}^{\infty} \sum_{m=-n}^n \left\{ \mathbf{h}_{n,m}^{\text{inc}} j_n(\kappa r) \mathbf{curl}_{S^2} Y_{n,m}(\hat{x}) \right. \\ &\quad \left. + \mathbf{e}_{n,m}^{\text{inc}} \left[\frac{j_n(\kappa r) + \kappa r j_n'(\kappa r)}{i\kappa r} \nabla_{S^2} Y_{n,m}(\hat{x}) + \frac{j_n(\kappa r)}{i\kappa r} n(n+1) Y_{n,m}(\hat{x}) \mathbf{e}_r(\mathbf{x}) \right] \right\} \quad (\text{C.1a})\end{aligned}$$

and

$$\begin{aligned}\mathbf{H}^{\text{inc}}(\mathbf{x}) &= \sum_{n=1}^{\infty} \sum_{m=-n}^n \left\{ -\mathbf{e}_{n,m}^{\text{inc}} j_n(\kappa r) \mathbf{curl}_{S^2} Y_{n,m}(\hat{x}) \right. \\ &\quad \left. + \mathbf{h}_{n,m}^{\text{inc}} \left[\frac{j_n(\kappa r) + \kappa r j_n'(\kappa r)}{i\kappa r} \nabla_{S^2} Y_{n,m}(\hat{x}) + \frac{j_n(\kappa r)}{i\kappa r} n(n+1) Y_{n,m}(\hat{x}) \mathbf{e}_r(\mathbf{x}) \right] \right\} \quad (\text{C.1b})\end{aligned}$$

In (C.1), the modal coefficients have the following expression for any $\delta > 0$,

$$\mathbf{e}_{n,m}^{\text{inc}} = -\frac{i\kappa\delta}{j_n(\kappa\delta) + \kappa\delta j_n'(\kappa\delta)} \frac{1}{n(n+1)} \int_{\{|\mathbf{x}|=\delta\}} (\mathbf{n} \times \mathbf{E}^{\text{inc}})(\mathbf{x}) \cdot \mathbf{curl}_{S^2} \overline{Y_{n,m}}(\hat{x}) \, ds \quad (\text{C.2a})$$

$$\mathbf{h}_{n,m}^{\text{inc}} = -\frac{1}{j_n(\kappa\delta)} \frac{1}{n(n+1)} \int_{\{|\mathbf{x}|=\delta\}} (\mathbf{n} \times \mathbf{E}^{\text{inc}})(\mathbf{x}) \cdot \nabla_{S^2} \overline{Y_{n,m}}(\hat{x}) \, ds \quad (\text{C.2b})$$

where \mathbf{n} denotes the outward normal unit vector to $\mathcal{B}(0, \delta)$.

Lemma 3. *The sums of dipoles in the modal decomposition of the incident field are given by*

$$\sum_{m=-1}^1 \mathbf{e}_{1,m}^{\text{inc}} \nabla_{\mathcal{S}^2} Y_{1,m} = \frac{i}{2j_{1,1}} \gamma_t \mathbf{E}^{\text{inc}}(0); \quad \sum_{m=-1}^1 \mathbf{e}_{1,m}^{\text{inc}} Y_{1,m} = \frac{i}{2j_{1,1}} \gamma_n \mathbf{E}^{\text{inc}}(0) \quad (\text{C.3a})$$

$$\sum_{m=-1}^1 \mathbf{h}_{1,m}^{\text{inc}} \nabla_{\mathcal{S}^2} Y_{1,m} = \frac{i}{2j_{1,1}} \gamma_t \mathbf{H}^{\text{inc}}(0); \quad \sum_{m=-1}^1 \mathbf{h}_{1,m}^{\text{inc}} Y_{1,m} = \frac{i}{2j_{1,1}} \gamma_n \mathbf{H}^{\text{inc}}(0) \quad (\text{C.3b})$$

where $j_{1,1}$ = denotes the first coefficient in the expansion of the spherical Bessel function j_n , see Proposition 3.

Proof. The result is obtained by identifying the Taylor expansion of $(\mathbf{E}^{\text{inc}}, \mathbf{H}^{\text{inc}})$ in a neighborhood of 0

$$\mathbf{E}^{\text{inc}}(\mathbf{x}) = \mathbf{E}^{\text{inc}}(0) + O_{r \rightarrow 0}(r); \quad \mathbf{H}^{\text{inc}}(\mathbf{x}) = \mathbf{H}^{\text{inc}}(0) + O_{r \rightarrow 0}(r)$$

with the expansion of the modal decomposition in a neighborhood of 0 given by

$$\begin{aligned} \mathbf{E}^{\text{inc}}(\mathbf{x}) &= \frac{2j_{1,1}}{i} \sum_{m=-1}^1 \mathbf{e}_{1,m}^{\text{inc}} \left[\nabla_{\mathcal{S}^2} Y_{1,m} + Y_{1,m} \mathbf{e}_r \right] + O_{r \rightarrow 0}(r) \\ \mathbf{H}^{\text{inc}}(\mathbf{x}) &= \frac{2j_{1,1}}{i} \sum_{m=-1}^1 \mathbf{h}_{1,m}^{\text{inc}} \left[\nabla_{\mathcal{S}^2} Y_{1,m} + Y_{1,m} \mathbf{e}_r \right] + O_{r \rightarrow 0}(r). \end{aligned}$$

□

C.2 Analytical decomposition of the scattered field

According to (B.18), the solution of the exterior Maxwell problem (2.6) have an analytical solution. Actually, the scattered fields $(\mathbf{E}_\delta, \mathbf{H}_\delta)$ can be decomposed in the basis of singular solutions of the Maxwell equations,

$$\begin{aligned} \mathbf{E}_\delta(\mathbf{x}) &= \sum_{n=1}^{\infty} \sum_{m=-n}^n \mathbf{h}_{n,m}(\delta) h_n^{(1)}(\kappa r) \mathbf{curl}_{\mathcal{S}^2} Y_{n,m}(\hat{x}) \\ &\quad + \mathbf{e}_{n,m}(\delta) \left[\frac{h_n^{(1)}(\kappa r) + \kappa r h_n^{(1)' }(\kappa r)}{i\kappa r} \nabla_{\mathcal{S}^2} Y_{n,m}(\hat{x}) + \frac{h_n^{(1)}(\kappa r)}{i\kappa r} n(n+1) Y_{n,m}(\hat{x}) \mathbf{e}_r \right] \end{aligned} \quad (\text{C.4a})$$

and

$$\begin{aligned} \mathbf{H}_\delta(\mathbf{x}) &= \sum_{n=1}^{\infty} \sum_{m=-n}^n -\mathbf{e}_{n,m}(\delta) h_n^{(1)}(\kappa r) \mathbf{curl}_{\mathcal{S}^2} Y_{n,m}(\hat{x}) \\ &\quad + \mathbf{h}_{n,m}(\delta) \left[\frac{h_n^{(1)}(\kappa r) + \kappa r h_n^{(1)' }(\kappa r)}{i\kappa r} \nabla_{\mathcal{S}^2} Y_{n,m}(\hat{x}) + \frac{h_n^{(1)}(\kappa r)}{i\kappa r} n(n+1) Y_{n,m}(\hat{x}) \mathbf{e}_r \right] \end{aligned} \quad (\text{C.4b})$$

In (C.4), the modal coefficients depend on the small parameter δ through the expression (B.17)

$$\mathbf{e}_{n,m}(\delta) = \frac{i\kappa\delta}{h_n^{(1)}(\kappa\delta) + \kappa\delta h_n^{(1)' }(\kappa\delta)} \frac{1}{n(n+1)} \int_{\{|\mathbf{x}|=\delta\}} (\mathbf{n} \times \mathbf{E}^{\text{inc}})(\mathbf{x}) \cdot \mathbf{curl}_{\mathcal{S}^2} \overline{Y_{n,m}}(\hat{x}) \, ds \quad (\text{C.5a})$$

$$\mathbf{h}_{n,m}(\delta) = \frac{1}{h_n^{(1)}(\kappa\delta)} \frac{1}{n(n+1)} \int_{\{|\mathbf{x}|=\delta\}} (\mathbf{n} \times \mathbf{E}^{\text{inc}})(\mathbf{x}) \cdot \nabla_{\mathcal{S}^2} \overline{Y_{n,m}}(\hat{x}) \, ds \quad (\text{C.5b})$$

Remark 28. Identifying (C.2) and (C.5), we observe that

$$\mathbf{e}_{n,m}(\delta) = -\frac{j_n(\kappa\delta) + \kappa\delta j'_n(\kappa\delta)}{h_n^{(1)}(\kappa\delta) + \kappa\delta h_n^{(1)' }(\kappa\delta)} \mathbf{e}_{n,m}^{\text{inc}}; \quad \mathbf{h}_{n,m}(\delta) = -\frac{j_n(\kappa\delta)}{h_n^{(1)}(\kappa\delta)} \mathbf{h}_{n,m}^{\text{inc}}. \quad (\text{C.6})$$

This relation makes evident the dependence in δ .

The following proposition gives the Taylor expansion of the exact solution $(\mathbf{E}_\delta, \mathbf{H}_\delta)$ at the fifth order. That allows to find the third order far-field term again given by (2.10) and also the expression of the collected model presented in Section 5.

Proposition 5. *The analytical solution $(\mathbf{E}_\delta, \mathbf{H}_\delta)$ have the Taylor series expansion when δ tends to 0,*

$$\begin{aligned} \mathbf{E}_\delta(\mathbf{x}) = & (\kappa\delta)^3 \left\{ \left(\frac{1}{2} - \frac{3(\kappa\delta)^2}{10} \right) h_1^{(1)}(\kappa r) \gamma_t \mathbf{H}^{\text{inc}}(0) \times \mathbf{e}_r \right. \\ & \left. - \left(1 + \frac{3(\kappa\delta)^2}{10} \right) \frac{h_1^{(1)}(\kappa r) + \kappa r h_1^{(1)' }(\kappa r)}{i\kappa r} \gamma_t \mathbf{E}^{\text{inc}}(0) - 2 \left(1 + \frac{3(\kappa\delta)^2}{10} \right) \frac{h_1^{(1)}(\kappa r)}{i\kappa r} \gamma_n \mathbf{E}^{\text{inc}}(0) \mathbf{e}_r \right\} \\ & + O_{\delta \rightarrow 0}(\delta^5) \end{aligned}$$

and

$$\begin{aligned} \mathbf{H}_\delta(\mathbf{x}) = & (\kappa\delta)^3 \left\{ \left(1 - \frac{3(\kappa\delta)^2}{10} \right) h_1^{(1)}(\kappa r) \gamma_t \mathbf{E}^{\text{inc}}(0) \times \mathbf{e}_r \right. \\ & \left. + \left(\frac{1}{2} - \frac{3(\kappa\delta)^2}{10} \right) \frac{h_1^{(1)}(\kappa r) + \kappa r h_1^{(1)' }(\kappa r)}{i\kappa r} \gamma_t \mathbf{H}^{\text{inc}}(0) + 2 \left(\frac{1}{2} - \frac{3(\kappa\delta)^2}{10} \right) \frac{h_1^{(1)}(\kappa r)}{i\kappa r} \gamma_n \mathbf{H}^{\text{inc}}(0) \mathbf{e}_r \right\} \\ & + O_{\delta \rightarrow 0}(\delta^5). \end{aligned}$$

Proof. By injecting the expressions (C.6) and (C.3) into (C.4), we obtain

$$\begin{aligned} \mathbf{E}_\delta = & -\frac{j_1(\kappa\delta)}{h_1^{(1)}(\kappa\delta)} \frac{i}{2j_{1,1}} h_1^{(1)}(\kappa r) \gamma_t \mathbf{H}^{\text{inc}}(0) \times \mathbf{e}_r \\ & - \frac{j_1(\kappa\delta) + \kappa\delta j'_1(\kappa\delta)}{h_1^{(1)}(\kappa\delta) + \kappa\delta h_1^{(1)' }(\kappa\delta)} \frac{i}{2j_{1,1}} \left[\frac{h_1^{(1)}(\kappa r) + \kappa r h_1^{(1)' }(\kappa r)}{i\kappa r} \gamma_t \mathbf{E}^{\text{inc}}(0) + 2 \frac{h_1^{(1)}(\kappa r)}{i\kappa r} \gamma_n \mathbf{E}^{\text{inc}}(0) \mathbf{e}_r \right] + \mathfrak{E}_{\delta,2}(\mathbf{x}) \end{aligned}$$

and

$$\begin{aligned} \mathbf{H}_\delta = & \frac{j_1(\kappa\delta) + \kappa\delta j'_1(\kappa\delta)}{h_1^{(1)}(\kappa\delta) + \kappa\delta h_1^{(1)' }(\kappa\delta)} \frac{i}{2j_{1,1}} h_1^{(1)}(\kappa r) \gamma_t \mathbf{E}^{\text{inc}}(0) \times \mathbf{e}_r \\ & - \frac{j_1(\kappa\delta)}{h_1^{(1)}(\kappa\delta)} \frac{i}{2j_{1,1}} \left[\frac{h_1^{(1)}(\kappa r) + \kappa r h_1^{(1)' }(\kappa r)}{i\kappa r} \gamma_t \mathbf{H}^{\text{inc}}(0) + 2 \frac{h_1^{(1)}(\kappa r)}{i\kappa r} \gamma_n \mathbf{H}^{\text{inc}}(0) \mathbf{e}_r \right] + \mathfrak{H}_{\delta,2}(\mathbf{x}) \end{aligned}$$

where the remainders $\mathfrak{E}_{\delta,2}$ and $\mathfrak{H}_{\delta,2}$ are of second order ($n \geq 2$) into the expansions (C.4). We remark that $\mathfrak{E}_{\delta,2}$ and $\mathfrak{H}_{\delta,2}$ are in $O(\delta^5)$ when δ tends to 0. Then, we expand the coefficients depending on δ

$$\begin{aligned} \frac{j_1(\kappa\delta)}{h_1^{(1)}(\kappa\delta)} &= \frac{j_{1,1}}{h_{1,-2}} (\kappa\delta)^3 + \left[\frac{j_{1,3}}{h_{1,-2}} - \frac{j_{1,1} h_{1,0}}{(h_{1,-2})^2} \right] (\kappa\delta)^5 + O_{\delta \rightarrow 0}(\delta^6) \\ \frac{j_1(\kappa\delta) + \kappa\delta j'_1(\kappa\delta)}{h_1^{(1)}(\kappa\delta) + \kappa\delta h_1^{(1)' }(\kappa\delta)} &= -\frac{2j_{1,1}}{h_{1,-2}} (\kappa\delta)^3 - \left[\frac{2j_{1,1} h_{1,0}}{(h_{1,-2})^2} + \frac{4j_{1,3}}{h_{1,-2}} \right] (\kappa\delta)^5 + O_{\delta \rightarrow 0}(\delta^6) \end{aligned}$$

and we inject them into the previous expansions in order to obtain the result. \square

The following proposition gives the Taylor expansion of the exact solution $(\mathbf{E}_\delta(\delta \cdot), \mathbf{H}_\delta(\delta \cdot))$ at the first order. That allows to find the first near-field term again, given by (2.14).

Proposition 6. *The analytical solution $(\mathbf{E}_\delta(\delta \cdot), \mathbf{H}_\delta(\delta \cdot))$ have the Taylor series expansion in fast variable, when δ tends to 0,*

$$\begin{aligned}\mathbf{E}_\delta(\delta \mathbf{X}) &= \frac{1}{R^3} \left[2\gamma_n(\mathbf{E}^{\text{inc}}(0)) \mathbf{e}_r - \gamma_t(\mathbf{E}^{\text{inc}}(0)) \right] + O_{\delta \rightarrow 0}(\delta) \\ \mathbf{H}_\delta(\delta \mathbf{X}) &= -\frac{1}{2R^3} \left[2\gamma_n(\mathbf{H}^{\text{inc}}(0)) \mathbf{e}_r - \gamma_t(\mathbf{H}^{\text{inc}}(0)) \right] + O_{\delta \rightarrow 0}(\delta).\end{aligned}$$

Proof. Thanks to the Taylor series expansion of $(\mathbf{E}_\delta, \mathbf{H}_\delta)$ in Proposition 5, we have

$$\begin{aligned}\mathbf{E}_\delta(\delta \mathbf{X}) &= (\kappa\delta)^3 \left[-\frac{h_1^{(1)}(\kappa\delta R) + \kappa\delta R h_1^{(1)' }(\kappa\delta R)}{i\kappa\delta R} \gamma_t(\mathbf{E}^{\text{inc}}(0)) - 2\frac{h_1^{(1)}(\kappa\delta R)}{i\kappa\delta R} \gamma_n(\mathbf{E}^{\text{inc}}(0)) \mathbf{e}_r \right] + O_{\delta \rightarrow 0}(\delta) \\ \mathbf{H}_\delta(\delta \mathbf{X}) &= (\kappa\delta)^3 \left[\frac{h_1^{(1)}(\kappa\delta R) + \kappa\delta R h_1^{(1)' }(\kappa\delta R)}{2i\kappa\delta R} \gamma_t(\mathbf{H}^{\text{inc}}(0)) + \frac{h_1^{(1)}(\kappa\delta R)}{i\kappa\delta R} \gamma_n(\mathbf{H}^{\text{inc}}(0)) \mathbf{e}_r \right] + O_{\delta \rightarrow 0}(\delta).\end{aligned}$$

According to the Laurent series expansions of the spherical Hankel function of the first kind, we have

$$-\frac{h_1^{(1)}(\kappa\delta R) + \kappa\delta R h_1^{(1)' }(\kappa\delta R)}{i\kappa\delta R} = \frac{\mathfrak{h}_{1,-2}}{i}(\kappa\delta R)^{-3} + O(\delta^{-1}) \quad -2\frac{h_1^{(1)}(\kappa\delta R)}{i\kappa\delta R} = -\frac{2\mathfrak{h}_{1,-2}}{i}(\kappa\delta R)^{-3} + O(\delta^{-1}).$$

Then, we obtain easily the result by substituting the previous expansions into the one of $(\mathbf{E}_\delta(\delta \cdot), \mathbf{H}_\delta(\delta \cdot))$. \square

References

- [1] H. Ammari and H. Kang. *Reconstruction of small inhomogeneities from boundary measurements*. Springer, 2004.
- [2] H. Ammari, S. Moskow, and M. S. Vogelius. Boundary integral formulae for the reconstruction of electric and electromagnetic inhomogeneities of small volume. *ESAIM: Control, Optimisation and Calculus of Variations*, 9:49–66, 2003.
- [3] H. Ammari, M. S. Vogelius, and D. Volkov. Asymptotic formulas for perturbations in the electromagnetic fields due to the presence of inhomogeneities of small diameter ii. the full maxwell equations. *Journal de mathématiques pures et appliquées*, 80(8):769–814, 2001.
- [4] H. Barucq, J. Chabassier, H. Pham, and S. Tordeux. Numerical robustness of single-layer method with Fourier basis for multiple obstacle acoustic scattering in homogeneous media. *Wave Motion*, 2017.
- [5] A. Bendali. Numerical analysis of the exterior boundary value problem for the time-harmonic maxwell equations by a boundary finite element method. ii. the discrete problem. *Mathematics of Computation*, 43(167):47–68, 1984.
- [6] A. Bendali, P.-H. Cocquet, and S. Tordeux. Approximation by multipoles of the multiple acoustic scattering by small obstacles in three dimensions and application to the foldy theory of isotropic scattering. *Archive for Rational Mechanics and Analysis*, 219(3):1017–1059, 2016.

- [7] J. Blitz. *Electrical and magnetic methods of non-destructive testing*, volume 3. Springer Science & Business Media, 2012.
- [8] V. Bonnaillie-Noël, D. Brancherie, M. Dambrine, F. Herau, S. Tordeux, and G. Vial. Multi-scale expansion and numerical approximation for surface defects. In *ESAIM: Proceedings*, volume 33, pages 22–35. EDP Sciences, 2011.
- [9] A. Buffa, M. Costabel, and D. Sheen. On traces for $H(\text{curl}, \Omega)$ in lipschitz domains. *Journal of Mathematical Analysis and Applications*, 276(2):845 – 867, 2002.
- [10] M. Cassier and C. Hazard. Multiple scattering of acoustic waves by small sound-soft obstacles in two dimensions: mathematical justification of the foldy-lax model. *Wave Motion*, 50(1):18–28, 2013.
- [11] D. P. Challa, G. Hu, and M. Sini. Multiple scattering of electromagnetic waves by finitely many point-like obstacles. *Mathematical Models and Methods in Applied Sciences*, 24(05):863–899, 2014.
- [12] X. Claeys. *Analyse asymptotique et numérique de la diffraction d’ondes par des fils minces*. PhD thesis, Université de Versailles-Saint Quentin en Yvelines, 2008.
- [13] P.-H. Cocquet. *Etude mathématique et numérique de modes homogénéisés de métamatériaux*. PhD thesis, Université Paul Sabatier-Toulouse III, 2012.
- [14] D. Colton and R. Kress. *Integral equation methods in scattering theory*, volume 72. SIAM, 2013.
- [15] D. G. Crighton, A. P. Dowling, J. Ffowcs-Williams, M. Heckl, F. Leppington, and J. F. Bartram. *Modern methods in analytical acoustics lecture notes*, 1992.
- [16] M. Dauge, S. Tordeux, and G. Vial. Selfsimilar perturbation near a corner: matching versus multiscale expansions for a model problem. In *Around the Research of Vladimir Maz’ya II*, pages 95–134. Springer, 2010.
- [17] A. de La Bourdonnaye. Décomposition de $H^{-1/2}(\text{div}_{\Gamma}, \Gamma)$ et nature de l’opérateur de Steklov-Poincaré du problème extérieur de l’électromagnétisme. *Comptes rendus de l’Académie des sciences. Série 1, Mathématique*, 316(4):369–372, 1993.
- [18] M. Duruflé. *Intégration numérique et éléments finis d’ordre élevé appliqués aux équations de Maxwell en régime harmonique*. PhD thesis, 2006. Thèse de doctorat dirigée par Cohen, Gary Chalom Sciences. Mathématiques appliquées Paris 9 2006.
- [19] W. Eckhaus. *Matched asymptotic expansions and singular perturbations*. 1973.
- [20] L. L. Foldy. The multiple scattering of waves. I. General theory of isotropic scattering by randomly distributed scatterers. *Physical Review*, 67(3-4):107, 1945.
- [21] L. Fraenkel. On the method of matched asymptotic expansions: Part I: A matching principle. In *Mathematical Proceedings of the Cambridge Philosophical Society*, volume 65, pages 209–231. Cambridge University Press, 1969.
- [22] K. A. Fuller and D. W. Mackowski. Electromagnetic scattering by compounded spherical particles. *Light scattering by nonspherical particles: theory, measurements, and applications*, page 226, 2000.

- [23] M. Ganesh and S. C. Hawkins. A high-order algorithm for multiple electromagnetic scattering in three dimensions. *Numerical Algorithms*, 50(4):469–510, 2009.
- [24] A. M. Il'in. *Matching of asymptotic expansions of solutions of boundary value problems*, volume 102. American Mathematical Society Providence, RI, 1992.
- [25] B. G. Korenev. *Bessel functions and their applications*. CRC Press, 2003.
- [26] J. Labat. Représentations modales pour la diffraction d'ondes électromagnétiques. Master's thesis, Université de Pau et des Pays de l'Adour, Sept. 2016.
- [27] B. Laud. *Electromagnetics*. New Age International, 1987.
- [28] V. Mattesi. *Propagation des ondes dans un domaine comportant des petites hétérogénéités: modélisation asymptotique et calcul numérique*. PhD thesis, Pau, 2014.
- [29] V. Maz'Ya, S. Nazarov, and B. Plamenevskij. *Asymptotic theory of elliptic boundary value problems in singularly perturbed domains*, volume 1. Birkhäuser, 2012.
- [30] P. Monk. *Finite element methods for Maxwell's equations*. Oxford University Press, 2003.
- [31] J.-C. Nédélec. *Acoustic and electromagnetic equations: integral representations for harmonic problems*, volume 144. Springer Science & Business Media, 2001.
- [32] V. Péron. *Modélisation mathématique de phénomènes électromagnétiques dans des matériaux à fort contraste*. PhD thesis, Université Rennes 1, 2009.
- [33] R. E. Raab and O. L. De Lange. *Multipole theory in electromagnetism: classical, quantum, and symmetry aspects, with applications*, volume 128. Oxford University Press on Demand, 2005.
- [34] L. F. R. S. Rayleigh. X. on the electromagnetic theory of light. *The London, Edinburgh, and Dublin Philosophical Magazine and Journal of Science*, 12(73):81–101, 1881.
- [35] B. Thierry. *Analysis and Numerical Simulations of Time Reversal and Multiple Scattering*. Theses, Université Henri Poincaré - Nancy I, Sept. 2011.
- [36] S. Tordeux. *Méthodes Asymptotiques pour la Propagation des Ondes dans les Milieux comportant des Fentes*. Theses, Université de Versailles-Saint Quentin en Yvelines, Dec. 2004.
- [37] M. Van Dyke. *Perturbation Methods in Fluid Mechanics*. Parabolic Press, 1975.
- [38] B. Veihelmann, T. Nousiainen, M. Kahnert, and W. Van der Zande. Light scattering by small feldspar particles simulated using the gaussian random sphere geometry. *Journal of Quantitative Spectroscopy and Radiative Transfer*, 100(1-3):393–405, 2006.
- [39] G. Vial. *Analyse multi-échelle et conditions aux limites approchées pour un problème avec couche mince dans un domaine à coin*. PhD thesis, 2003.
- [40] D. Volkov. *An inverse problem for the time harmonic Maxwell's equations*. PhD thesis, 2003.
- [41] T. Wriedt, J. Hellmers, E. Eremina, and R. Schuh. Light scattering by single erythrocyte: comparison of different methods. *Journal of Quantitative Spectroscopy and Radiative Transfer*, 100(1-3):444–456, 2006.



**RESEARCH CENTRE
BORDEAUX – SUD-OUEST**

200 avenue de la Vieille Tour
33405 Talence Cedex

Publisher
Inria
Domaine de Voluceau - Rocquencourt
BP 105 - 78153 Le Chesnay Cedex
inria.fr

ISSN 0249-6399